Cranfield University

HAE-IN LEE

# COOPERATIVE CONTROL OF MULTI-UAVS UNDER COMMUNICATION CONSTRAINTS

School of Aerospace, Transport and Manufacturing
Autonomous Vehicles Dynamics and Control

PhD thesis
Academic Year: 2015–2018

Supervisors: Dr. Hyo-Sang Shin, Prof. Antonios Tsourdos
October 2018

Cranfield University

School of Aerospace, Transport and Manufacturing
Autonomous Vehicles Dynamics and Control

PhD thesis

Academic Year: 2015–2018

Hae-In Lee

# Cooperative Control of Multi-UAVs Under Communication Constraints

Supervisors: Dr. Hyo-Sang Shin, Prof. Antonios Tsourdos
October 2018

# Abstract

This research aims to develop an analysis and control methodology for the multiple unmanned aerial vehicles (UAVs), connected over a communication network. The wireless communication network between the UAVs is vulnerable to errors and time delays, which may lead to performance degradation or even instability. Analysis on the effects of the potential communication constraints in the multiple UAV control is a critical issue for successful operation of multiple UAVs. Therefore, this thesis proposes a systematic method by incorporating three steps: proposing the analysis method and metrics considering the wireless communication dynamics, designing the structure of the cooperative controller for UAVs, and applying the analysis method to the proposed control in representative applications.

For simplicity and general insights on the effect of communication topology, a networked system is first analysed without considering the agent or communication dynamics. The network theory specifies important characteristics such as robustness, effectiveness, and synchronisability with respect to the network topology. This research not only reveals the trade-off relationship among the network properties, but also proposes a multi-objective optimisation (MOO) method to find the optimal network topology considering these trade-offs.

Extending the analysis to the networked control system with agent and communication dynamics, the effect of the network topology with respect to system dynamics and time delays should be considered. To this end, the effect of communication dynamics is then analysed in the perspective of robustness and performance of the controller. The key philosophy behind this analysis is to approximate the networked control system as a trans-

fer function, and to apply the concepts such as stability margin and sensitivity function in the control theory.

Through the analysis, it is shown that the information sharing between the agents to determine their control input deteriorates the robustness of their stability against system uncertainties. In order to compensate the robustness and cancel out the effect of uncertainties, this thesis also develops two different adaptive control methods. The proposed adaptive control methods in this research aim to cope with unmatched uncertainty and time-varying parameter uncertainty, respectively. The effect of unmatched uncertainty is reduced on the nominal performance of the controller, using the parameter-robust linear quadratic Gaussian method and adaptive term. On the other hand, time-varying parameter uncertainty is estimated without requiring the persistent excitation using concurrent learning with the directional forgetting algorithm. The stability of the tracking and parameter estimation error is proved using Lyapunov analysis.

The proposed analysis method and control design are demonstrated in two application examples of a formation control problem without any physical interconnection between the agents, and an interconnected slung-load transportation system. The performance of the proposed controllers and the effect of topology and delay on the system performance are evaluated either analytically or numerically.

# Keywords

Unmanned Aerial Vehicle, Network Theory, Networked Control System, Adaptive Control, Formation Control, Slung-Load Transportation System

# Contents

# List of Figures

# List of Tables

# Nomenclature

| | |
|---|---|
| $N$ | The number of vehicles / agents / nodes |
| $f_{core}$ | Fraction of core nodes |
| $k$ | Total degree |
| $p(\cdot)$ | Probability density function |
| $P(\cdot)$ | The cumulative density function |
| $\gamma$ | Exponent in the power-law distribution |
| $\zeta(\cdot;\cdot)$ | Hurwitz zeta function |
| $\langle\cdot\rangle$ | Average value |
| $S$ | The size of the largest cluster |
| $\phi$ | Probability of the percolation |
| $d_{ij}$ | Geodesic path from the node $i$ to $j$ |
| $L$ | Laplacian matrix of a graph |
| $\lambda$ | Eigenvalue |
| $\psi$ | Network states |
| $c$ | Diffusion rate constant |
| $G(s)$ | Transfer function of agent dynamics |
| $C(s)$ | Transfer function of measurement dynamics |
| $x(t)$ | System states |
| $r(t)$ | Reference input |
| $y(t)$ | Observed outputs |
| $e(t)$ | Error between the reference input and outputs / reference states and states |

| | |
|---|---|
| $H(s)$ | Transfer function of communication dynamics |
| $K(s)$ | Transfer function of controller |
| $n$ | The number of states |
| $m$ | The number of inputs |
| $l$ | The number of outputs |
| $\mathscr{N}$ | The number of communication hops |
| $\tau_{ij}$ | Communication delay from agent $i$ to $j$ |
| $T$ | Accessing delay of each communication hop |
| $\lambda(\cdot)$ | Set of eigenvalues of a matrix |
| $\mathfrak{N}(\cdot,\cdot,\cdot)$ | The number of clockwise encirclements of the point by the locus of a transfer function as $s$ traverses the closed contour |
| $\bar{\sigma}(\cdot)$ | Maximum singular value of a matrix |
| $S(s)$ | Sensitivity function |
| $\Delta(t)$ | Parameterised uncertainty |
| $W^*(t)$ | True parameter matrix |
| $\Phi(x(t))$ | Basis vector |
| $p$ | The number of basis |
| $N^*$ | Weight matrix |
| $\varepsilon$ | System parameter variation |
| $q$ | The number of system parameter variation |
| $w_{PR}$ | Weight of the parameter-robust linear quadratic Gaussian method |
| $\Gamma$ | Adaptation gain |
| $\sigma$ | $\sigma$-mod gain |
| $V(\cdot,\cdot)$ | Lyapunov function |
| $q(t)$ | Filtered vector of $\Phi(x(t))$ |
| $c(t)$ | Filtered vector of $\Delta(t)$ |
| $\Omega(t)$ | Information matrix |
| $M(t)$ | Auxiliary matrix |

| | |
|---|---|
| $\Psi(\cdot,\cdot)$ | Transition matrix |
| $h(t)$ | Step function |
| $\mathbb{C}$ | Direction cosine matrix |
| $g$ | Gravitational acceleration |
| $K_t$ | Thrust coefficient of a rotor |
| $K_r$ | Torque coefficient of a rotor |
| $K_c$ | Control allocation coefficient |
| $d$ | Distance between the rotors |

**List of Abbreviations**

| | |
|---|---|
| UAV | Unmanned Aerial Vehicle |
| MOO | Multi-Objective Optimisation |
| EGT | Evolutionary Game Theory |
| TDMA | Time Division Multiple Access |
| MIMO | Multi-Input-Multi-Output |
| SISO | Single-Input-Single-Output |
| CRHP | Closed-Right-Hand-Plane |
| GM | Gain Margin |
| PM | Phase Margin |
| DM | Delay Margin |
| IFL | Internal Feedback Loop |
| AC | Adaptive Control |
| MRAC | Model Reference Adaptive Control |
| FE | Finite Excitation |
| PE | Persistence of Excitation |
| CL | Concurrent Learning |
| PRLQG | Parameter-Robust Linear Quadratic Gaussian |
| LQR | Linear Quadratic Regulator |

| | |
|---|---|
| LQG | Linear Quadratic Gaussian |

# Chapter 1

# Introduction

## 1.1 Background and Motivation

Recently, incorporating multiple unmanned aerial vehicles (UAVs) is getting increasing attention for its versatile applications for both military and civilian uses. In multi-UAV operations, the importance of the wireless communication network is increasing correspondingly. The wireless communication network among the multiple UAVs enhances the scalability and reliability by eliminating the necessity to be connected to the ground station directly. However, the more the UAVs are dependent on each others' communication network, the more the performance could be degraded by the communication constraints, such as transmission range, bandwidth, error, and time delay [1]. The problem is even more crucial for small UAVs using unreliable sensors and transmitters due to their limited payload or cost effectiveness. Depending on the control design or system dynamics, even a trivial uncertainty may evoke cascading effects over the whole network of UAVs and eventually the failure of the mission [2]. The necessity and challenges to cope with this issue have been numerously emphasised in various applications including military systems [3, 4], urban deployments [5], and civilian uses [6].

There have been numerous works indirectly related with this issue. On the control of UAVs, many control techniques, such as robust control and adaptive control, have been

proposed to handle the systems with uncertainties. On the communication dynamics, there have been attempts in the field of network calculus to model the departures and arrivals of data packets. The network calculus is an attempt to model the communication in the data packet level and quantify the service curves. Ciucu and Fidler [7, 8, 9] reviewed deterministic and stochastic network calculus. Whereas deterministic network calculus provides conservative bounds to the service curve, stochastic network calculus estimates the bounds into feasible regions using probability functions. Jiang and Liu [10] focused on stochastic network calculus, and Lin *et al.* [11] reviewed the application of stochastic network calculus.

However, the linkage between the two fields of study has been hardly studied to answer the question: how much effect the communication dynamics has on the control of UAVs. The reasons behind would include that it has been only recent years that the operation of networked UAVs has been getting dramatic attention, compared with the development of classical control theory. Also, it is difficult to combine these fields of study as the communication dynamics is nonlinear, stochastic, and finite-field [12] to be considered in analysing the control of UAVs.

In the view of control design for UAVs, the focus would be the impact of wireless communication on the control metrics such as robustness and performance, rather than the detailed behaviours of data packets in the communication. This research first aims to propose a systematic approach to analyse and design the networked UAVs with considerations of communication dynamics, by combining the concepts of control theory and network theory. This research then concentrates on developing control algorithms, which can retain desirable robustness and performance, for the networked multiple UAVs.

## 1.2 Research Objectives

The main objectives of this research fall into two folds: the first objective is to propose a systematic approach to consider communication dynamics into the analysis of the net-

worked UAV system and the second to develop its control algorithms that guarantee desirable performance. The analysis method is proposed to quantify the effects of communication topology and dynamics on the robustness and performance of the networked UAVs. Adaptive control algorithms are then proposed to alleviate the effects of uncertainties that propagate through the network, based on the analysis results. Specific objectives are suggested as:

1. **Analysis on networked system** In order to obtain a general idea on the analysis, the characteristics of a general networked system without considering communication and UAV dynamics are analysed with respect to different network topologies.

2. **Analysis on networked control system** Extending the analysis to communication and system dynamics, the robustness and performance measures of the networked control system are defined. The effect of communication and UAV dynamics is analysed with respect to different network topologies.

3. **Adaptive control design for unmatched uncertainties** To compensate the robustness and performance metrics obtained from the analysis method, the controller is designed. An adaptive control technique is proposed to cope with the unmatched uncertainties that propagate through the network. The unmatched uncertainties may occur from the physical interconnection between the agents, such as in slung-load transportation system.

4. **Adaptive control design for time-varying uncertainties** Another adaptive control technique is designed to handle the time-varying uncertainties without requiring persistent excitation.

5. **Application** Two application examples are presented to validate the analysis framework and the proposed control methods: formation control and slung-load system. The numerical simulations on the representative application examples are conducted to support the analysis.

## 1.3 Theoretical Basis

This section presents some important theories closely relevant to the main objective of this thesis: combination of network theory and control theory. The detailed literature review with respect to each specific objectives is given in the rest of the thesis where relevant.

First, the network theory is the study of graphs, which are composed of nodes and edges. The networked system of multiple UAVs with communication among them can be formulated as a graph; neglecting the detailed communication and UAV dynamics, the properties in the network theory can be applied directly. The concepts in the network theory have been developed in numerous fields of study, such as computational science, electrical engineering, economics, and operational research. The important traditional concepts include Laplace matrix, centrality measure, geodesic path, and percolation phenomenon [13]. These concepts are used throughout the thesis, but especially for the analysis on networked system.

With consideration of communication and system dynamics, the study on networked control systems has been developed. Developed relatively recently compared with network theory, the studies on networked control systems focus on the effect of communication on the control or estimation of each vehicles composing the network. The challenging issues include band-limited channels, sampling time, delay, and packet dropouts [14]. One of the main objectives of this thesis is to develop an analysis method to quantify the robustness and performance of the networked control system.

In the control theory, the concepts of stability, stability margin, and sensitivity function of multi-input-multi-output (MIMO) system are mainly utilised for the robustness and performance metrics [15]. Also, for the control design, model-reference adaptive control (MRAC) method and LQ-based controllers [16, 17] are used. More relevant control concepts and techniques to specific objectives are introduced in the rest of the thesis.

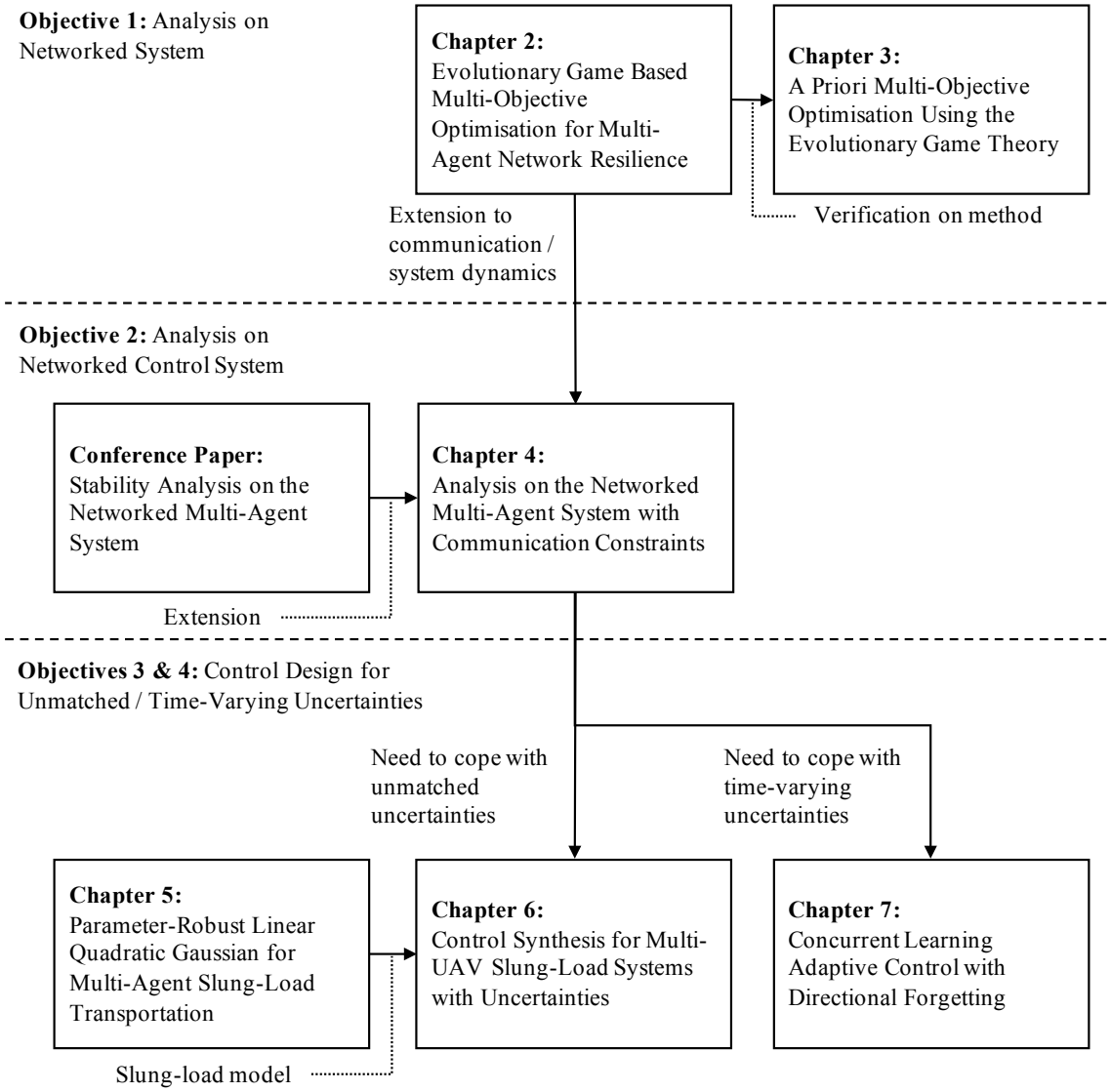


Figure 1.1: Main structure of the thesis

## 1.4 Thesis Overview and Contributions

This thesis is paper-based and hence the rest of this thesis from Chapter 2 to 7 is composed of six main papers. Each of the chapters contains its abstract and introduction, providing the context of the research, relevant literature, and contributions to this thesis. The methodology, results, and conclusions of the chapters are consistent with the publications, except for some changes in the notation and terminology for their completeness and consistency.

The connections between the chapters, papers, and research objectives are illustrated

in Fig. 1.1. The major chapters closely related with each research objectives 1, 2, 3 and 4 are Chapters 2, 4, 6 and 7, respectively. Chapter 2 deals with the analysis of networked system, and later extended to the networked control system in Chapter 4. Chapters 6 and 7 propose control methods for unmatched and time-varying uncertainties, respectively. The rest of the chapters support these main chapters; Chapter 3 further verifies the proposed method in Chapter 2, and Chapter 5 provides mathematical model of slung-load system for Chapter 6. The research objective 5 is handled in the overall chapters and then summarised in Chapter 8: general discussions. Each blocks in Fig. 1.1 are briefly overviewed, underpinning the contributions of each publications.

**Chapter 2**

- Title: Evolutionary Game Based Multi-Objective Optimisation for Multi-Agent Network Resilience

- Conference: 30th Congress of the International Council of the Aeronautical Sciences (ICAS2016), Daejeon, Korea, 2016

Chapter 2 is presented to achieve the research objective: analysis on networked system. Without considering the communication or system dynamics, the main properties of a general networked system are analysed. In addition to analysing the network properties with respect to different network topologies, the optimal network topology is obtained by formulating the problem into a multi-objective optimisation (MOO) problem. A new MOO method is proposed to solve the problem, which uses the evolutionary game theory (EGT) to consider the trade-offs between the objective functions.

The contribution of this chapter is threefold. First, the main contribution on this thesis is that a general idea on the effect of network topology is obtained. The trade-offs between the network topologies suggest that the extension to the networked control systems may also retain similar characteristics. This corresponds to the conclusions of Chapter 4. Second, in the view of network theory, this research suggests a guideline to design

the network topology considering the trade-offs between the network properties. This is applicable not only to networked UAV systems, but also to various fields including multi-agent systems, sensor network, or automated highway systems. Third, in the perspective of MOO methods, the proposed EGT based method is newly proposed to solve a MOO problem, considering the trade-offs between the objective functions. The proposed method is further developed and verified in Chapter 3.

**Chapter 3**

- Title: A Priori Multi-Objective Optimisation Using the Evolutionary Game Theory
- Journal: European Journal of Operational Research
  Status: In revision to submit

In Chapter 3, the proposed MOO method in Chapter 2 is extended and verified. The applicability of the method is not limited to the networked control as in Chapter 2, but extended to general benchmark problems. As the main objective of the proposed EGT based MOO method is to consider the trade-offs of the objective functions in optimisation, the concept of trade-off and EGT related notions are detailed. The method is validated with well-known benchmark MOO problems, comparing with other MOO methods.

In this thesis, this chapter is a supporting part for Chapter 2, providing the methodological approach for optimising the network topology. However, the main contribution on this research lies in solving the MOO problems in a simple way to consider the trade-offs. The optimal decision variables can be computed in consistent computational time, regardless of the complexity of the MOO problems.

**Chapter 4**

- Title: Stability Analysis on the Networked Multi-Agent System
- Journal: IEEE Transactions on Automatic Control
  Status: Submitted

Chapter 4 mainly focuses on the analysis on the networked control system. A new analysis method is proposed to consider the networked control system as a single transfer function, which enables to quantify the robustness of system stability and the performance metrics. The application of the analysis method on case studies suggest the effect of network topology, communication dynamics, and agent dynamics on the analysis metrics. The result reveals the trade-offs between the robustness and performance metrics, and often instability depending on the network topology and system dynamics.

The contribution of this chapter is twofold. First, the contribution of this research on the thesis is that the effect of network topology on the robustness and performance of the controller is obtained. The trade-off relationship together with Chapter 2 provides a guide to design a network. Second, another contribution on the thesis is the effect of system dynamics on the system stability. Depending on the networked system dynamics – including agent dynamics, controller, and communication dynamics – the networked control system could be unstable or the stability margin could be critical. This suggests the controller to be carefully designed to suppress the effects of uncertainties to compensate the critical stability margins, supporting the rationale behind Chapters 5 to 7.

**Conference Paper**

- Title: Stability Analysis on the Networked Multi-Agent System
- Conference: European Control Conference (ECC2018), Limassol, Cyprus, 2018

This research is conducted to achieve the research objective: analysis on the networked control system. The analysis in Chapter 2 is extended to consider the communication and system dynamics, and the analysis metrics are changed to control theory based metrics. The analysis on delay margins of simple agent dynamics and initial simulation results have been presented, and the analysis is later extended to other robustness and performance metrics and simulation results in Chapter 4. The main results and findings of this paper are therefore incorporated in Chapter 4.

**Chapter 5**

- Title: Parameter-Robust Linear Quadratic Gaussian Technique for Multi-Agent Slung-Load Transportation

- Journal: Aerospace Science and Technology
  Status: Published, Vol. 71, pp. 119-127, 2017

In Chapter 5, the slung-load transportation system with multiple UAVs is introduced, which contains unmatched structured uncertainties. The slung-load dynamics is modelled using spherical coordinates, and the modelling is verified with numerical simulations. The controller is designed with parameter-robust linear quadratic Gaussian (PRLQG) method to obtain the nominal control performance with respect to different payload variations.

This chapter is a supporting part of Chapter 6, where the modelling of the slung-load dynamics and the PRLQG-based baseline controller are used. The contribution on the modelling part is that the slung-load system is modelled with minimal state-space representation, which enables to apply the optimal control methods directly. Also, consideration of the slung-load system as an application example is a challenging but important point in this thesis, as the physical interconnections between the UAVs influence on the stability of the networked control system and may create unmatched uncertainties.

Note that this paper has been submitted in 2014, but gone through major corrections since 2016. The modelling part has been conducted before the PhD study, and the detailed analysis on the PRLQG control method has been added during the PhD. This paper provides the mathematical model and baseline controller for Chapter 6, which proposes a control synthesis for unmatched and nonlinear uncertainties.

**Chapter 6**

- Title: Control Synthesis for Multi-UAV Slung-Load Systems with Uncertainties

- Conference: European Control Conference (ECC2018), Limassol, Cyprus, 2018

Chapter 6 is presented for the research objective: adaptive control design for unmatched uncertainties. The control design is extended from Chapter 5 to model-reference adaptive control (MRAC) in order to cope with both unmatched and matched uncertainties. The stability condition of the tracking and parameter estimation error is proven with Lyapunov stability analysis.

The main contribution of this chapter is that the controller is designed to suppress the effects of unmatched as well as matched nonlinear uncertainties on the stability of the networked control system. As the results in Chapter 4 suggest that the stability margin of the networked control systems could be critically low, it is beneficial to design the controllers to retain its nominal performance under the existence of potential type of uncertainties.

**Chapter 7**

- Title: Concurrent Learning Adaptive Control with Directional Forgetting
- Journal: IEEE Transactions on Automatic Control
  Status: In revision to resubmit

In Chapter 7, the adaptive control method is designed to cope with time-varying uncertainties. The concurrent learning method with directional forgetting algorithm is used to relax the persistent excitation requirement while identifying time-varying parameters. The sufficient and necessary conditions for Lyapunov and exponential stability of the tracking and parameter estimation error are derived.

The contribution of the chapter is the design of the controller to suppress the effects of time-varying parameters. In this thesis, the control method can be used to compensate the critical stability margins of the networked control system, as stated in Chapter 4. The proposed control technique is also expected to be applicable to other systems with time-varying parameters, where the persistent excitation is not guaranteed.

# References

[1] H. S. Shin. “UAV Swarms : Decision Making Paradigms”. In: *Encyclopedia of Aerospace Engineering*. John Wiley: Chichester, 2014, pp. 1–34.

[2] I. Akyildiz, W. Su, Y. Sankarasubramaniam, and E. Cayirci. “Wireless sensor networks: a survey”. In: *Computer Networks* 38.4 (2002), pp. 393–422.

[3] T. Samad, J. S. Bay, and D. Godbole. “Network-centric systems for military operations in urban terrain: The role of UAVs”. In: *Proceedings of the IEEE* 95.1 (2007), pp. 92–107.

[4] M. Hauge, L. Landmark, and M. Amanowicz. “Selected Issues of QoS Provision in Heterogenous Military Networks”. In: *International Journal of Electronics and Telecommunications* 60.1 (2014), pp. 7–13.

[5] G. Pau and R. Tse. “Challenges and opportunities in immersive vehicular sensing: Lessons from urban deployments”. In: *Signal Processing: Image Communication* 27.8 (2012), pp. 900–908.

[6] P. Carvalhal, C. Santos, M. Ferreira, L. Silva, and J. Afonso. “Design and Development of a Fly-by-Wireless UAV Platform”. In: *Aerial Vehicles* (2009), pp. 1–12.

[7] F. Ciucu and J. Schmitt. “Perspectives on network calculus: no free lunch, but still good value”. In: *SIGCOMM Comput. Commun. Rev.* 42.4 (2012), pp. 311–322.

[8] M. Fidler. “Survey of deterministic and stochastic service curve models in the network calculus”. In: *IEEE Communications Surveys & Tutorials* 12.1 (2010), pp. 59–86.

[9] M. Fidler and A. Rizk. “A Guide to the Stochastic Network Calculus”. In: *IEEE Communications Surveys & Tutorials* PP.99 (2014), pp. 1–1.

[10] Y. Jiang and Y. Liu. *Stochastic Network Calculus*. Springer Berlin Heidelberg, 2008.

[11] C. Lin, Y. Deng, and Y. Jiang. “On applying stochastic network calculus”. In: *Frontiers of Computer Science* 7.6 (2013), pp. 924–942.

[12] S. Y. Park and A. Sahai. “Network Coding meets Decentralized Control: Network Linearization and Capacity-Stabilizablilty Equivalence”. In: *arXiv* (2013), pp. 4817–4822. arXiv: 1308.5045.

[13] M. E. J. Newman. “Networks. An introduction”. In: *Oxford University Press* (2010), p. 772.

[14] J. P. Hespanha, P. Naghshtabrizi, and Y. Xu. “A survey of recent results in networked control systems”. In: *Proc. of the IEEE* 95.1 (2007), pp. 138–162.

[15] J. D. Blight, R. Lane Dailey, and D. Gangsaas. “Practical control law design for aircraft using multivariable techniques”. In: *International Journal of Control* 59.1 (1994), pp. 93–137.

[16] J. Doyle and G. Stein. “Multivariable feedback design: Concepts for a classical/modern synthesis”. In: *Automatic Control, IEEE Transactions on* 26.1 (1981), pp. 4–16.

[17] G. Stein and M. Athans. “The LQG / LTR Procedure for Multivariable Feedback Control Design”. In: *IEEE Transactions on Automatic Control* 32.2 (1987), pp. 105–114.

# Chapter 2

# Evolutionary Game Based Multi-Objective Optimisation for Multi-Agent Network Resilience


## Abstract

This research presents multi-objective optimisation (MOO) problem for network resilience. The scale free core-periphery structure is parameterised to formulate the network properties as objective functions. Optimising the conflicting network properties, an evolutionary game based approach is used to find the weightings of the weighted sum method. Numerical results show the optimal weightings and network structures depending on the size of network.


## 2.1 Introduction

Modern aerospace technologies often incorporate complex structures of networks. The more complicated and intensive the dependency on network connection is, the more the functionality suffers from node failure or communication malfunction. Furthermore,

wireless communication networks are vulnerable to the cyber-physical failure. It is an important issue to model the failing vertices as a percolation process and to design a resilient topology in autonomous operations.

There have been several attempts to find robust and efficient networks. Motter *et al.* [18] have addressed the conflict between robustness and synchronisability, and other properties including global and local efficiency have been detailed later [19]. As an option to improve the overall network properties, Peixoto *et al.* [20] propose the core-periphery topology, but the detailed topology and consideration of conflicting network properties remain illusive.

This chapter aims to find the network topology for enhancing network properties, considering the networked system without any dynamics. The main idea is to formulate this issue into a MOO problem, where the conflicting properties of network are objective functions and the topology of network is a decision variable. As the full topology is determined by a large number of variables, this research proposes a single parameter design method assuming scale free core-periphery network.

Solving the formulated MOO problem, this chapter suggests to use the evolutionary game based MOO method [21]. It is based on the weighted-sum method, while the weightings are determined by an evolutionary game. The main advantage is the consideration of solution's survivability in the other criteria without any expert decision or use of aggregation coefficient while providing low computational load. The main contribution thus lies in suggesting a new perspective on formulating the resilient network and applying a suitable MOO method, which has not been applied comprehensively.

This chapter is composed as follows: the first part summarises the definitions and characteristics of scale free core-periphery topology. Then finding the optimal network structure is formulated into MOO problem. The evolutionary game based method is explained in section 2.4, and examined through numerical simulations in section 2.5. Finally, conclusions and future works are addressed.

## 2.2 Scale Free Core-Periphery Network

### 2.2.1 Definition

The core-periphery network with $N$ nodes is defined with core nodes and periphery nodes [22]. Defining the fraction of core nodes as $f_{core}$, core nodes of the number $Nf_{core}$ are connected with each other, and peripheral nodes of the rest are connected randomly either to the core or to the periphery. Note that $f_{core}$ is determined so that $Nf_{core}$ is an integer.

The number of edges connected to each node is decided by the total degree $k$. The scale free network follows the power-law distribution, defined with the probability and cumulative density function, $p(k)$ and $P(K)$ respectively:

$$\begin{aligned} p(k) &= \frac{k^{-\gamma}}{\zeta(\gamma;k_{min}) - \zeta(\gamma;N)} \\ P(K) &= \frac{\zeta(\gamma;k_{min}) - \zeta(\gamma;K+1)}{\zeta(\gamma;k_{min}) - \zeta(\gamma;N)} \\ \zeta(\gamma;a) &\triangleq \sum_{k=a}^{\infty} k^{-\gamma} \simeq \frac{a^{-\gamma+1}}{\gamma-1} \end{aligned} \tag{2.1}$$

where $\gamma$ is an exponent in the power-law distribution, and $\zeta(\gamma;a)$ is the Hurwitz zeta function for normalisation. The long-tail effect of the probability distribution is eliminated by constraining the degree $k_{min} \leq k \leq N-1$ [13].

The structure of scale free core-periphery network is thus determined by three parameters: $f_{core}$, $k_{min}$ and $\gamma$. By the definition of core-periphery nodes, the probability of $k \geq Nf_{core} - 1$ is $f_{core}$, which means the cumulative density function satisfies

$$\frac{\zeta(\gamma;k_{min}) - \zeta(\gamma;Nf_{core})}{\zeta(\gamma;k_{min}) - \zeta(\gamma;n)} = 1 - f_{core} \tag{2.2}$$

Also, the average degree is fixed for that the unlimited degree enhances all the theo-

retical properties. The average degree can be computed as

$$\langle k \rangle = \frac{\zeta(\gamma; k_{min}) - \zeta(\gamma+1; N)}{\zeta(\gamma; k_{min}) - \zeta(\gamma; N)} \tag{2.3}$$

where $\langle \cdot \rangle$ denotes the average value. From the definition of the Hurwitz zeta function, existence of the average degree requires $\gamma > 2$.

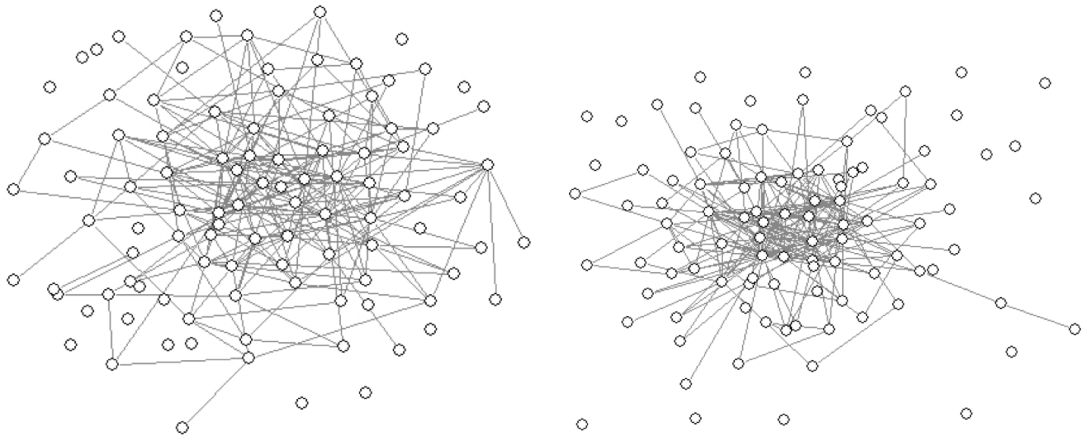

(a) Homogeneous Network (b) Heterogeneous Network

Figure 2.1: Visualisation of the scale free networks

Using Eqn. (2.2) and Eqn. (2.3), $f_{core}$ and $k_{min}$ are computed from $\gamma$, where the average degree $\langle k \rangle$ is fixed. Therefore, the design of network is simplified into a single-parameter problem with $\gamma$. Increase in $\gamma$ results in large $k_{min}$, and the network has homogeneous degree over the nodes. On the contrary, decrease in $\gamma$ yields a heterogeneous network with highly concentrated nodes. The number of core nodes remains similar, but the number of periphery nodes connected directly to the core is larger in heterogeneous networks than in the homogeneous. Both homogeneous and heterogeneous networks are visualised in Fig. 2.1 using the Pajek program [23]. While $\langle k \rangle$ is fixed to 3, Fig. 2.1 (a) is plotted with $\gamma = 5$ and (b) with $\gamma = 3$. Although the size of network is large – a hundred – the visualisation clearly shows homogeneity and heterogeneity respectively.

### 2.2.2 Properties

The network properties are classified into three main categories – robustness, efficiency and synchronisability [18, 19] – which are derived from the percolation process.

The percolation process is crucial in understanding the network properties, especially robustness. The percolation is a phenomenon where some fraction of nodes and edges are removed. The analysis on the percolation phenomenon in the generated network enables to model the cyber-physical failure of the autonomous system and to compute the remaining network functionality. From this analysis, the size of the largest cluster with respect to the occupational probability is obtained, where the cluster is defined with the groups of nodes connected to each other and the occupational probability is the portion of remaining nodes [13].

Robustness is the ability of a network to maintain its function under the presence of failure by taking a detour or multi-hop communication. The value is determined by the area of $S$–$\phi$ plot below the critical size of the largest cluster, $S_c$:

$$J_1 = \int_0^{S_c} \phi dS \tag{2.4}$$

where $\phi$ is the probability of the percolation.

Efficiency is the measure of how the nodes communicate their information each other. The global efficiency is proportional to the closeness centrality, which is the average length of a geodesic path $d_{ij}$ as,

$$J_2 = \left(\langle d_{ij} \rangle\right)^{-1} \tag{2.5}$$

where $i$ and $j$ are the indices of nodes.

Synchronisability depends on the speed of diffusion along the connections, which is

determined by the eigenvalues of the Laplacian matrix $L$,

$$J_3 = \frac{\lambda_N}{\lambda_2}, \qquad \frac{d\psi}{dt} + cL\psi = 0 \tag{2.6}$$

where $\psi$ is the network state, $c$ is the diffusion rate constant, $\lambda_N$ is the maximum eigenvalue, and $\lambda_2$ is the minimum non-zero eigenvalue of the Laplacian matrix.

Note that the network properties chosen are not explicitly expressed as functions of $\gamma$. Instead, the properties are computed with respect to various $\gamma$ with Monte-Carlo simulation, and fitted into second-order polynomial.

## 2.3 Multi-Objective Optimisation Problem Formulation

To find the optimal network structure, an optimisation problem is formulated with its objective functions set as the network properties. As the design of network depends on a single parameter, the MOO problem is formulated as

$$\begin{aligned} \max_{\gamma} \quad & J_1, J_2, J_3 \\ \text{subject to} \quad & \gamma > 2 \end{aligned} \tag{2.7}$$

The objective functions may conflict with each other; enhancement in one objective deteriorates at least one of the rests. The weighted sum method aggregates multiple weighted objectives into a single cost function as

$$\begin{aligned} \max_{\gamma} \quad & J = w_1 J_1 + w_2 J_2 + w_3 J_3 \\ \text{subject to} \quad & \gamma > 2 \end{aligned} \tag{2.8}$$

This method is the most widely used thanks to its simplicity [24], but difficulties arise when determining the weightings, which are resolved in this research by using the evolutionary game theory (EGT).

## 2.4 Evolutionary Game Based Multi-Objective Optimisation

### 2.4.1 Payoff Matrix

The core concept of the evolutionary game based MOO method is that the optimisation problem is a type of non-cooperative game. Among the conflicting objectives, improving an objective deteriorates at least one of the others. One needs to consider both gain and loss of choosing which objective to be optimised. optimising the ratios of gain to loss, called trade-offs, it is expected that more weighting is applied to the objectives that are sensitive to the choice of which objective to be optimised. It is compared to the concept of equilibrium in the game theory.

Finding the equilibrium in a non-cooperative game requires analysing the players' utility to formulate a payoff matrix [25]. The decision variables and cost functions act as players, and which objectives to be optimised are the possible strategies. The weightings of a MOO problem correspond to the Nash equilibrium of the mixed strategies. Therefore, the payoff matrix is composed such that objective functions comprise the rows and optimal decision variables with respect to each criterion are substituted to the columns. For the problem formulation in Eqn. (3.3), the payoff matrix $A$ is composed as

$$A = \begin{bmatrix} J_1(\gamma_1^*) & J_1(\gamma_2^*) & J_1(\gamma_3^*) \\ J_2(\gamma_1^*) & J_2(\gamma_2^*) & J_2(\gamma_3^*) \\ J_3(\gamma_1^*) & J_3(\gamma_2^*) & J_3(\gamma_3^*) \end{bmatrix} \tag{2.9}$$

where $\gamma_i^*$ is the optimal $\gamma$ for the $i$-th objective.

The normalisation method and the form of cost function affect the characteristics of the payoff matrix. Different scales of each cost function have an effect of varying absolute and relative importance, and thus the cost functions are normalised in each step. The

normalised payoff matrix $\bar{A}$ is composed as

$$\bar{A}_{ij} = \frac{J_i(\gamma_i^*) - J_i^-}{J_i^+ - J_i^-} \tag{2.10}$$

where $J_i^+$ and $J_i^-$ are the maximum and minimum value of $i$-th objective respectively.

### 2.4.2 Replicator Equation

Using the payoff matrix, the fitness of mixed strategies $p_i$ evolves in each time step through the replicator equation,

$$\dot{p}_i = p_i(e_i A p^T - p A^T p) \tag{2.11}$$

where $e_i \in \mathbb{R}^3$ is a vector with one at the $i$-th element and zeros at the other.

The evolutionary stable solution $\bar{p}$ is computed with an augmented matrix as

$$\begin{bmatrix} \bar{p}^T \\ a \end{bmatrix} = \begin{bmatrix} A & -1_{3\times 1} \\ -1_{1\times 3} & 0 \end{bmatrix}^{-1} \begin{bmatrix} 0_{3\times 1} \\ 1 \end{bmatrix} \tag{2.12}$$

where $a$ is an auxiliary constant to match the matrix dimension.

A single solution exists when the augmented matrix is invertible. If the problem is singular, infinitely many solutions exist but the average solution is used. The stability of the dynamics is determined by the eigenvalues of the payoff matrix, and guarantee of stability is easily shown in the MOO problems [26].

## 2.5 Optimal Network Structure

The optimal network structure is obtained from the proposed approach. The algorithm of the proposed approach is summarised in Fig. 2.2. Given the average degree $\langle k \rangle$, objective functions for the optimisation problem are derived. Then, optimal degree exponent $\gamma$ is obtained using the evolutionary game based MOO method. The optimal leads to the

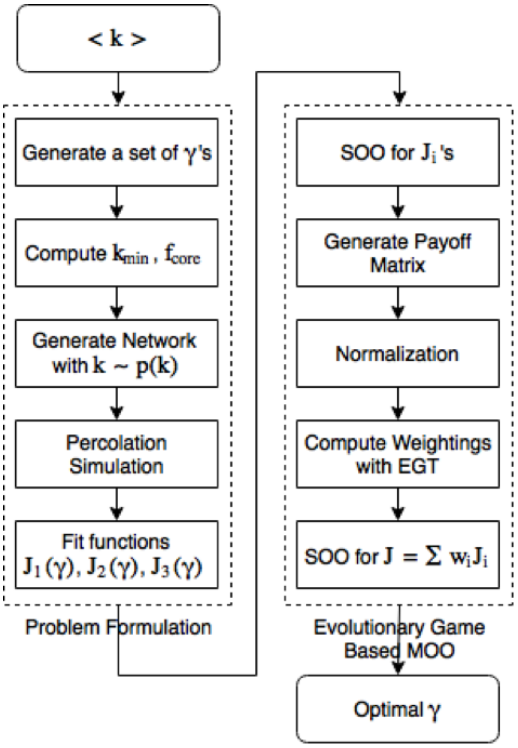


Figure 2.2: Algorithm of the evolutionary game based MOO method

| Network Parameter | Value | Description |
|---|---|---|
| $N$ | 100 | The number of nodes |
| $\gamma_{max}$ | 5 | Upper bound of exponent |
| $\langle k \rangle_0$ | 30 | Initial average degree |
| $\Delta \langle k \rangle$ | 3 | Change in average degree |

Table 2.1: Network parameter specification

optimal structure of the network.

Numerical simulation is conducted with different $\langle k \rangle$'s. Physical limit of multi-agent network such as transmission power and coverage decides $\langle k \rangle$; for instance, given the fixed transmission power, spread of the networked vehicles reduces $\langle k \rangle$. Exploiting the advantage of the propose approach that the weightings are determined dynamically, the simulation is composed with reducing $\langle k \rangle$ as:

$$\langle k \rangle = \langle k \rangle_0 - \Delta \langle k \rangle t \tag{2.13}$$

where $t$ is the simulation time. The values of simulation parameters are specified in Table

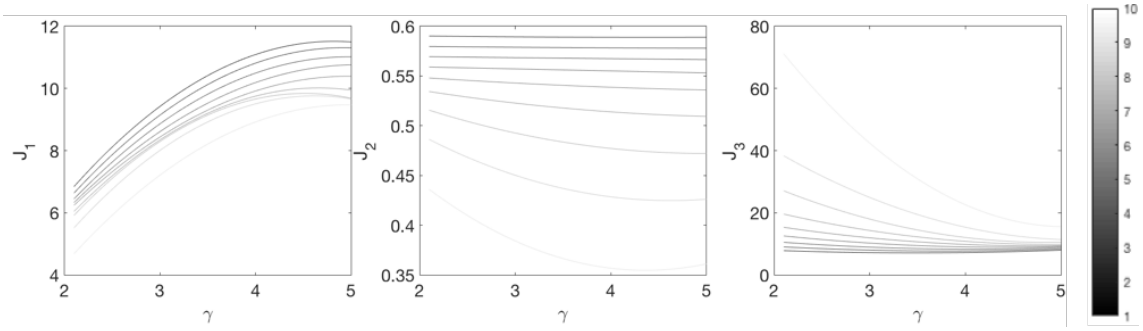


(a) Average at $1 \leq t \leq 10$

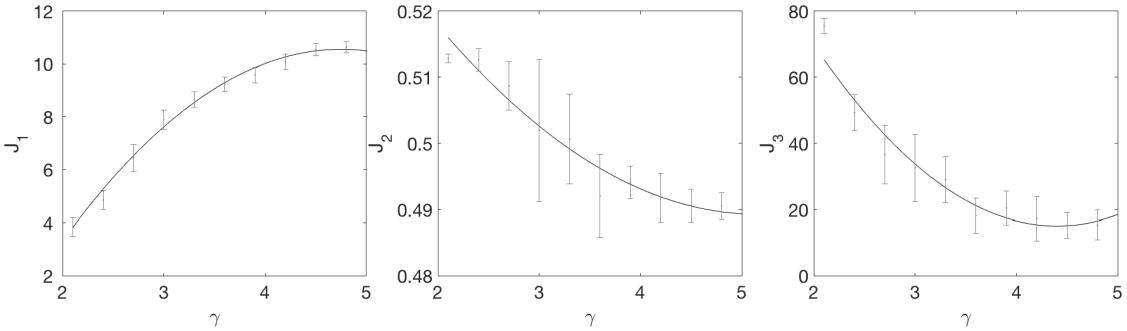


(b) Average and variance at $t = 10$

Figure 2.3: Objective functions – network properties

Table 2.1.

The objective functions are obtained with Monte-Carlo simulations with 10 runs generating the different networks and same degree distribution, and then are fitted into second-order polynomial. In the MOO part, each single objective optimisation is conducted using 'fmincon' from MATLAB. The evolutionary stable solutions are evolved 100 times at each run.

The objective functions with respect to $\gamma$ are shown in Fig. 2.3. Three figures show different network properties – robustness, efficiency, and synchronisability. In Fig. 2.3 (a), the brightness of the lines indicates the simulation time. Whereas the change in robustness stays similar throughout the simulation, efficiency and synchronisability varies in their minimum and maximum values. It can be concluded that efficiency and synchronisability are more sensitive to network structure when the transmission power is small or requires large coverage area. Since the relationships between the network properties and $\gamma$ is obtained only by numerical simulations, the variance of Monte-Carlo simulation at the

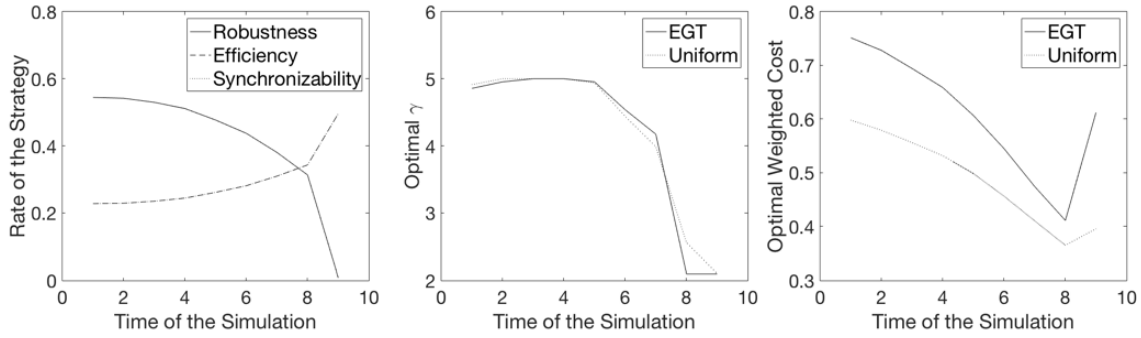


Figure 2.4: Results of the evolutionary game based MOO method

time step $t = 10$ is shown in Fig. 2.3 (b).

Using the obtained objective functions, the evolutionary game based MOO method is implemented. The resultant optimal weightings, decision variable, and cost are shown in Fig. 2.4. In Fig. 2.4 (a), the weightings on robustness decrease while efficiency and synchronisability increases almost simultaneously with the decrease of $\langle k \rangle$. This corresponds to the fact that efficiency and synchronisability are more sensitive in the later part of simulations. Increase of weightings on sensitive cost functions implies that the evolutionary game base approach is successfully considering the trade-offs. In Fig. 2.4 (b), the optimal network structure is implied by optimal $\gamma$. It is more advantageous to formulate a homogenous network when the transmission power is not enough or desired coverage is broad, while a heterogeneous network is better in the other case.

For validating the performance of evolutionary game based approach, the optimisation result using uniform weightings, one third on each objective function, is compared. Fig. 2.4 (b) shows that similar optimal network structures are obtained in each method, but Fig. 2.4 (c) shows that the evolutionary game based approach results in the increase of maximum weighted cost.

## 2.6 Conclusions

In this chapter, design of scale free core-periphery networks is formulated into a single parameter problem, and the network properties are optimised using the evolutionary game

based MOO method. Numerical simulation is conducted with different average degrees, which are relevant to the size of network by the transmission power or coverage. The results suggest that a homogeneous network is advantageous in a concentrated network with either sufficient transmission power or narrow coverage, whereas a heterogeneous network is of more importance in the other case. The parameter of the network structure is given by the optimal exponent of the degree distribution. This research is expected to suggest a guide for designing a topology in the various fields including multi-agent or sensor network design.

Further studies are focused on mobile network system. Most of the previous works on mobile networks [26, 27] have been dedicated to maximise connectivity, which is similar to synchronisability, not considering the other properties. The results often result in a rendezvous formation without a constraint on coverage. We expect that controlling the multiple agents to form an optimal degree distribution from this research may suggest more robust, efficient and fast synchronising network.

# References

[13] M. E. J. Newman. “Networks. An introduction”. In: *Oxford University Press* (2010), p. 772.

[18] A. E. Motter, C. Zhou, and J. Kurths. “Network synchronization, diffusion, and the paradox of heterogeneity”. In: *Physical Review E - Statistical, Nonlinear, and Soft Matter Physics* 71.1 (2005), pp. 1–10.

[19] B. Wang, H. Tang, C. Guo, Z. Xiu, and T. Zhou. “Optimization of network structure to random failures”. In: *Physica A: Statistical Mechanics and its Applications* 368.2 (2006), pp. 607–614.

[20] T. P. Peixoto and S. Bornholdt. “Evolution of robust network topologies: Emergence of central backbones”. In: *Physical Review Letters* 109.11 (2012), pp. 1–5.

[21] C. Leboucher, H. S. Shin, S. Le Menec, A. Tsourdos, A. Kotenkoff, P. Siarry, and R. Chelouah. “Novel Evolutionary Game Based Multi-Objective Optimisation for Dynamic Weapon Target Assignment”. In: *the 19th World Congress The International Federation of Automatic Control* 2010 (2014), pp. 3936–3941.

[22] P. Holme. “Core-periphery organization of complex networks”. In: *Physical Review E - Statistical, Nonlinear, and Soft Matter Physics* 72.4 (2005).

[23] V. Batagelj and A. Mrvar. “Pajek – program for large network analysis”. In: *Connections* (1999), pp. 47–57.

[24] K. Deb. *Multi-objective optimization using evolutionary algorithms: an introduction*. John Wiley & Sons, LTD., 2011.

[25] M. Kok. “A Note on the Pay-off Matrix in Multiple Objective Programming”. In: *European Journal of Operational Research* 26.1 (1986), pp. 96–107.

[26] J. Hofbauer and K. Sigmund. “Evolutionary Game Dynamics”. In: *Bulletin of the American Mathematical Society* 40.4 (2003), pp. 479–519.

[27] M. M. Zavlanos and G. J. Pappas. “Potential fields for maintaining connectivity of mobile networks”. In: *IEEE Transactions on Robotics* 23.4 (2007), pp. 812–816.

# Chapter 3

# A Priori Multi-Objective Optimisation Using the Evolutionary Game Theory

## Abstract

This chapter develops an *a priori* Multi-Objective Optimisation (MOO) approach based on the evolutionary game theory (EGT). One of the main challenges in the *a priori* MOO approaches is determination of the weightings of each objective. In this chapter, the problem of determining the weightings is formulated as an evolutionary game of optimal solutions of individual single-objective optimisation problems and weightings are obtained by solving this game. The properties of the proposed evolutionary game based approach are also investigated through trade-off analysis. The analysis results suggest that the proposed approach determines the weightings such that the trade-offs at the corresponding solution of the MOO problem becomes identical. As a part of validation, numerical simulations are performed with well-known benchmark MOO problems. The simulation results confirm that the analysis results are valid.

## 3.1 Introduction

MOO refers to the process of simultaneously optimising a set of more than one objective in a systematic manner [28] and is also known as vector optimisation, multi-objective programming, or multi-criteria optimisation. The application of MOO is ubiquitous, e.g., engineering design, operational management, strategic management, public sector planning, and etc. [29]. The objectives in the MOO problems are generally conflicting and these problems seldom have a unique solution [30]. Consequently, it is often non-trivial and difficult to solve MOO problems.

Because of an extensive range of applications and inherent complexity of MOO, there have been comprehensive researches on MOO algorithms [31]. Depending on when the user-preference is utilised, MOO algorithms can be classified into three categories: *a priori*, *a posteriori*, or interactive [32]. *a priori* methods heavily rely on the preference information and usually yield a single optimal solution, whereas *a posteriori* methods find multiple non-dominated solutions without any prior information. The resultant set of non-dominated solutions, defined as Pareto-optimal set [33], allows the decision maker to select a solution in accordance with his/her preference. Combining the characteristics of *a priori* and *a posteriori* methods, the optimisation and decision making process iteratively evolve in interactive methods.

Although which approach is better than the other is clearly debatable and subjective, *a priori* methods are widely used thanks to their simplicity and intuitiveness [28]. In MOO problems with dynamically evolving systems and/or time-critical systems, the possibility for the user or operator to intervene in each optimisation procedure is minimal. Therefore, in this type of the MOO problem, advantages of the *a priori* approach can be accentuated. A critical issue with *a priori* methods including the weighted sum method is determination of the user-defined preference information: how to aggregate the multiple objectives into a single objective function [34].

The main motivation of this chapter is the challenge in determining the weightings of objectives in *a priori* methods considering dynamically evolving systems and systems

require time-critical decision making. Non-existence of an absolutely dominant solution among conflicting objectives makes the decision on appropriate weightings cumbersome. Although moving away from a solution along a feasible search direction improves most of objectives in the MOO problem, but it is likely to impair a few objectives or even just one objective. This implies that the performance may still be degraded, especially if the impaired objective is critical. Therefore, it could be important to examine the trade-offs among the candidate solutions of the MOO problem and its result could be used in finding weightings of the objectives. Note that the trade-offs are defined as limit effects of deviation along a feasible direction from a given decision and it is measured by relative changes in objectives.

There have been several attempts to resolve the difficulties in finding the appropriate weightings for given MOO problems. The weighted compromise programming [35] uses the ratio of positive axis intercepts. Later, Messec [36] suggested the conversion method from design metrics to form the aggregated objective function. Both methods, however, do not implement the trade-off information of the problem structure.

This chapter develops an *a priori* MOO algorithm that determines the weightings in consideration of the trade-offs among the potential solutions. The main proposition is to leverage the evolutionary game theory (EGT), so the proposed method is named evolutionary game based *a priori* MOO.

The rational behind this proposition is that selecting the weightings in *a priori* methods can be considered as an evolutionary game problem in which optimising each objective corresponds to a strategy. In this game, we can evaluate the change in the costs results from a small deviation of an optimal individual, that is the solution obtained from optimising the corresponding single objective. The concept of this change is identical to that of the trade-off. If the trade-off of an optimal individual is small compared with others, optimising the corresponding objective becomes more important in the game. Solving the evolutionary game will result in the weighting of the optimal individual inverse proportional to the trade-off. EGT consequently enables determination of the weightings

reflecting the the trade-offs.

Obtaining the weightings using the EGT was first attempted in [21]. The MOO problem considered in [21] was a Weapon Target Assignment (WTA) problem where several objectives need to be optimised and time-critical decision making is of great importance. The proposed algorithm was expected to enable consideration of the individual solutions' survivability in other criteria without any expert decision or use of aggregation coefficients. As the main purpose was to briefly study its feasibility and demonstrate its potential in the WTA problem, the rigorous development, analysis, and validation of the algorithm remained the subject of another study.

Under this background, this chapter first develops an improved evolutionary game based *a priori* MOO algorithm, named *EGMOO*. The main considerations of this development are to propose how to convert the MOO problem to a evolutionary game of selecting the weightings, and to provide the closed-form solution of the converted game. In order to mitigate the issue results from the different scales of the objectives, this chapter utilises normalised objectives in the evolutionary game dynamics. Selecting a proper normalisation method for the evolutionary game, this chapter investigates a few normalisation methods [37, 38].

This chapter then focuses on the analysis and validation of the proposed *a priori* MOO algorithm. In the analysis, we examine the properties of the proposed algorithm, including incommensurability, stability and singularity, through the dynamics of the evolutionary game. Then, the proposed evolutionary game based approach is validated by performing the trade-off analysis, which is common in MOO algorithms [39, 40, 41, 42, 43, 44, 45, 46, 47]. In order to demonstrate the validity of the evolutionary game based approach, this chapter also performs numerical simulations with benchmark problems commonly used for the validation of the MOO algorithms. In the discussion of the simulation results, the trade-off of the solution point of the proposed approach is compared with the optimal trade-off obtained from the whole Pareto-optimal set.

The rest of the chapter is organised as follows: Section 3.2 introduces the definition

of the multi-objective problem and two classical *a priori* MOO methods. Section 3.3 describes the decision process for determining the weightings based on the EGT approach. The performance of the proposed evolutionary game based MOO algorithm is evaluated with the trade-off analysis explained in 3.4. The problem settings and numerical results are presented in Section 3.5. Finally, the conclusion and future works are proposed in Section 3.6.

## 3.2 Multi-Objective Optimisation

An MOO problem is generally defined with multiple cost functions, constraints, and bounds as

$$\begin{aligned} &\text{minimise } f_m(\boldsymbol{x}), \quad m = 1,2,\cdots,M \\ &\text{subject to } g_j(\boldsymbol{x}) \geq 0, \quad j = 1,2,\cdots,J \\ &\qquad\qquad h_k(\boldsymbol{x}) = 0, \quad k = 1,2,\cdots,K \\ &\qquad\qquad x_i^{lb} \leq x_i \leq x_i^{ub}, \quad i = 1,2,\cdots,n \end{aligned} \tag{3.1}$$

where the number of cost functions, $M$, is larger than 2, and $\boldsymbol{x}$ is a vector of $n$ decision variables. Equality and inequality constraints can either exist or not.

As stated in Introduction, this research develops an *a prior* method where the MOO problem is reformulated to a single-objective optimisation problem using the EGT approach. The two classical *a priori* methods are the weighted sum method and the min-max goal programming approach.

Let us first briefly review the weighted sum method. For more detail, the reader is referred to [34]. The weighted sum method integrates multiple objectives, which are pre-multiplied by the weighting vector $\boldsymbol{w}$, into a single cost function. The MOO problem is

therefore reformulated as

$$\begin{aligned} \text{minimise } f(\boldsymbol{x}) &= \sum_{m=1}^{M} w_m f_m(\boldsymbol{x}) \\ \text{subject to } g_j(\boldsymbol{x}) &\geq 0, \quad j = 1,2,\cdots,J \\ h_k(\boldsymbol{x}) &= 0, \quad k = 1,2,\cdots,K \\ x_i^{lb} \leq x_i &\leq x_i^{ub}, \quad i = 1,2,\cdots,n \end{aligned} \tag{3.2}$$

where $w_m$'s are the weightings for the corresponding cost functions $f_m$'s.

The weighted sum method is one of the most widely used MOO methods thanks to its simplicity and intuitiveness in finding the non-dominated solutions. It is also proven that any Pareto-optimal solution can be reached by the weighted sum method when the MOO problem is convex.

However, one critical drawback of this method is that the performance is highly sensitive to the selection of the weightings. Obtaining the proper weightings involves a few difficulties including ambiguousness of reflecting the decision maker's preference information, problem dependency, and incommensurability in the multiple objectives.

Another limitation of the weighted sum method occurs when dealing with non-convex optimisation problems. The solutions of the weighted sum methods are proven to be Pareto-optimal, but likely to be distributed either in the boundary or in the nonuniform parts of the non-convex Pareto-optimal set. Subsequently, even if the weightings are determined adequately overcoming the difficulties listed above, the resultant optimal solution may converge to the identical or indifferent points of the other weightings.

Now, let us recall goal programming and its properties in brief. Again, the reader is referred to [34] for more detail. Goal programming uses additional pre-defined preference information beside the relative importance of the multiple objectives: the goal of the optimisation. Minimising the deviations from the solutions to the designated target objectives, the min-max goal programming approach converts an MOO problem into the

following single-objective optimisation problem:

$$\begin{aligned} &\text{minimise } \gamma \\ &\text{subject to } f_m(\boldsymbol{x}) - \gamma w_m \leq f_{goal,m}, \quad m = 1, \cdots, M \\ &\qquad g_j(\boldsymbol{x}) \geq 0, \quad j = 1, 2, \cdots, J \\ &\qquad h_k(\boldsymbol{x}) = 0, \quad k = 1, 2, \cdots, K \\ &\qquad x_i^{lb} \leq x_i \leq x_i^{ub}, \quad i = 1, 2, \cdots, n \end{aligned} \tag{3.3}$$

where $\gamma$ is the deviation from the goal, $f_{goal}$.

Unlike the weighted sum method, it is proven that the min-max goal programming approach is able to find all the Pareto-optimal solutions in both the convex and non-convex MOO problems. Note that capability in finding the entire Pareto-optimal solutions is important to properly determine the weightings in *a priori* approaches. This is because, although *a priori* methods compute a single optimum, accessibility to the Pareto-optimal set should be secured to reflect the effects of different weighting sets in the solutions.

Similar to the weighted sum method, it is critical to determine appropriate weightings in the min-max goal programming approach since its performance is dependent on the these weightings. Moreover, utilising the concept of goal might introduce additional complexity to the problem.

The proposed MOO method in this chapter can utilise both the weighted-sum method and min-max goal programming approach, since the proposed approach focuses in determining the proper weightings. In cases that the estimation of goal is difficult, the weighted-sum method is more appropriate while min-max goal programming approach should be used for non-convex MOO problems. For this reason, in Chapter 2, the weighted-sum method has been used considering that determining the goal of network properties. In this chapter, however, most of the benchmark problems incorporate non-convex Pareto-optimal front, and thus the goal programming approach has been utilised.

## 3.3 Evolutionary Game Based Approach

The overview of the proposed evolutionary based *a priori* MOO algorithm is depicted in Fig. 3.1. As shown in Fig. 3.1, given the MOO problem, the proposed MOO algorithm first individually solve each single objective optimisation (SOO) problem. The optimal solutions obtained from SOO problems are named *optimal individuals* and denoted as $\boldsymbol{x}_m^*$ for $m \in \{1,\ldots,M\}$. The *optimal individual* can be a solution vector or an average of multiple solution vectors of the corresponding SOO problem. Then, the algorithm formulate a payoff matrix, $A$, from the *optimal individuals* obtained and corresponding cost functions, $f_m$. Once, the payoff matrix is given, the proposed MOO algorithm solve the evolutionary game to find a Evolutionary Stable Strategy (ESS). The weightings of each objective can be then obtained from this ESS. Next, the algorithm solve the MOO problem with the weightings obtained from the ESS. Note that, if the min-max goal programming approach is selected as an *a priori* MOO method like in this chapter, the goals, $f_{goal,m}$, should be provided to formulate the MOO problem as shown in Eqn. (3.3). These goals can be obtained from individual SOO performed for each objective or simply set to be identical to *optimal individuals*.

Now, let us discuss how to formulate the evolutionary game of determining the weightings in detail. MOO is a type of non-cooperative game where the decision variables act as players and multiple criteria correspond to strategies. The players adopt mixed strategies generating the fitness or a probability distribution over possible actions, which is related to the weightings of each objective in the MOO problem. The concept of Nash equilibrium, the point on which each player maximises his or her payoff assuming the others' payoff being fixed, can be interpreted in terms of optimisation, i.e. maximising the worst-case value. In order to mitigate the stiffness of the weighted-sum of the cost functions on the Nash equilibrium point, less fitness is assigned on more stiffly changing strategy. However, the purpose of the decision making of the weightings is exactly opposite; more weightings should be assigned to the cost function with larger slope in MOO problems. Therefore, the decision making problem of selecting the weightings is

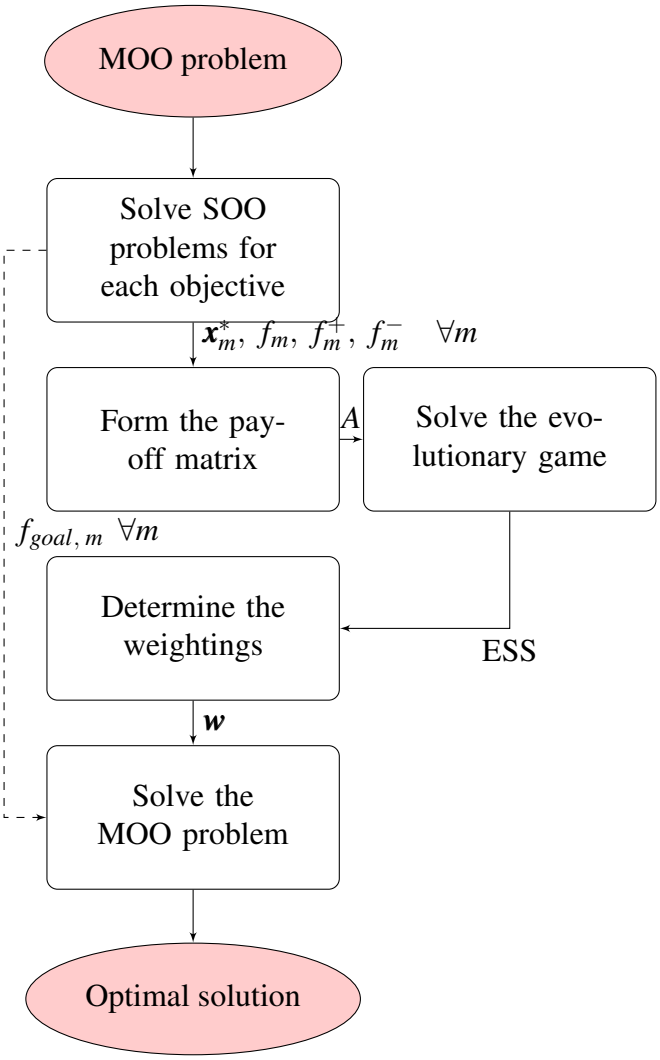


Figure 3.1: Flowchart of the proposed evolutionary game based *a priori* MOO: $f_m^+$ and $f_m^-$ denote the maximum and minimum vlaues of the corresponding cost function $f_m$.

subsequently converted to the problem of finding the negative value of the fitness in Nash equilibrium.

Fig. 3.2 visualises the inverse relationship between the Nash equilibrium and the desired weightings of the objectives in a simple MOO problem with $M = 2$. Two cost functions are plotted in straight lines as the payoff linearises the trade-offs between the objectives. The mixed strategy plotted flat in a red line, maximising the minimum value, is therefore a Nash equilibrium solution. The fitness is inversely proportional to the trade-offs caused by the change of decision variables. Hence, the weightings can be designed as the difference between the fitness and 1's. Utilisation of the game theory generalises

this concept, i.e. enables to expand the decision making of the weightings to the general number of objectives.

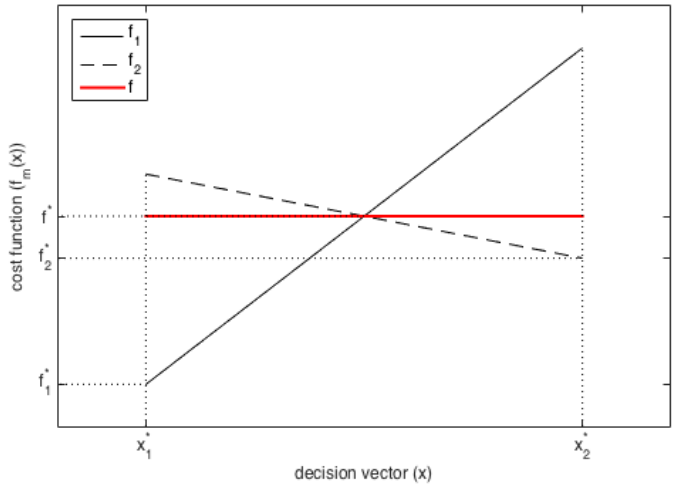


Figure 3.2: The equilibrium in the two-objective optimisation problem

The effect of the changes in weightings on the solution space is shown in Fig. 3.3. Let us suppose that the original weightings of the objectives, $f_1$ and $f_2$, are set to be $(\omega_1, \omega_2) = (0.5, 0.5)$. If we apply the evolutionary game, the weighting of $f_2$ becomes larger than that of $f_1$ as the $f_2$ value more rapidly changes as illustrated in Fig. 3.2, e.g. compared with the case of $(\omega_1, \omega_2) = (0.3, 0.7)$. In Fig. 3.3, the optimal solutions for the two sets of the weightings are marked as a circle and star shape on the solution space. From Fig. 3.3, we can deduce that adjusting the weightings drives the slope at the optimal solution close to "-1" in the weighted solution space. This implies that the trade-offs of each weighted objective in the proposed approach tend to be identical.

There are two major views on finding the equilibrium, static and dynamic approaches. Even though the final result may be the same, the dynamic approach complements the game dynamics that is not observed in the static approach. The converging pattern of the fitness is characterised by the game dynamics, which is defined as a feedback loop of each player's payoff change results from the others' action. When an MOO problem is time-variant, change in the weightings can be either relaxed or tightened according to the time span in a feedback loop. As shown in Fig. 3.4, the gradient of evolution is straightforward

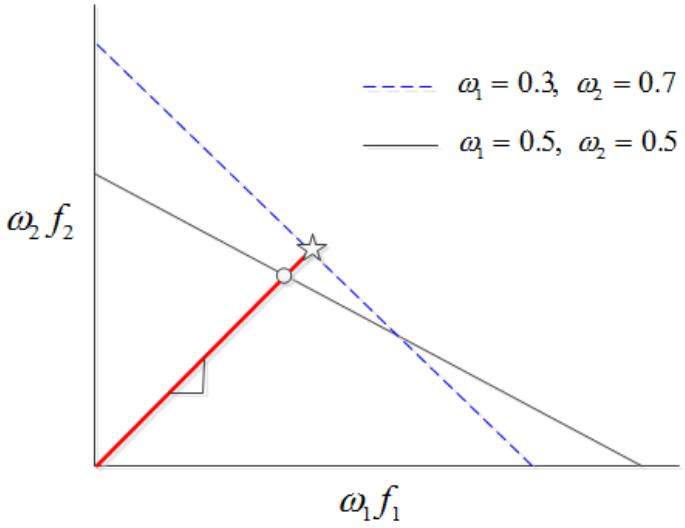


Figure 3.3: Effect of the changes in weightings on the solution space

to the equilibrium, so that the cease in the middle results in the intermediate value between the initial and the stable value. Therefore, this research applies EGT, the most renowned concept of the dynamic approach, in the decision making of the weightings.

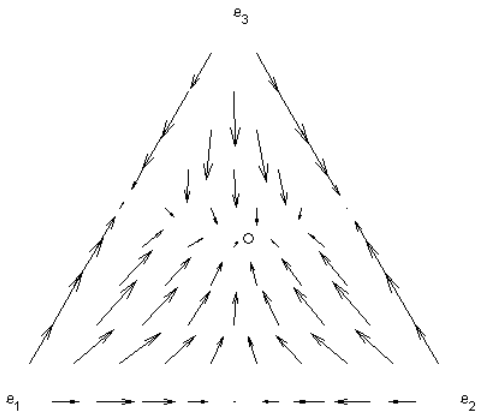


Figure 3.4: The relaxation of evolution in time-variant system

Following subsections will explain how to compose and normalise the payoff of each player from the MOO problem. Moreover, for the implementation of the resultant payoff matrix into the game dynamics, salient issues such as non-existence, singularity, and stability will be discussed.

### 3.3.1 Payoff Matrix

The payoff matrix defined in this research is the same as the payoff matrix commonly used in other MOO methods [25]. As the weightings of an MOO problem are correspondent to the fitness of cost functions in game theory, objective functions comprise the rows and different decision variables are substituted to each column. Therefore, the payoff matrix can be defined with multiple decision variables and criteria as

$$A = \begin{array}{c} \\ f_1 \\ f_2 \\ \vdots \\ f_M \end{array} \begin{array}{c} \begin{array}{cccc} \boldsymbol{x}_1^* & \boldsymbol{x}_2^* & \dots & \boldsymbol{x}_M^* \end{array} \\ \begin{pmatrix} f_1(\boldsymbol{x}_1^*) & f_1(\boldsymbol{x}_2^*) & \dots & f_1(\boldsymbol{x}_M^*) \\ f_2(\boldsymbol{x}_1^*) & f_2(\boldsymbol{x}_2^*) & \dots & f_2(\boldsymbol{x}_M^*) \\ \vdots & \vdots & & \vdots \\ f_M(\boldsymbol{x}_1^*) & f_M(\boldsymbol{x}_2^*) & \dots & f_M(\boldsymbol{x}_M^*) \end{pmatrix} \end{array} \tag{3.4}$$

where $\boldsymbol{x}_i^* \in S$ denotes an *optimal individual* for each cost function $f_i$, and $S$ is a solution space.

Due to the incommensurability issue, the payoff defined in Eqn. (3.4) cannot be directly used. Normalisation of this payoff matrix must be preceded to resolve the incommensurability. Nonlinear normalisation methods, such as the one implemented in another decision making algorithm, TOPSIS (technique for order preference by similarity to an ideal solution) [37], are not under consideration in this research due to their dependency on units. Two commonly used linear normalisation methods are given as

$$A_{ij} = \frac{f_{ij}}{f_i^+} \tag{3.5}$$

$$A_{ij} = \frac{f_{ij} - f_i^-}{f_i^+ - f_i^-} \tag{3.6}$$

where $f_{ij} = f_i(\boldsymbol{x}_j^*)$, $f_i^-$ is the minimum and $f_i^+$ is the maximum value of each cost function. Given the first normalisation method described in Eqn. (3.5), the normalised value $A_{ij}$ becomes less sensitive to the change in the value of the cost function $f_{ij}$ as the maxi-

mum value $f_i^+$ gets larger. Let us suppose the changes in two objectives are the same, but the maximum value of the one objective is much smaller than the other. Then, although the changes in the cost functions are the same, the normalised cost with the smaller maximum value is more stiffly changing compared to the other. From the proposed evolutionary game, it is clear that the more weighting will be selected for the one with the smaller maximum value, which is undesirable. On the other hand, in the normalisation method defined in Eqn. (3.6), the normalised cost is determined only by the unit change in the cost functions. Using this normalisation method, the weightings will be selected by evaluating the relative change in the range between the minimum and maximum values of the cost function, not the absolute scale of the cost function. This coincides with the main idea of the proposed evolutionary game based approach. Therefore, the second normalisation method is utilised in the proposed MOO algorithm, i.e.:

$$\begin{aligned} A &= \{A_{ij}\} \\ A_{ij} &= \frac{f_{ij} - f_i^-}{f_i^+ - f_i^-} \end{aligned} \tag{3.7}$$

### 3.3.2 Evolving Dynamics and Stability

Using the payoff matrix, the fitness on the stable equilibrium evolves in each time step through the game dynamics. Assuming no mutation or recombination process, the resultant fitness is determined only by its initial value. Evolving dynamics of the fitness is defined by the replicator equation as follows [48].

$$\dot{p}_i = p_i(e_i A p^T - p A p^T) \tag{3.8}$$

where $A \in \mathbb{R}_{M\times M}$ is the payoff matrix, and $p \in \mathbb{R}_{1\times M}$ is the fitness for each strategy. Here, $e_i \in \mathbb{R}_{1\times M}$ is a vector with one at the $i^{th}$ element and zeros at the others and $p_i$ denotes the proportion of the $i^{th}$ strategy in the population.

The converging point of fitness after infinite iterations can be estimated analytically.

Without the uncertainties of mutation or recombination, result of the replicator equation is fixed with respect to the initial guess of the fitness. Also, it is proven that there exists at least one Nash equilibrium in any evolutionary game [26]. In order to find Nash equilibrium, two relevant concepts are explored: a rest point and stability. Nash equilibrium is defined as a rest point which is stable whereas strict Nash equilibrium requires the rest point to be asymptotically stable.

First, analytical expression of a rest point, $\bar{p}$, is derived from that the derivative of the game dynamics becomes zero at the point.

$$e_i A \bar{p}^T - \bar{p} A \bar{p}^T = 0 \tag{3.9}$$

Rearranging the equation yields the following relationship.

$$A \bar{p}^T = \bar{p} A \bar{p}^T \mathbf{1}_{n\times 1} = k \mathbf{1}_{n\times 1} \tag{3.10}$$

Using the fact that summation of the weightings is always 1, the solution is computed with an augmented matrix as follows.

$$\begin{pmatrix} \bar{p}^T \\ k \end{pmatrix} = \begin{pmatrix} A & -\mathbf{1}_{n\times 1} \\ \mathbf{1}_{1\times n} & 0 \end{pmatrix}^{-1} \begin{pmatrix} \mathbf{0}_{n\times 1} \\ 1 \end{pmatrix} \tag{3.11}$$

When the augmented matrix is invertible, a single rest point exists for the replicator equation. On the contrary, if the problem is singular, infinitely many equilibria exist. The duplicated rows and columns are reduced to make the matrix full rank. Also, all the components in $\bar{p}$ must be non-negative to stay inside the solution set. Even though the analytical solution of $\bar{p}$ has a negative value, the population does not evolve further to the solution.

Second, a point is stable when the following relationship is accomplished.

$$p^T A p < \bar{p}^T A p \qquad for\ \forall p \quad such\ that \quad p^T A \bar{p} = \bar{p}^T A \bar{p} \tag{3.12}$$

The stability of the dynamics is determined by the eigenvalues of the payoff matrix $A$; real value of more than two eigenvalues must be negative to make the system stable [49]. In the payoff matrix of MOO problems, the diagonal terms are zero after the normalisation and thus stability is always guaranteed.

## 3.4 Trade-Off Analysis

For the validation of MOO methods, it is required to select proper performance indices. Performance of MOO methods is usually evaluated either on the searching methods for the Pareto-optimal set or on the decision-making algorithms. Metrics such as error ratio, set coverage metric, generational distance, and maximum Pareto-optimal front error are relevant to the performance of optimisation methods converging towards the Pareto-optimal front [50]. Distribution along the Pareto-optimal front is assessed by spacing, spread, or chi-square-like deviation measure [50]. Metrics of decision-making algorithms include closeness, uniformity, and consistency, all of which are computed by multiple decision makers and the decision table [51]. As the proposed approach is not not required to find any Pareto-optimal set or decision table, none of these metrics are applicable.

The main purpose of the evolutionary game based approach is to compute the weightings reflecting the trade-off information. The trade-off refers to the relative changes in one cost function with respect to the those in other costs. For the validation, the trade-off information in the proposed approach should be investigated and compared to reference approaches. Note that the concept of trade-off, also known as marginal rate of substitution, is often adopted in interactive methods. Therefore, this research defines a performance index using the trade-off utilised in interactive methods.

Let us discuss about the trade-off in more detail. The trade-off information applied in interactive methods are categorised into two, partial and global trade-off. The partial or local trade-off is an approximation of the slope tangent to the Pareto-optimal. Definition

of the partial trade-off of $f_1$ with respect to $f_2$ and its approximation are given as

$$T_{ij}(\bar{\boldsymbol{x}}) = \frac{f_i(\bar{\boldsymbol{x}}) - f_i(\boldsymbol{x})}{f_j(\bar{\boldsymbol{x}}) - f_j(\boldsymbol{x})} \simeq \frac{\nabla f_i^T(\bar{\boldsymbol{x}})\boldsymbol{d}}{\nabla f_j^T(\bar{\boldsymbol{x}})\boldsymbol{d}} \tag{3.13}$$

where $\boldsymbol{d}$ is a vector of change in decision variables such that $\boldsymbol{x} = \bar{\boldsymbol{x}} + \alpha\boldsymbol{d} \in S$ for a constant $\alpha \geq 0$.

An interactive or *a posteriori* optimisation method using the partial trade-off is suggested by Miettinen [44]. The Miettinen's method computes the objective trade-off information from the structure of the problem with the Karush–Kuhn–Tucker multipliers, and selects a new Pareto-optimal solution with the desirable trade-off specified by the decision maker.

The advantage of using the partial trade-off as a performance index would minimal computational load. The partial trade-off is available as a byproduct of finding the Pareto-optimal set using the Karush–Kuhn–Tucker multipliers. A potential issue is that the desirable partial trade-off must be specified by the decision maker with precision, which is often difficult.

The global trade-off is defined as a limit effect of changing from a given decision along the Pareto-optimal set. Like the partial trade-off, the global trade-off is measured by relative changes in costs. The definition of the global trade-off and its relevant set are given by [47]:

$$T_{ij}(\bar{\boldsymbol{x}}) = \begin{cases} \sup\limits_{\boldsymbol{x} \in S_j^<(\bar{\boldsymbol{x}})} \dfrac{f_i(\boldsymbol{x}) - f_i(\bar{\boldsymbol{x}})}{f_j(\bar{\boldsymbol{x}}) - f_j(\boldsymbol{x})}, & \text{for } S_j^<(\bar{\boldsymbol{x}}) \neq \phi \\ -\infty, & \text{for } S_j^<(\boldsymbol{x}) = \phi \end{cases} \tag{3.14}$$

$$S_j^<(\bar{\boldsymbol{x}}) = \{\boldsymbol{x} \in S | f_j(\boldsymbol{x}) < f_j(\bar{\boldsymbol{x}}),\ f_k(\boldsymbol{x}) \geq f_k(\bar{\boldsymbol{x}}),\ \forall k \neq j\}$$

where $S$ denotes the Pareto-optimal set.

If the solution set is properly efficient, the global trade-off is bounded with system

control parameters. The boundedness is obtained as

$$\begin{cases} T_{ij}(\bar{\boldsymbol{x}}) \leq \frac{\lambda_j+\rho_j}{\rho_i} \\ T_{ji}(\bar{\boldsymbol{x}}) \leq \frac{\lambda_i+\rho_i}{\rho_j} \end{cases} \tag{3.15}$$

where the control parameters $\rho_i$ and $\lambda_i$ mean relative and absolute importance, respectively. If we select the bound of the trade-off as $\beta$, then the following two equations must hold

$$\begin{cases} \frac{\lambda_j+\rho_j}{\rho_i} = \beta_{ij} \\ \frac{\lambda_i+\rho_i}{\rho_j} = \beta_{ji} \end{cases} \tag{3.16}$$

In iterative method, $\lambda_i$ and $\lambda_j$ are determined by the user interactively. Once $\lambda_i$ and $\lambda_j$ are given, we can obtain $\rho_i$ and $\rho_j$ from Eqn. (3.16). Unlike in the partial trade-off, the desirable trade-off doesn't need to be specified with precision, but only its desirable bound, $\beta_{ij}$, is required to be defined. Therefore, this research uses the global trade-off to define a performance index for the validation of the proposed approach.

Note that, as shown in the payoff matrix given in Eqn. (3.4), the absolute importance of each objective is identical. Therefore, for the investigation of the properties of the proposed MOO algorithm, it needs to set to be unity. Furthermore, the bound, $\beta_{ij}$, is the parameter that the user defines interactively by examining the quality of the solution from the current trial decision of $\beta_{ij}$. However, as the proposed evolutionary based approach aims to make the all values of the trade-offs identical to their average, all $\beta_{ij}$'s should be set to be the average of the corresponding trade-offs.

In order to selects a new Pareto-optimal solution meeting the desirable trade-off conditions, iterative approaches generally defines a new optimisation problem: find the solution, $\boldsymbol{x}^*$, which minimises the following cost function

$$\begin{aligned} J(\boldsymbol{x}) = \max_{i,\,j} \{ & (\lambda_i + \rho_i)\left(f_i(\boldsymbol{x}) - f_i(\boldsymbol{x}_i^*)\right) \\ & + \rho_j \left(f_j(\boldsymbol{x}) - f_j(\boldsymbol{x}_j^*)\right) \} \end{aligned} \tag{3.17}$$

while satisfying the boundedness condition of the global trade-offs. The cost in this problem implies the maximum difference between all actual trade-offs and the corresponding bound at the point $\boldsymbol{x}$. Hence, this problem is to minimise this maximum difference that enables to find a point $\boldsymbol{x}$ on the Pareto optimal front where the difference between the actual trade-offs and the bound is minimised. One of the representative examples of using this cost function is Interactive Decision-Making Algorithm (GIDMA) suggested by Kaliszewski [47].

If the proposed evolutionary based approach indeed makes the all values of the trade-offs identical, its solution should be the same as the optimal solution of the optimisation problem whose cost function is given by Eqn. (3.17). Therefore, the performance index in this research can be further defined as

$$PI(\boldsymbol{x}_{EG}) = \left| \frac{J(\boldsymbol{x}_{EG}) - J^*}{J^- - J^*} \right| \tag{3.18}$$

where $J^*$ and $J^-$ denote the cost of the optimal solution obtained by GIDMA and the worst cost, for $\lambda_i = \lambda_j = 1$ and $\beta_{ij} = \mu\left(T_{ij}(\bar{\boldsymbol{x}})\right)$. Here, $\mu\left(T_{ij}(\bar{\boldsymbol{x}})\right)$ denotes the average of the trade-offs $T_{ij}$ over $\bar{\boldsymbol{x}}$. This performance index will be utilised for the validation of the proposed evolutionary game based algorithm.

## 3.5 Validation

In order to validate the performance of the proposed algorithm, this section performs numerical simulations on two types of well-known benchmark problems: static and dynamic. The validation will be conducted by evaluating the performance index defined in Eqn. (3.18) and computation time.

There are various popular test suites for MOO, such as SCH, FON, KUR, POL, and VNT [52]. Most of these benchmark problems focus on the search for Pareto-optimal front and the form of Pareto-optimal front in these test suites may contain distinctive features that are not common in real world problems.

However, the purpose of applying the benchmark problems is to compute the trade-off information, and thus complicated forms or duplicated Pareto-optimal fronts may not be necessary. To this end, three problems of the Zitzler–Deb–Thiele (ZDT) problem set [50] – ZDT1, ZDT2, and ZDT3 – and Miettinen's problem are used in the trade-off analysis are selected as static optimisation test cases. The other problems of the ZDT set – ZDT4, ZDT5, and ZDT6 – are excluded in this research, as these problems are designed to test the performance of the algorithm on finding multiple, thin, and nonuniform Pareto-optimal fronts, respectively. For dynamics optimisation test suites, Deb–Thiele–Laumanns–Zitzler's problem set (DTLZ) [52, 53] is chosen.

### 3.5.1 Benchmark Problems

This subsection introduces formulation of the benchmark problems and analyses the characteristics of the corresponding Pareto-optimal front through visualisation.

ZDT test problems with two objective functions can be formulated with the following structure.

$$\begin{cases} f_1(\boldsymbol{x}) & = f_1(x_1, x_2, \cdots, x_k) \\ f_2(\boldsymbol{x}) & = g(x_{k+1}, \cdots, x_n) \times h(f_1, g) \end{cases}, \qquad k < n \tag{3.19}$$

where the function $f_1$ tests the diversity along the Pareto-optimal front, $g$ tests the convergence to the front, and $h$ determines the shape of the Pareto-optimal front, such as convexity, non-convexity and discontinuity.

The problem ZDT1 has a convex Pareto-optimal set, which is basic and relatively easy to find the Pareto-optimal front. Increasing the number of decision variables, $n$, the test function enables to evaluate the algorithm's capability to handle large number of decision

variables. The relevant functions are defined as follows.

$$\text{ZDT1}: \begin{cases} f_1(\boldsymbol{x}) & = x_1 \\ g(\boldsymbol{x}) & = 1 + \frac{9}{n-1}\sum_{i=2}^{n} x_i \\ h(\boldsymbol{x}) & = 1 - \sqrt{f_1/g} \end{cases} \tag{3.20}$$

Second, ZDT2 has a non-convex Pareto-optimal set so that the simple weighted-sum methods are unable to find the intermediate values of Pareto-optimal solutions. The functions $f_1$, $g$, and $h$ are defined as

$$\text{ZDT2}: \begin{cases} f_1(\boldsymbol{x}) & = x_1 \\ g(\boldsymbol{x}) & = 1 + \frac{9}{n-1}\sum_{i=2}^{n} x_i \\ h(\boldsymbol{x}) & = 1 - (f_1/g)^2 \end{cases} \tag{3.21}$$

Third, the Pareto-optimal set of ZDT3 is discontinuous due to its sine-function in $h$. As the definition of Pareto-optimal set is that all the solutions contained in the set are not strictly dominant to each other, nondominated parts of sine-function are not defined as Pareto-optimal resulting in a discontinuous Pareto-optimal front. The functions are defined as

$$\text{ZDT3}: \begin{cases} f_1(\boldsymbol{x}) & = x_1 \\ g(\boldsymbol{x}) & = 1 + \frac{9}{n-1}\sum_{i=2}^{n} x_i \\ h(\boldsymbol{x}) & = 1 - \sqrt{f_1/g} - (f_1/g)\sin(10\pi f_1) \end{cases} \tag{3.22}$$

The decision variables at the Pareto-optimal front are derived when all the values of $x_2, x_3, \cdots, x_n$ are 0. The solution varies along the Pareto-optimal depending on the value of $x_1$ varying inside its upper and lower bounds.

The Pareto-optimal fronts of ZDT1, ZDT2, and ZDT3 with analytic solutions are shown in Fig. 3.5. The shapes of convex, non-convex, and discontinuous Pareto-optimal fronts are fixed regardless of the number of decision variables. All the decision variables

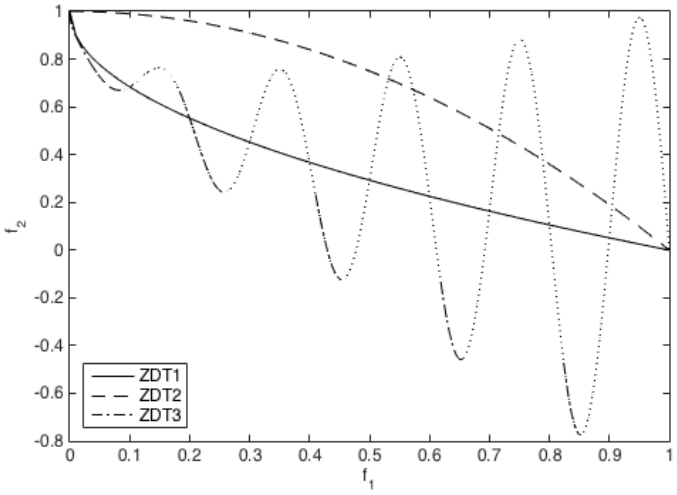


Figure 3.5: The Pareto-optimal fronts of the ZDT problems

are bounded from 0 to 1, and thus the function $f_1$ varies from 0 to 1. From the dotted line of sinusoidal function in ZDT3, only line-dotted parts are defined as Pareto-optimal.

Miettinen's problem is designed to test the trade-off analysis in case of a irregular shape of the Pareto-optimal front in three-dimensional space. The problem incorporates three conflicting objective functions and two decision variables as follows.

Miettinen's problem :

$$\begin{cases} f_1(x_1,x_2) = \phi(x_1,x_2) \\ f_2(x_1,x_2) = \phi(x_1,x_2-1) \\ f_3(x_1,x_2) = \phi(x_1-1,x_2) \\ \psi(x_1,x_2) = x_1^2 + x_2^2 \\ \phi(x_1,x_2) = \psi(x_1,x_2) - \exp(-50\psi(x_1,x_2)) \end{cases} \tag{3.23}$$

The analytic solution of Miettinen's problem is given when the decision variables $x_1$ and $x_2$ satisfy the following inequalities.

$$x_1 \geq 0, \quad x_2 \geq 0, \quad x_1 + x_2 \leq 1 \tag{3.24}$$

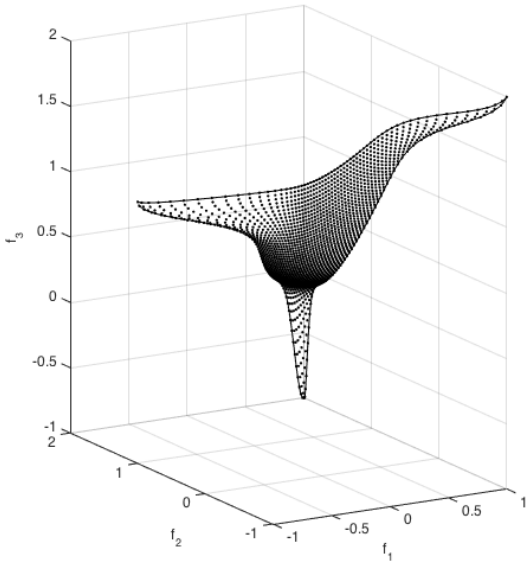


Figure 3.6: The Pareto-optimal front of the Miettinen's problem

The shape of the Pareto-optimal front of the Miettinen's problem is visualised in Fig. 3.6.

The DTLZ test problems can expand the optimisation problem to the general number of objective functions and to the time-variant problem. The formulation is given as

$$\text{DTLZ}: \begin{cases} f_1(\boldsymbol{x}) = (1+g(\boldsymbol{x}_M)+K(t))\cos(\frac{x_1\pi}{2})\cdots\cos(\frac{x_{M-1}\pi}{2}) \\ f_2(\boldsymbol{x}) = (1+g(\boldsymbol{x}_M))\cos(\frac{x_1\pi}{2})\cdots\sin(\frac{x_{M-1}\pi}{2}) \\ \quad\vdots \\ f_M(\boldsymbol{x}) = (1+g(\boldsymbol{x}_M))\sin(\frac{x_1\pi}{2}) \\ g(\boldsymbol{x}_M) = G(t)+\sum_{x\in\boldsymbol{x}_M}(x_i-G(t))^2 \end{cases} \tag{3.25}$$

where $\boldsymbol{x}_M = \{x_M,\cdots,x_n\}$, $n \geq M$, and the functions $G(t)$ and $K(t)$ determine the time-variant properties.

The analytic solutions of the Pareto-optimal front are derived when $\boldsymbol{x}_M$ is zero and $x_1, x_2, \cdots, x_M$ varies from 0 to 1.

The resultant Pareto-optimal front is a circle in two-dimension and a sphere in three

dimensional space, and therefore it is non-convex Pareto-optimal set problem. The radius and eccentricity depends on the time-variant functions $G(t)$ and $K(t)$. The Pareto-optimal front of the three-objective problem is plotted as ellipsoids in Fig. 3.7.

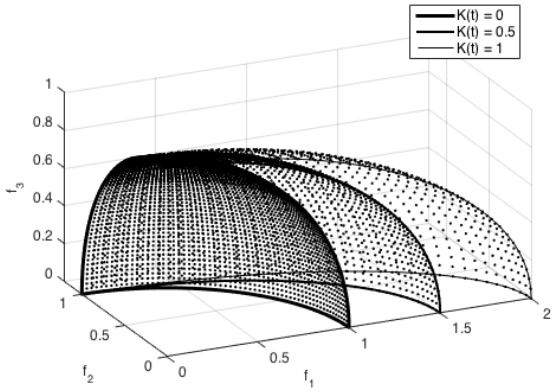


Figure 3.7: The Pareto-optimal fronts of the DTLZ problems

### 3.5.2 Simulation Settings

The optimisation algorithm selected to solve SOO problems is the sequential quadratic programming (SQP) method. As the cost functions are nonlinear and twice continuously differentiable, the SQP algorithm is an efficient solver.

The trade-off analysis is then conducted to evaluate the performance of the proposed approach. The *a posteriori* MOO to find the Pareto-optimal front, of which the trade-off is computed, is handled with the repetitive min-max goal programming approach. In other words, the Pareto-optimal front is found from repeating SOO with different weightings. For a fair comparison, like in the proposed evolutionary game based approach, SQP is used as the solver for each SOO problem.

The evolutionary game based approach requires $(M+1)$ times of single-objective optimisations. On the other hand, the number of single-objective optimisation processes required for obtaining the full Pareto-optimal front is the same as the number of Pareto-optimal solutions, denoted as $N$. If the front is continuous, this number might become infinite. For the fair comparison on the computation time with GIDMA, this number needs

Table 3.1: Benchmark problem simulation parameter specification

| Test Problem | The Number of Objectives ($M$) | The Number of Decision Variables ($n$) |
|---|---|---|
| ZDT1 | 2 | 30 |
| ZDT2 | 2 | 30 |
| ZDT3 | 2 | 30 |
| Miettinen's | 3 | 2 |
| DTLZ2 M3 | 3 | 10 |
| DTLZ2 M4 | 4 | 10 |
| DTLZ2 M5 | 5 | 10 |

to be limited to a reasonable value. In this research, the parameter $N$ is fixed as 100 in two-objective optimisation problems, and approximately 1800 in the others, reflecting the complexity in the shape of the Pareto-optimal front. The computational time is measured directly by the MATLAB built-in function computing the elapsed time. Note that the two algorithms are tested in Matlab 2016a and the specification of the machine run the algorithms is OS X 2.8 GHz Mac mini with 16 GB RAM. The absolute elapsed time varies depending on the specification of the machine, but the relative time consumed for each algorithm could be useful for the computation time comparison.

The number of objectives and variables of each benchmark problem are specified and summarised in Table 3.1. It is worth to note that the Pareto-optimal front is determined only by $k$ number of decision variables, where $k = M - 1$, in all the benchmark problems. If exists, the number of elements of the set $\boldsymbol{x}_M$ determines the computational complexity in finding the Pareto-optimal front.

### 3.5.3 Simulation Results

#### Time-invariant weighting determination

For time-invariant systems, the ZDT test suites, the Miettinen's problem, and DTLZ tests with $G(t) = 0$ and $K(t) = 0.5$ are considered.

The performance comparison results are summarised in Table 3.2. In the table, PI denotes the performance index given in Eqn. (3.18). The Pareto-optimal front and the

Table 3.2: Performance of time-invariant optimisation

| Test Problem | PI | The Computation Time (sec) | |
|---|---|---|---|
| | | GIDMA | EGT |
| ZDT1 | 0.0346 | 5.93 | 0.747 |
| ZDT2 | 0.0041 | 6.228 | 0.769 |
| ZDT3 | 7.8386e-4 | 12.823 | 0.821 |
| Miettinen's | 0.2553 | 43.198 | 0.679 |
| DTLZ2 M3 | 0.0128 | 45.287 | 1.22 |
| DTLZ2 M4 | 0.0835 | 95.371 | 1.23 |

correspondent trade-off along the $f_1$ axis in ZDT problems suites is given in Fig. 3.8. The scale of the objective function $f_2$ is plotted on the left y-axis and that of normalised trade-off on the right y-axis. The two-objective optimisation problems yields a payoff matrix with 0's at the diagonal terms and 1's at the off-diagonal terms, which implies that the resultant weightings are just even. Although the evolutionary game based approach and its weightings are simple, the result of EGMOO is almost the same with the solution found by GIDMA in ZDT2 and ZDT3. As stated in Section 3.4, the solution found by GIDMA is considered as the optimal solution in the trade-off analysis. Note that Regarding the result for ZDT1, it seems the difference in the solutions is graphically large. However, as shown in the Table 3.2, the PI remains small, that is around 3.5%.

The Miettinen's problem shows more irregular pattern in both Pareto-optimal front and the trade-off along $f_1$ and $f_2$ axis as shown in Fig. 3.9 (a). As the Pareto-optimal front is asymmetric, the solution of EGT is located approximately in the centre of the Pareto-optimal front, whereas the GIDMA solution is placed at the lower edges of the Pareto-optimal front. As represented in Table 3.2, the error represented by PI is still around 25.53%.

In DTLZ problems, the evolutionary stable solution tends to provide the optimal solution confirming the trade-off analysis results. Note that although the trade-off error represented by PI remains small, it becomes larger as the dimension of the problem increases in the DTLZ benchmark problem. For visualisation, the results of the three-objective problem in the DTLZ set, DTLZ2 M3, are depicted in Fig. 3.9 (b). Even though the problem

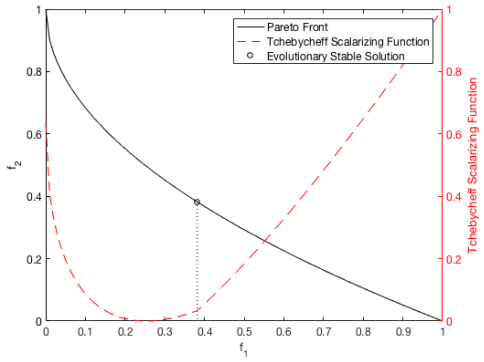


(a) ZDT1

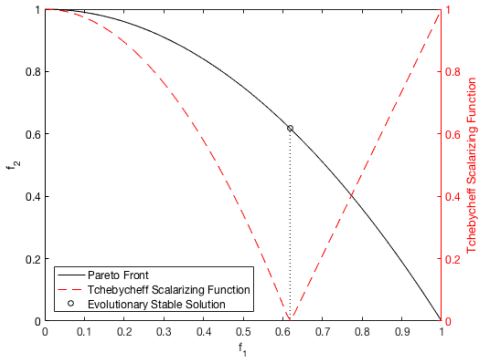


(b) ZDT2

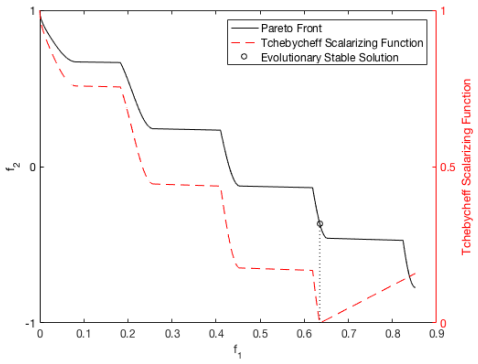


(c) ZDT3

Figure 3.8: The evolutionary stable solution and its trade-off in the ZDT problems

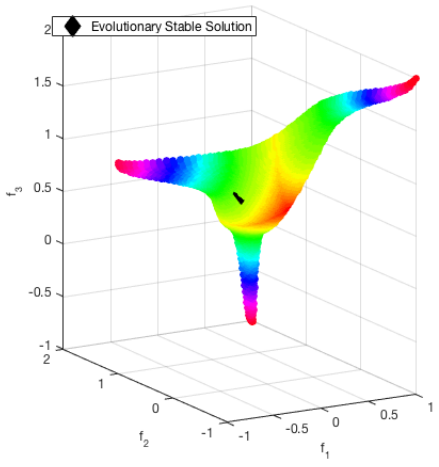


(a) Miettinen's

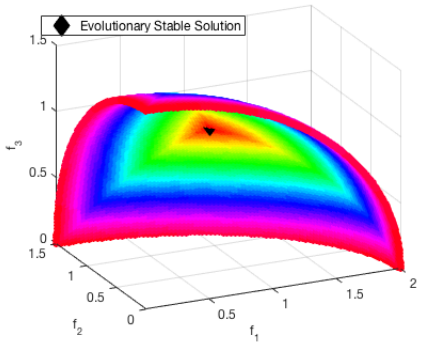


(b) DTLZ2 M3

Figure 3.9: The evolutionary stable solution and its trade-off in the Miettinen's and DTLZ2 M3 problem

has a ellipsoidal Pareto-optimal front, which is not exactly symmetric, EGMOO results in a solution close to the GIDMA solution.

The simulation results for the trade-offs in general confirm that the trade-off analysis of the proposed approach is valid regardless of convexity or non-convexity of the Pareto-optimal front: the proposed approach determines the weightings that can provide an MOO solution whose trade-offs become identical.

Now, let us investigate the performance of the proposed evolutionary game based approach on the computational time, compared with that of GIDMA. The results on the computational time are again summarised in Table 3.2. The computational time exponentially increases as the complexity in the size and shape of the Pareto-optimal front increases in GIDMA. On the contrary, EGMOO provides relatively consistent computational time while providing the similar results to GIDMA. This implies that, for the MOO problems which require time-critical decision making, EGMOO is much more appropriate to be implemented.

**Time-variant weighting determination**

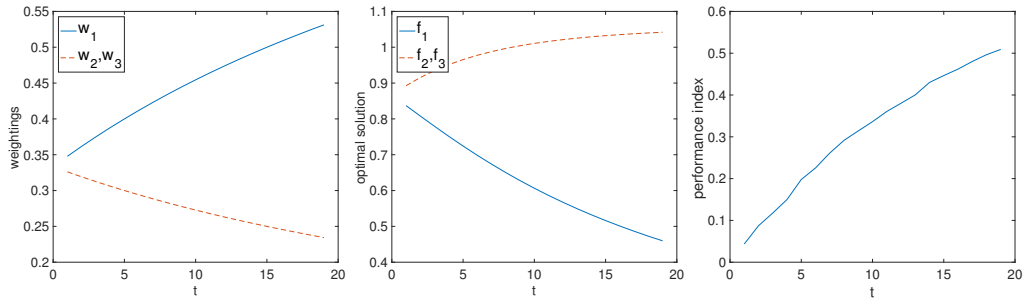


Figure 3.10: The weightings and evolutionary stable solution at time-variant systems

The time-variant systems are considered to observe the weightings dynamically determined by the evolutionary game based approach. The DTLZ problem is linearly varied with the function from $K(t) = 0$ to $K(t) = 1$.

In Fig. 3.10, the weightings of each cost function and the resultant cost of the optimisation is plotted. The weightings of the function $f_1$ increase as the radius along the $f_1$ axis

increases from 1 to 2, while the other weightings are the same as the formulation is symmetric. When the problem is extended to $M = 4$ and $M = 5$, the ratio of the weightings is maintained but the scale is normalised to match the summation with 1. Subsequently, the cost of $f_1$ increases more rapidly than that of the other objectives even considering that the overall scale of $f_1$ is expanding in double. The average cost over the time span is 0.0320 and the whole computation time is 1.792 sec, which is fairly short considering that the trade-off analysis take 5.223 sec.

## 3.6 Conclusions

This chapter develops an a priori approach for MOO problems involving dynamically evolving systems and/or time-critical systems. A main challenge with *a priori* methods is how to determine the user-defined preference information, i.e. how to aggregate the multiple objectives into a single objective function [34]. Therefore, determination of the weightings of objectives is of paramount in *a priori* methods. This chapter formulates this determination problem as an evolutionary game of *optimal individuals* and obtains the weightings by solving this game. Note that each *optimal individual* is defined as the optimal solution of the single objective optimisation problem with each objective. In the game, to mitigate the stiffness of the weighted-sum of the cost functions on the Nash equilibrium point, less fitness is assigned on more stiffly changing strategy. Since the purpose of decision making on the weightings is exactly opposite, the proposed approach assigns more weighting to the objective function with less fitness. This research also investigates the properties of the proposed evolutionary game based approach by theoretical analysis including trade-off analysis. Here, the trade-off, also known as marginal rate of substitution, refers to the relative changes in one cost function with respect to the those in other costs and is a common concept used in MOO approaches. The analysis results suggest that the proposed evolutionary game based approach finds weightings such that the trade-offs at a MOO solution becomes identical to their mean value. We also per-

form numerical simulations with well-known benchmark problems in MOO to validate the analysis results. The simulation results confirm that the proposed approach makes the trade-offs of each weighted objective identical to the mean at its solution. Moreover, they also show that the computational time of the evolutionary game based approach is in general consistent regardless the complexity of the problem. This indicates that the proposed approach can be indeed applied to MOO problems involving dynamically evolving or time-critical systems.

# References

[21] C. Leboucher, H. S. Shin, S. Le Menec, A. Tsourdos, A. Kotenkoff, P. Siarry, and R. Chelouah. "Novel Evolutionary Game Based Multi-Objective Optimisation for Dynamic Weapon Target Assignment". In: *the 19th World Congress The International Federation of Automatic Control* 2010 (2014), pp. 3936–3941.

[25] M. Kok. "A Note on the Pay-off Matrix in Multiple Objective Programming". In: *European Journal of Operational Research* 26.1 (1986), pp. 96–107.

[26] J. Hofbauer and K. Sigmund. "Evolutionary Game Dynamics". In: *Bulletin of the Anerican Mathematical Society* 40.4 (2003), pp. 479–519.

[28] R. T. Marler and J. S. Arora. "Survey of multi-objective optimization methods for engineering". In: *Structural and Multidisciplinary Optimization* 26.6 (2004), pp. 369–395.

[29] T. Stewart, O. Bandte, H. Braun, N. Chakraborti, M. Ehrgott, M. Göbelt, Y. Jin, H. Nakayama, S. Poles, and D. Di Stefano. "Real-world applications of multiobjective optimization". In: *Multiobjective Optimization: Interactive and Evolutionary Approaches*. Springer, 2008, pp. 285–327.

[30] P. Korhonen. "Multiple objective programming support". In: *Encyclopedia of optimization* (2009), pp. 2503–2511.

[31] Y. Collette and P. Siarry. *Multiobjective Optimization: Principles and Case Studies*. Springer, 2003, p. 315.

[32] C.-L. Hwang and A. S. M. Masud. *Multiple Objective Decision Making - Methods and Applications*. Springer Berlin Heidelberg, 1979, p. 357.

[33] V. Changkong and Y. Y. Haimes. *Multiobjective decision making theory and methodology*. New York: Elsevier Science Publishing Co., Inc., 1983.

[34] K. Deb. "Classical Methods". In: *Multi-objective optimization using evolutionary algorithms*. John Wiley & Sons, LTD., 2011, pp. 47–75.

[35] T. W. Athan and P. Y. Papalambros. "A note on weighted criteria methods for compromise solutions in multi-objective optimization". In: *Engineering Optimization* 27.2 (1996), pp. 155–176.

[36] A. Messac. "From dubious construction of objective functions to the application of physical programming". In: *AIAA Journal* 38.1 (2000), pp. 155–163.

[37] S. Opricovic and G. H. Tzeng. "Compromise solution by MCDM methods: A comparative analysis of VIKOR and TOPSIS". In: *European Journal of Operational Research* 156.2 (2004), pp. 445–455.

[38] H. Mausser. "Normalization and Other Topics in Multi Objective Optimization". In: *Proceedings of the Fields-MITACS Industrial Problems Workshop* (2006), pp. 89–101.

[39] K. Miettinen. *Nonlinear multiobjective optimization*. Vol. 12. Springer US, 1999, p. 320.

[40] S. Zionts. "The Interactive Surrogate Worth Trade-Off (ISWT) Method for Multiobjective Decision-Making". In: *Lecture Notes in Economics and Mathematical Systems*. Springer Berlin Heidelberg, 1978, pp. 42–47.

[41] M. Sakawa. “Interactive Multiobjective Optimization by the Sequential Proxy Optimization Technique (SPOT)”. In: *IEEE Transactions on Reliability* R-31.5 (1982), pp. 386–396.

[42] J.-B. Yang. “Gradient projection and local region search for multiobjective optimisation”. In: *European Journal of Operational Research* 112.2 (1999), pp. 432–459.

[43] M. Sakawa and H. Yano. “Trade-off rates in the hyperplane method for multiobjective optimization problems”. In: *European Journal of Operational Research* 44.1 (1990), pp. 105–118.

[44] P. Eskelinen and K. Miettinen. “Trade-off analysis approach for interactive nonlinear multiobjective optimization”. In: *OR Spectrum* 34.4 (2011), pp. 803–816.

[45] I. Kaliszewski and W. Michalowski. “Efficient Solutions and Bounds on Tradeoffs 1,2”. In: *Optimization* 94.2 (1997), pp. 381–394.

[46] S. Zionts. “A multiple criteria method for choosing among discrete alternatives”. In: *European Journal of Operational Research* 7.2 (1981), pp. 143–147.

[47] I. Kaliszewski. “Using trade-off information in decision-making algorithms”. In: *Computers & Operations Research* 27.May 1998 (2000), pp. 161–182.

[48] M. Pelillo. “Replicator equations, maximal cliques, and graph isomorphism.” In: *Neural computation* 11.8 (1999), pp. 1933–1955.

[49] H. Ohtsuki and M. Nowak. “The replicator equation on graphs”. In: *Journal of Theoretical Biology* 243.1 (2006), pp. 86–97.

[50] K. Deb. “Salient Issues of Multi-Objective Evolutionary Algorithms”. In: *Multi-objective optimization using evolutionary algorithms*. John Wiley & Sons, LTD., 2011, pp. 324–370.

[51] J. Pang and J. Liang. “Evaluation of the results of multi-attribute group decision-making with linguistic information”. In: *Omega* 40.3 (2012), pp. 294–301.

[52] K. Deb, L. Thiele, M. Laumanns, and E. Zitzler. “Scalable Multi-Objective Optimization Test Problems”. In: *Proceedings of the Congress on Evolutionary Computation (CEC-2002)* 2 (2002), pp. 825–830.

[53] M. Farina, K. Deb, and P. Amato. “Dynamic Multiobjective Optimization Problems: Test Cases Approximation and Applications”. In: *IEEE Transactions on Evolutionary Computation* 8.5 (2004), pp. 311–326.

# Chapter 4

# Analysis on the Networked Multi-Agent System with Communication Constraints

## Abstract

In this chapter, a new analysis method on the multi-agent system is proposed to evaluate the robustness and performance of the networked control. The main idea is to model the networked control system as a multi-output-multi-input transfer function and to apply the robustness and performance metrics defined in linear control theory. The strength of this problem formulation is the applicability for general agent dynamics, controllers, and communication characteristics, extending its potential feasibility. This chapter defines the stability of the networked system, its robustness metric against uncertainties, and the performance metric for reference input tracking. The case studies with first-, second-, and higher order dynamics show the theoretical effects of network topology and agent dynamics on the robustness, and as a result, a trade-off between the robustness and performance metrics is suggested. The numerical simulations verify the analysis results of the case studies.

## 4.1 Introduction

The operation of the networked multi-agent systems is getting increasing attention for its versatile applications: unmanned aerial vehicles (UAVs), mobile sensor networks, automated highway systems, etc. [14] However, there have been not many works considering the communication constraints on the control of agents, despite their influence on the stability of the networked control system. The communication is limited in its capacity, delayed, and often incorporates incorrect information, but analysing their effect on the control system is challenging for its stochastic and finite-field dynamics.

Previous studies have coped with this issue by defining the difference between the real and transmitted states as the unknown perturbation. Under the assumption that the perturbed error is bounded, the necessary and sufficient conditions for the closed-loop stability were obtained [54]. In order to specify the communication constraints, Lin *et al.* [55] proposed that the stability is mainly influenced by the time delay and the major source of the communication delay is the accessing delay, which is constant in some protocols such as time division multiple access (TDMA) protocols [56]. Assuming the constant delay, the stability analysis is more detailed. By augmenting the state-space representation with the delayed states, either the location of the closed-loop poles [57] or the Schur stability [58, 59, 55] of the system matrix was evaluated. Tan and Liu [60] applied the Schur stability of the networked system to a consensus problem, and Schwager *et al.* [61, 62] provided a detailed implementation on quad-rotor UAVs, with an analytic solution of the stability conditions for a first- and second-order agent dynamics. For the first-order consensus problem, the analysis has been extended to time-varying delays using Lyapunov stability [63].

This chapter proposes a generalised analysis framework on the networked multi-agent system that can consider the effects of general agent and communication dynamics on the robustness and performance. A key idea of the approach is that if the communication dynamics can be modelled as a transfer function, such as the time delay as exponential function and the data rate as zero-order-holder, any analysis tool in linear control theory

can be applied. In [64], a similar approach has been taken for a first-order agent dynamics to analyse the effect of time delay, which has been assumed to be identical in every control input. In this research, the applicability of the analysis framework is extended to general agent and communication dynamics, and its analysis metrics include stability margin and tracking performance evaluation.

The problem formulation is generalised to consider the effects of higher-order agent dynamics including physical interconnections among the agents, and of the accessing delay that is a potential cause of destabilising the network. The stability of the networked multi-agent system is defined with Routh–Hurwitz and Nyquist criterion to evaluate the margins of gain/phase variation and time delay that do not destabilise the system. Here, the stability margin of the networked multi-agent system necessarily involves multi-input-multi-output (MIMO) transfer function analysis, of which the earlier concept has been proposed by Kim [65]. The stability margin is extended to consider simultaneous gain and phase variation, and the effects of communication network topology and agent dynamics on the margin are detailed in this research. The sensitivity function is also evaluated to quantify the reference tracking performance. The analysis results on first- and second-order agent dynamics are compared with the previous works in [61, 64], which are partly consistent with this work. The analysis, in this chapter, is not limited to simple agent dynamics but extended to higher-order systems, revealing the physical insights on which network topology and system dynamics is beneficial for the robustness and performance. The analysis results are validated through numerical simulations.

## 4.2 Problem Formulation

The block diagram of the networked system with three agents is shown in Fig. 4.1. The whole network is mainly composed of two parts: the agent dynamics with its controller and observer, and the communication dynamics. The agent dynamics, including the possible interconnections among the agents, is denoted as $G(s) \in \mathbb{R}^{n\times m}$. The outputs are

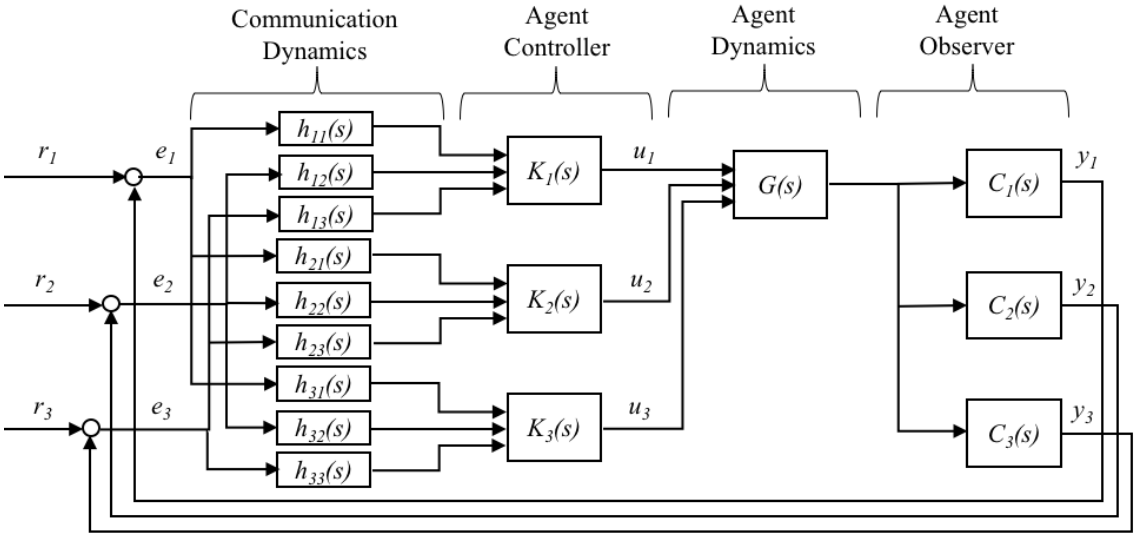


Figure 4.1: Block diagram of the networked control system

obtained in each agent with its transfer function $C_i(s) \in \mathbb{R}^{l_i \times n}$. The difference between the reference inputs $r_i(t) \in \mathbb{R}^{l_i}$ and the observed outputs $y_i(t) \in \mathbb{R}^{l_i}$, denoted as $e(t) \in \mathbb{R}^{l_i}$, is transmitted from $j$-th to $i$-th agent through the communication dynamics $h_{ij}(s) \in \mathbb{R}$. Each agent computes its control input $u_i(t) \in \mathbb{R}^{m_i}$ based on the received outputs with the transfer function $K_i(s) \in \mathbb{R}^{m_i \times l}$. Formulation of each transfer function and the closed-loop dynamics is discussed in this section.

### 4.2.1 Agent Dynamics

Consider a state-space representation for the networked agent dynamics as:

$$\dot{x}(t) = Ax(t) + Bu(t), \tag{4.1}$$

where the system matrices $A \in \mathbb{R}^{n \times n}$ and $B \in \mathbb{R}^{n \times m}$ are assumed to be constant and controllable. Then, the transfer function of the MIMO system is given as:

$$G(s) = (sI_n - A)^{-1}B, \tag{4.2}$$

**Algorithm 1:** $\mathscr{N}$-hop flooding algorithm (implemented by robot $i$)

**Require:** *Robot i has a clock t synchronised with the rest of the robots in the network.*
initialise $\hat{y}_{ii} = y_i(0)$ and $\tau_{ii} = 0$;
initialise $\hat{y}_{ij} = 0$ and $\tau_{ij} = \infty$ for $j \neq i$;
initialise $\hat{y}_{ij}^{\min} = 0$ and $\tau_{ij}^{\min} = \infty$ for $j \neq i$;
**for** $t = 0$ *to* $\infty$ **do**
  **if** *it is robot i's turn to broadcast* **then**
    broadcast $\hat{y}_i = [\hat{y}_{i1}^T \cdots \hat{y}_{iN}^T]^T$;
    broadcast $\tau_i = [\tau_{i1} \cdots \tau_{iN}]^T$;
  **end**
  **else if** *broadcast received from robot k with* $\hat{y}_k$ *and* $\tau_k$ **then**
    **for** $j = 1$ *to* $N$ **do**
      **if** $\tau_{kj} < \mathscr{N}$ *and* $\tau_{kj} < \tau_{ij}^{\min}$ **then**
        update $\hat{y}_{ij}^{\min} = \hat{y}_{kj}$ and $\tau_{ij}^{\min} = \tau_{kj}$;
      **end**
    **end**
  **end**
  update $\hat{y}_{ii} = y_i(t)$ and $\tau_{ij}^{\min} = \tau_{ij}^{\min} + 1$ for $j \neq i$;
  update $\hat{y}_{ij} = \hat{y}_{ij}^{\min}$ and $\tau_{ij} = \tau_{ij}^{\min}$ for $j \neq i$;
**end**

where $I_n \in \mathbb{R}^{n \times n}$ is the identity matrix. The control law for each vehicle $i$ is assumed to be linear as:

$$U_i(s) = -K_i(s)\Big[h_{i1}(s)Y_1^T(s), \cdots, h_{iN}(s)Y_N^T(s)\Big]^T, \tag{4.3}$$

where the capital letters $U_i(s)$ and $Y_i(s)$ denote the Laplace transforms of $u_i(t)$ and $y_i(t)$, respectively. The observed states $Y_i(s)$ are obtained with the observers as:

$$Y_i(s) = C_i(s)X(s), \tag{4.4}$$

where $X(s)$ is the Laplace transform of $x(t)$.

### 4.2.2 Communication Dynamics

The network protocol using the flooding algorithm is considered for its physical applicability. The main idea of the flooding algorithm is that each agent copies the outdated

outputs. Each agent takes turn to broadcast its output, while the others receive it to avoid the interference. The time slot is allocated equally by time $T$, similar to TDMA protocol. After all the agents take their turns, the networked agents have the outdated outputs of the connected agents with different time delays. The flooding algorithm thus enables the multi-hop communication with constant delays proportional to the time slot $T$ and the number of minimum turns to transmit the data from $j$-th to $i$-th agent as $\tau_{ij}$. The detailed flooding algorithm is shown in Algorithm 1, which is a modified algorithm of [61] to consider $\mathscr{N}$-hop communication.

The delayed communication is modelled as:

$$h_{ij}(s) = e^{-\tau_{ij}Ts}. \tag{4.5}$$

The exponential function complicates the characteristic equation, and the closed-loop transfer function has a non-causality issue. To analyse the stability, the delay is approximated to a rational function with Pade approximation as:

$$h_{ij}(s) \simeq \frac{1-\tau_{ij}Ts/2}{1+\tau_{ij}Ts/2}. \tag{4.6}$$

### 4.2.3 Networked Dynamics

The open-loop transfer function of the whole networked system is derived from Fig. 4.1 as:

$$G_{OL}(s) = C(s)G(s)(K(s) \circ H(s)), \tag{4.7}$$

where $\circ$ is the Hadamard product, and the augmented matrices are defined as:

$$\begin{aligned} C(s) &= [C_1^T(s), \cdots, C_N^T(s)]^T \in \mathbb{R}^{l \times n} \\ K(s) &= [K_1^T(s), \cdots, K_N^T(s)]^T \in \mathbb{R}^{m \times l} \\ H(s) &= \begin{bmatrix} h_{11}(s)\mathbf{1}_{m_1 \times l_1} & \cdots & h_{1N}(s)\mathbf{1}_{m_1 \times l_N} \\ \vdots & \ddots & \vdots \\ h_{N1}(s)\mathbf{1}_{m_N \times l_1} & \cdots & h_{NN}(s)\mathbf{1}_{m_N \times l_N} \end{bmatrix} \\ &\in \mathbb{R}^{m \times l} \end{aligned} \tag{4.8}$$

The corresponding MIMO closed-loop transfer function from the reference input to the system states is

$$G_{CL}(s) = (I_l + G_{OL}(s))^{-1} G_{OL}(s). \tag{4.9}$$

If the dynamics of each agent is identical with the same system matrices $A_I$ and $B_I$, the agents are not interconnected with others, i.e. $n = Nn_i$, and the communication dynamics is negligible, i.e. $H(s) = \mathbf{1}_{m \times l}$, the open-loop transfer function is simplified as:

$$G_{OL}^*(s) = L \otimes (C_I(s) G_I(s) K_I(s)), \tag{4.10}$$

where $L \in \mathbb{R}^{N \times N}$ is the Laplacian matrix of a graph, $\otimes$ stands for the Kronecker product, $K_I(s) \in \mathbb{R}^{m_i \times l_i}$ is the control of each agent, $C_I(s)\mathbb{R}^{l_i \times n_i}$ is the observer of each agent, and $G_I(s) \in \mathbb{R}^{n_i \times m_i}$ is the dynamics of each agent as:

$$G_I(s) = (sI_{n_i} - A_I)^{-1} B_I. \tag{4.11}$$

This simplified model is widely used in formation control, synchronisation, and consensus problems where the relative values between the agents are controlled. Despite the restrictive assumptions, it is worth analysing for its simplicity in showing a direct effect of the network topology on the system transfer function.

Note that the characteristics of a network topology is commonly represented with its

Laplacian matrix in network theory. The Laplacian matrix is defined as:

$$L = [l_{ij}], \quad l_{ij} = \begin{cases} \sum_{k=1}^{n} a_{ik}, & j = i \\ -a_{ij}, & j \neq i. \end{cases}, \tag{4.12}$$

where $a_{ij}$ is the elements of the adjacency matrix, representing the degrees from node $i$ to $j$. The eigenvalues of the Laplacian matrix infer to important characteristics of a network topology, such as connectivity and cyclic network, which is detailed along with its relationship on the networked system in Section 4.3.

## 4.3 Analysis Metrics

### 4.3.1 Stability

Two major criteria for the robustness and performance of the networked system are defined for analysis. Prior to evaluating the robustness of the system stability against uncertainties, disturbances, etc., the stability of the networked multi-agent system needs to be clarified.

**Definition 1** (Asymptotic stability)**.** *Suppose an equilibrium $x_e$ such that $Ax_e = 0$.*

- *The equilibrium $x_e$ is Lyapunov stable, if there exists a $\delta > 0$ such that, if $||x(0) - x_e|| < \delta$, then $||x(t) - x_e|| < \varepsilon$ for all $t \geq 0$.*
- *The equilibrium $x_e$ is asymptotically stable, if it is Lyapunov stable and there exists $\delta > 0$ such that, if $||x(0) - x_e|| < \delta$, then $\lim_{t \to \infty} ||x(t) - x_e|| = 0$.*

Regarding the equilibrium at the origin, i.e. $x_e = 0$, either the Routh–Hurwitz stability criterion or the Nyquist criterion states the sufficient and necessary condition for a linear time invariant system to be asymptotically stable. The criterions stated in [66] and [67] are used respectively.

**Lemma 1** (Routh–Hurwitz stability criterion)**.** *For a linear system $\dot{x}(t) = Ax(t)$, the equilibrium $x(t) = 0$ is asymptotically stable if and only if*

$$Re(\lambda) < 0, \quad \forall \lambda \in \lambda(A), \tag{4.13}$$

*where $Re(\cdot)$ is the real part of a value, and $\lambda(\cdot)$ denotes a set of eigenvalues of a matrix.*

**Lemma 2** (Nyquist criterion)**.** *Let $\Re(0, I_l + G_{OL}(s), \Omega_R)$ be the number of clockwise encirclements of the point 0 by the locus of $I_l + G_{OL}(s)$ as $s$ traverses the closed contour $\Omega_R$ in the complex plane in a clockwise sense. The Nyquist criterion states that a closed-loop system is asymptotically stable with respect to the origin if and only if the following equation is satisfied:*

$$\Re(0, I_l + G_{OL}(s), \Omega_R) = -P, \tag{4.14}$$

*where $P$ is the number of CRHP zeros of $G_{OL}(s)$, and the Nyquist contour $\Omega_R$ avoids imaginary zeros of $G_{OL}(s)$ by indentations of radius $1/R$.*

Using Lemma 1, proving the sufficient condition for the asymptotic stability of the networked system is straightforward.

**Theorem 1** (Asymptotic stability of the networked system)**.** *Suppose a networked system of the identical agents without physical coupling, the relative states of which are controlled with linear control $u(t) = -(L \otimes K_I)(x(t) - r)$. The states of the networked system, $x(t)$, asymptotically converge to the reference inputs $r$ if*

$$Re(\lambda) < 0, \quad \forall \lambda \in \lambda(A_I). \tag{4.15}$$

*Proof.* Define the error between the states and reference inputs as $e(t) \triangleq x(t) - r$. The error dynamics is obtained as:

$$\dot{e}(t) = A_r e(t) + B_r r(t) \tag{4.16}$$

where $A_r = A - B(L \otimes K_I)$.

The eigenvalues of the system matrix $A_r$ are obtained as:

$$\begin{aligned} \lambda(A_r) &= \lambda\left(I_N \otimes A_I - (I_N \otimes B_I)(L \otimes K_I)\right) \\ &= \lambda(A_I - L \otimes B_I K_I). \end{aligned} \tag{4.17}$$

From the properties of the Kronecker product, the eigenvalues can be decomposed as:

$$\begin{aligned} \lambda(A_r) \subseteq \Big\{ & \lambda_A - \lambda_L \lambda_{BK} \Big| \\ & \lambda_A \in \lambda(A_I), \lambda_L \in \lambda(L), \lambda_{BK} \in \lambda(B_I K_I) \Big\}. \end{aligned} \tag{4.18}$$

As the minimum eigenvalue of the graph Laplacian is 0, from Lemma 1, the equilibrium $e(t) = 0$ is asymptotically stable if

$$Re(\lambda) < 0, \quad \forall \lambda \in \lambda(A_I). \tag{4.19}$$

□

Note that the condition for asymptotic stability in Theorem 1 is restrictive. For instance, consider a networked system with $A_I = 0$ and $B_I = 1$, which does not satisfy the sufficient condition in Theorem 1. According to Definition 1, the networked system is asymptotically stable with respect to a set of equilibria $x(t) = \{\beta \mathbf{1}_{n\times 1} | \beta \in \mathbb{R}\}$ if the rank of the Laplacian is $N-1$ [68]. In case the relative states are considered important, such as formation control, consensus, and synchronisation problems, the networked system asymptotically solves the problem even with $A_I = 0$. Theorem 1 is applied for the reference tracking problems only, but provides a direct linkage with the robustness analysis in linear control theory.

### 4.3.2 Robustness

In linear control theory, the robustness of the stability is usually represented as stability margins – gain and phase margin. Unlike the classical stability margins of single-input-single-output (SISO) system, the stability margins of a multi-variable system involve both lower and upper bounds of the gain and phase variation as the following definition.

**Definition 2** (Stability margin in MIMO system)**.** *Given $GM_1$ and $GM_2$, any gains, $GM_1 < \gamma_i < GM_2$, inserted in the feedback loops either simultaneously or independently will not destabilise the closed-loop system. Similarly for $PM_1$ and $PM_2$, every loop may have a phase factor $e^{j\phi_i}$ with $PM_1 < \phi_i < PM_2$ and the system will remain closed-loop stable.*

Based on Lemma 2, the values of GM's and PM's are obtained by computing the minimum distance of the matrix $I_l + G_{OL}(s)$ from the singularity. Disk margin defines a disk such that any simultaneous phase and gain variations do destabilise the system if the perturbations remain inside the disk [15, 69]. The resultant GM's and PM's are symmetric, in case the characteristics of either the system or uncertainty is not known.

**Lemma 3** (Disk margin)**.** *Define a constant $\alpha(\omega)$ as:*

$$\alpha(\omega) = \frac{1}{\mu((I_l - G_{OL}(j\omega))(I_l + G_{OL}(j\omega))^{-1})}, \tag{4.20}$$

*where $\mu(\cdot)$ is defined as:*

$$\mu(M) = 1/\min_{\Delta}\{\bar{\sigma}(\Delta) : \det(I_l + M\Delta) = 0\}. \tag{4.21}$$

*Then, the gain and phase margins are guaranteed by*

$$GM = \frac{1 \mp \alpha^*}{1 \pm \alpha^*}, \quad PM = \pm 2\tan^{-1}\alpha^*, \tag{4.22}$$

*where $\alpha^* = \min_\omega \alpha(\omega)$.*

Here, the $\mu$-synthesis can specify the structure of uncertainty $\Delta$ [70]. If the uncertainty is diagonal, i.e. no coupling between the agents' uncertainties, $\mu(M)$ is the same as the size of maximum eigenvalue, $\max|\lambda(M)|$. With its off-diagonal terms, the value is upper bounded by the maximum singular value, $\bar{\sigma}(M)$. In the networked system, the uncertainty in the control $u(t)$ is contributed not only by its own model uncertainties and measurement errors, but also by the uncertainties of the connected agents and transmission errors between them. The stability margin from $\mu$-synthesis is therefore approximated to the eigenvalue when there is no interaction between any agents' control input, while the margin may decrease to singular value with the presence of interaction among all the agents' control.

Assuming there is no physical interconnection between the agents, the stability margin can be expressed as a function of $\lambda(L)$ and $\lambda(G_I(s))$ as the following theorem.

**Theorem 2** (Stability margin of the networked system)**.** *Suppose a networked system of the identical agents without physical coupling. The disk margin of the networked system is obtained as:*

$$\begin{aligned}\alpha(\omega) &= \min|\lambda((I_l + G^*_{OL}(j\omega))(I_l - G^*_{OL}(j\omega))^{-1})| \\ &= \min\Big\{|1+\lambda_L\lambda_G|/|1-\lambda_L\lambda_G|\Big| \\ &\qquad \lambda_L \in \lambda(L), \lambda_G \in \lambda(G_I(j\omega))\Big\}.\end{aligned} \tag{4.23}$$

Based on that the delay is mainly caused by the media accessing time, the delay is applied on each channel depending on the geodesic distance from the receiving to the transmitting agent, and does not effect on the agent itself. The delay margin is thus defined differently from the phase margin by

$$DM = \arg_T \det(I_l + G_{OL}(s)) = 0. \tag{4.24}$$

### 4.3.3 Performance

The reference tracking performance is evaluated through the sensitivity function defined as:

$$|S(s)| = \frac{1}{\underline{\sigma}(I_l + G_{OL}(s))}, \tag{4.25}$$

where $\underline{\sigma}(\cdot)$ is the minimum singular value of a matrix.

For improving the tracking performance, it is desirable to have a small value of $|S(s)|$ over low frequency domain. The following remark states the main characteristics of the sensitivity function in the networked system.

**Remark 1.** *For the networked system without physical interconnections, if the asymptotic stability condition in Theorem 1 holds, the minimum singular value of the matrix* $I_l + G^*_{OL}(s)$ *converges to* $\underline{\sigma}(I_l + L \otimes G_I(0))$ *over low frequency. Considering that the minimum singular value represents the size of a matrix, the increase in* $||L||$ *and* $||G_I(0)||$ *tends to diminish the sensitivity function* $|S(s)|$.

*Suppose a SISO agent dynamics* $G_I(s) = bk/\prod_{i=0}^{n_i}(s + a_i)$, *where* $a_i > 0$, $b > 0$, *and* $k > 0$ *are defined to satisfy the asymptotic stability condition in Theorem 1. Either the decrease of* $a_i$ *or increase of b increases the value of* $||G_I(0)||$, *and accordingly results in the decrease of* $|S(s)|$. *The findings can be summarised as:*

- *Effect of network topology: The increase in* $||L||$, *which corresponds to higher connectivity of a graph, improves the reference tracking performance.*

- *Effect of agent dynamics: The decrease of* $a_i$ *and increase of b or k is beneficial for the performance metric, implying that the slow convergence speed of individual agents is preferred for the performance of the whole network.*

Note that there has been a previous work on analysing the convergence speed by evaluating the eigenvalue of the error dynamics [64]. Whereas the previous work considers

$A_I = 0$ only, the approach can be extended to general $A_I$ as:

$$\lambda(A_r) \subseteq \Big\{ \lambda_A - \lambda_L \lambda_{BK} \Big| \lambda_A \in \lambda(A_I), \lambda_L \in \lambda(L), \lambda_{BK} \in \lambda(B_I K_I) \Big\}. \tag{4.26}$$

It is inferred from this equation that the increase in the network connectivity, control gain, and convergence speed of individual dynamics improves the convergence speed. However, under the assumption of accessing delay between the agents, the network connectivity and control gain also increase the effect of accessing delay, leading to the slow convergence. Considering the both aspects, the effect of network connectivity and control gain is obscure using this metric. Also, the error between the convergent value and the reference input is not considered in this metric. Hence, the sensitivity function $S(s)$, rather than the eigenvalue of the system matrix $\lambda(A_r)$, is suggested to evaluate the performance of the networked system.

## 4.4 Case Study

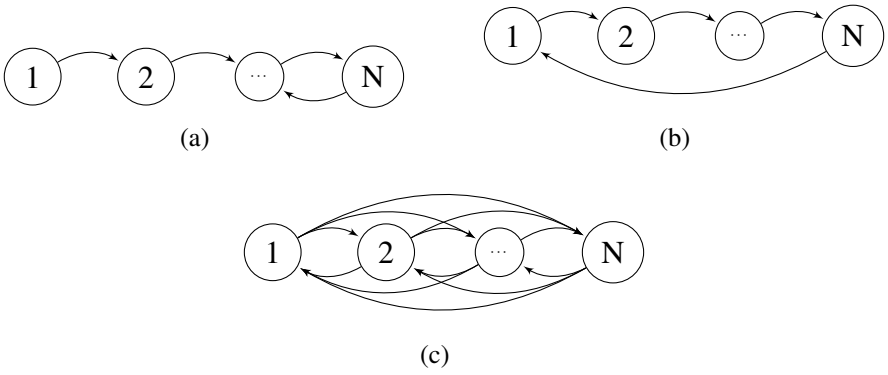


Figure 4.2: Different network topologies

In this section, case studies are presented to show how the proposed analysis framework can be applied to different networked systems. The networked systems of the identical agents without physical coupling are considered for the applicability of Theorem 1.

### 4.4.1 First-Order System

The dynamics of the first-order system is first considered as:

$$A_I = -a, \quad B_I = b, \quad C_I = 1, \tag{4.27}$$

where $a$ and $b$ are positive real constants to satisfy the stability condition in Theorem 1.

The open-loop transfer function is obtained as

$$G^*_{OL}(s) = \frac{bK(s) \circ H(s)}{s+a}. \tag{4.28}$$

Here, the relative states are controlled with a P-gain control, i.e. $K(s) = kL$.

The robustness analysis of the networked first-order system is shown in the following theorems.

**Theorem 3** (Stability margin of the first-order system)**.** *The analytic solution of the stability margin in Theorem 2 is obtained as:*

$$\begin{aligned} \alpha^* = \min \Bigg\{ & \sqrt{\frac{\omega^* + bk\lambda_i}{\omega^* - bk\lambda_i}} \Big| \\ & \lambda_L = \lambda_r + j\lambda_i,\ \lambda_L \in \lambda(L),\ \lambda_r, \lambda_i \in \mathbb{R} \Bigg\}, \end{aligned} \tag{4.29}$$

*where the frequency at which the margin is obtained, $\omega^*$, is computed for each $\lambda_L$ as:*

$$\omega^* = -a\frac{\lambda_r}{\lambda_i} - |\lambda_L| \sqrt{\frac{a^2}{b^2k^2\lambda_i^2} + 1}. \tag{4.30}$$

*When $\lambda_i = 0$ for all $\lambda_L$, the stability margin always satisfies $\alpha^* = 1$.*

*Proof.* The disk margin is obtained as:

$$\alpha^2(\omega) = \frac{(a + b\lambda_r)^2 + (\omega + bk\lambda_i)^2}{(a - b\lambda_r)^2 + (\omega - bk\lambda_i)^2}. \tag{4.31}$$

By differentiating the equation with respect to $\omega$, the extrema are obtained in $\omega^*$ such that

$$\lambda_i \omega^{*2} + 2a\lambda_r \omega^* - \lambda_i (a^2 + b^2 k^2 |\lambda_L|^2) = 0. \tag{4.32}$$

If $\lambda_i = 0$ for all $\lambda_L$, $\omega^*$ is 0 from the equation and $\partial \alpha^2 / \partial \omega$ is always negative for all $\omega > 0$. As the value of $\alpha$ approaches 1 in high frequency domain, the stability margin always satisfies $\alpha(\omega) \geq 1$.

If $\lambda_i \neq 0$, the minimum of $\alpha(\omega)$ is obtained at

$$\omega^* = -a\frac{\lambda_r}{\lambda_i} - |\lambda_L| \sqrt{\frac{a^2}{b^2 k^2 \lambda_i^2} + 1}. \tag{4.33}$$

□

From Theorem 3, it is inferred that if the network has an undirected graph in which the eigenvalue of the Laplacian matrix is real, the stability margin satisfies $\alpha^* = 1$. If there exists an imaginary part $\lambda_i \neq 0$, the increase of $|\lambda_L|$ and $\lambda_i / \lambda_r$ decreases the frequency $\omega^*$, and correspondingly the stability margin $\alpha^*$. Also, the decrease of $a$ and increase of $b$ deteriorates the stability margin.

Note that for the consensus problem with undirected graph, i.e. $a = 0$ and $\lambda_i = 0$, it is known that the phase margin is proportional to $1/|\lambda_L|$ [64]. The relationship between $\lambda_L$ and the disk margin $\alpha^*$ is different for the following reasons: the concept of $\alpha$ has been developed for an asymptotically stable system, i.e. no CRHP poles; and the value of $\alpha$ represents a conservative bound considering a simultaneous variation in gain and phase. However, the tendency that the increase of $|\lambda_L|$ decreases the margin remains with the generalised system dynamics $a$.

The delay margin of the networked first-order system is derived differently from the following theorem.

**Theorem 4** (Delay margin of the first-order system)**.** *The delay margin of the first-order system is infinite.*

*Proof.* The analytic solution of the closed-loop poles is derived from the characteristic equation as:

$$s = -\frac{f(k,T)}{c_3 T} \pm \frac{\sqrt{f(k,T)^2 - c_4 abkT^2 - c_5 bkT - c_6 T}}{c_3 T}, \tag{4.34}$$

where $f(k,T) = aT + c_1 bkT + c_2$ and $c_i$'s are non-negative real constants which vary depending on the communication graph. The closed-loop poles stay on the left-hand-plane regardless of the communication topology and time delay, resulting in the infinite delay margin. □

Remind that the delay margin is different from the phase margin obtained in Theorem 3. Under the assumption that an agent's own states are accessed instantly, the delay from the other agents does not destabilise the networked system.

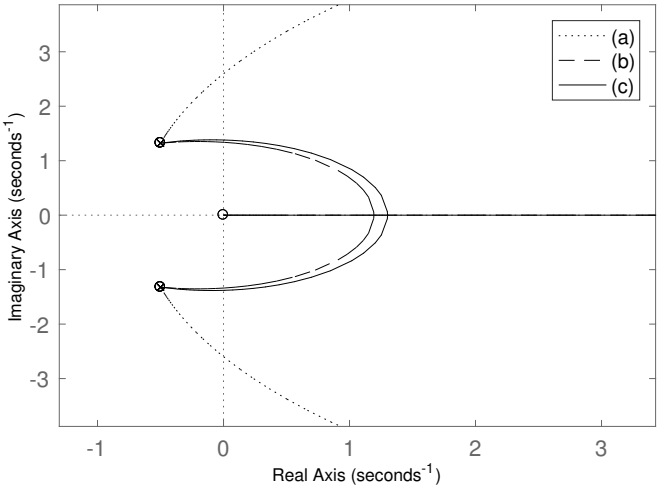


Figure 4.3: Root locus of the formation control with second-order dynamics

### 4.4.2 Second-Order System

The stability of the networked second-order system is analysed. The dynamics of the second-order system is generalised as:

$$A_I = \begin{bmatrix} 0 & 1 \\ -a_0 & -a_1 \end{bmatrix}, \quad B_I = \begin{bmatrix} 0 \\ b \end{bmatrix}, \quad C_I = \begin{bmatrix} 1 & 0 \end{bmatrix}, \tag{4.35}$$

where $a$, $b$ and $c$ are positive real constants. The relative value of the output is controlled with a P-gain control, $K(s) = kL$.

The open-loop transfer function is obtained as:

$$G^*_{OL}(s) = \frac{bK(s) \circ H(s)}{s^2 + a_1 s + a_0}. \tag{4.36}$$

The robustness of the networked second-order system is analysed in the following theorems.

**Theorem 5** (Stability margin or the second-order system)**.** *Suppose all eigenvalues of the Laplacian matrix are real. The disk margin is obtained as:*

$$\alpha^* = \left\{ \sqrt{\frac{2\omega^{*2} + a_0^2 - 2a_1 - 2bk\lambda_r}{2\omega^{*2} + a_0^2 - 2a_1 + 2bk\lambda_r}} \middle| \lambda_r \in \lambda_L \right\}, \tag{4.37}$$

*where $\omega^*$ is computed for each $\lambda_L$ as:*

$$\omega^* = \sqrt{a_1 + \sqrt{a_0^2 a_1 + b^2 k^2 \lambda_r^2}}. \tag{4.38}$$

*Proof.* The disk margin is obtained as:

$$\alpha^2(\omega) = \frac{(\omega^2 - a_0 + bk\lambda_r)^2 + (a_1\omega + bk\lambda_i)^2}{(\omega^2 - a_0 - bk\lambda_r)^2 + (a_1\omega - bk\lambda_i)^2}. \tag{4.39}$$

By differentiating the equation with respect to $\omega$, the extrema are obtained in $\omega^*$ such that

$$\begin{aligned} &2\lambda_r\omega^{*5} - 3a_1\lambda_i\omega^{*4} - 4a_0\lambda_r\omega^{*3} - (a_1^2 - 2a_0)a_1\lambda_i\omega^{*2} \\ &- 2a_1\lambda_r(a_1^2a_0 - a_0^2 + b^2k^2|\lambda_L|^2)\omega^* \\ &+ a_1\lambda_i(a_0^2 + b^2k^2|\lambda_L|^2) = 0. \end{aligned} \tag{4.40}$$

If $\lambda_i = 0$ for all $\lambda_L$, the minimum of $\alpha(\omega)$ is obtained at

$$\omega^* = \sqrt{a_1 + \sqrt{a_0^2a_1 + b^2k^2\lambda_r^2}}. \tag{4.41}$$

□

Unlike the first-order system, the disk margin of the second-order system with $\lambda_i = 0$ is less than 1, depending on the system dynamics and network connectivity. The tendency of the margin with respect to network topology $\lambda_L$ and system dynamics $a_0$, $a_1$, and $b$ remains similar to the conclusions made from Theorem 3.

Prior to computing the delay margin, its existence is first investigated through the root locus in Fig. 4.3. Three different communication graphs are considered as Fig. 4.2. The communication graphs (a) and (b) have the same average degree, whereas the graph (b) has the same average degree with maximum cyclic length, $N$, and the graph (c) is a fully connected graph. The effect of delay is shown as the non-minimum phase zero and the perturbation in the poles. As the gain $k$ increases, two poles cross the imaginary axis for all network topologies, implying that there exists a single upper bound for the gain $k$. The delay margin $T$ which makes this gain positive is computed in the following theorem.

**Theorem 6** (Delay margin of the second-order system)**.** *For a fully connected network, the delay margin is obtained as*

$$DM = \frac{4}{(N-2)a_1} \tag{4.42}$$

*Proof.* When the network is fully connected, the matrix in Eqn. (4.36), of which the deter-

minant is the characteristic equation, is symmetric with the diagonal terms $s^2+a_0s+a_1+bk(N-1)$ and the off-diagonal terms $-bk(1-sT/2)/(1+sT/2)$. For the determinant to be zero, the following equation is obtained.

$$\begin{aligned}&(s^2+a_1s+a_0+bk(N-1))(1+sT/2)\\&=-bk(1-sT/2) \text{ or } (N-1)bk(1-sT/2)\end{aligned} \tag{4.43}$$

Substituting $s=j\omega$, the closed-loop poles are on the imaginary axis if either of the following equations are satisfied.

$$\begin{cases}-T\omega^3+(bk(N-2)T+bT+2a_1)\omega=0\\-(a_1T+2)\omega^2+2bkN+2b=0\end{cases}$$
$$\text{or}\begin{cases}-T\omega^3+(2bk(N-1)T+bT+2a_1)\omega=0\\-(a_1T+2)\omega^2+2b=0\end{cases} \tag{4.44}$$

Considering that both the time slot $T$ and the control gain $k$ are positive, the condition for the closed-loop stability is obtained as

$$k\le\frac{a_1}{b}\cdot\frac{(2/T)^2+a_1(2/T)+b}{2(2/T)-(N-2)a_1},\quad T<\frac{4}{(N-2)a_1}. \tag{4.45}$$

□

Note that the resultant delay margin contradicts with the previous work [61]. For the same second-order system, the trivial solution from the previous work is periodic as:

$$T=\frac{\pi M}{\omega},\quad \omega=\frac{1}{2}\sqrt{-a_1^2+4(1+(N-1)k)b}, \tag{4.46}$$

where $M$ is a positive integer. This research provides more intuitive solution with lower degree of characteristic equation, simplifying the analysis.

### 4.4.3 Higher-Order System

For higher-order systems, the explicit expression of the stability margin is difficult to be obtained analytically. Instead, the stability margin of different network topologies and system dynamics is obtained numerically and shown in Fig. 8.1. In (i), (ii), (iii), and (iv), the values of $\lambda_r$, $\lambda_i$, $a_i$, and $b$ vary from 0 to 1 respectively, to show the relationship between each parameter and the stability margin. In the default case, the eigenvalue of the Laplacian matrix is set as $|\lambda_L| = 1/\sqrt{2}$ and $\lambda_i/\lambda_r = 1$, and the agent dynamics is defined as $G(s) = bk/\prod_{i=0}^{n_i}(s+a_i)$, where $a_i = 0.8$ for all $i$, $b = 0.2$, and $k = 1$.

The following remark is observed from Fig. 8.1, generalising the interpretations in Theorems 3 and 5.

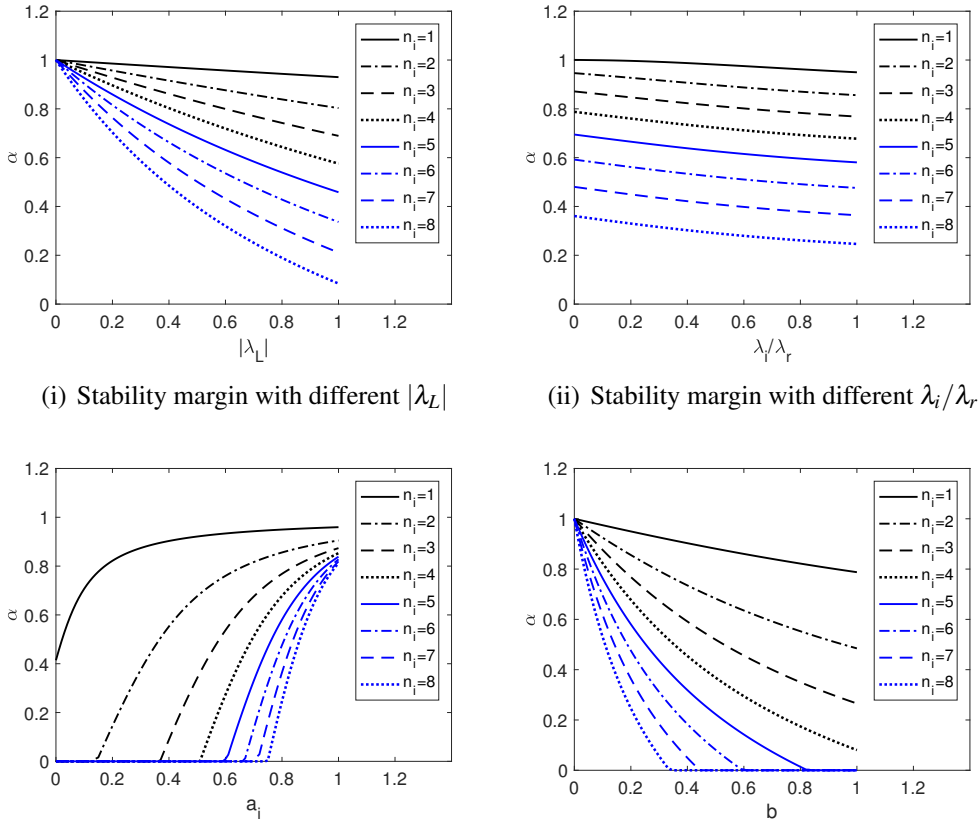


(i) Stability margin with different $|\lambda_L|$

(ii) Stability margin with different $\lambda_i/\lambda_r$

(iii) Stability margin with different $a_i$

(iv) Stability margin with different $b$

Figure 4.4: Stability margin with different network topologies & system dynamics

**Remark 2.**

- *Effect of network topology: From (i) and (ii), the increase of $|\lambda_L|$ and $\lambda_i/\lambda_r$ deteriorates the stability margin. It is known that $|\lambda_L|$ is relevant with the connectivity of a graph, and $\lambda_i/\lambda_r$ with the cyclic network. Also, even though it is not directly considered in the analysis, increase in the accessing delay has a similar effect on increasing $\lambda_i$ as a cyclic network, deteriorating the stability margin.*

- *Effect of agent dynamics: From (iii) and (iv), the increase of $a_i$'s and decrease of $b$ or $k$ improves the stability margin. The conclusion coincides with physical intuition: dependence more on the agent's own states than on the others' is beneficial for the stability margin.*

Comparing with Remark 1, it is notable that there is a trade-off between the robustness and performance. The effect of cyclic network or accessing delay is obscure in the performance metric, but the network connectivity and agent dynamics has a conflicting effect on the networked control system. When the connectivity of a graph is increased, the robustness is degraded while the performance is improved. Also, the increase of $a_i$'s compared with $b$ or $k$ implies that the agents are more dependent on their own states, increasing the robustness and losing the tracking performance of the whole system. This analysis result suggests that the network or control gain should be designed not to achieve both the robustness and performance, but to find a balance between them.

## 4.5 Numerical Simulations

### 4.5.1 Simulation Settings

The numerical simulations for the case studies are conducted to verify the robustness and performance analysis. The values for the agent dynamics are specified as $a = 2$ for the first-order system and $a_1 = 2$, $a_0 = 1$ for the second-order system. The value of $b$ is 1 for both cases. The reference input for the desired formation is given as a constant, $r(t) = [0.5345, 0.2673, -0.8018]^T$. The communication graphs (a), (b), and (c) in Fig. 4.2

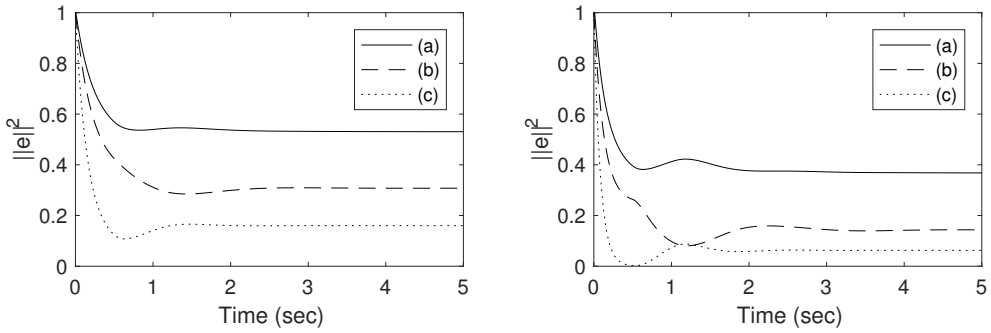


(i) $k = 1$, $T = 0.5$ sec (ii) $k = 2$, $T = 0.5$ sec

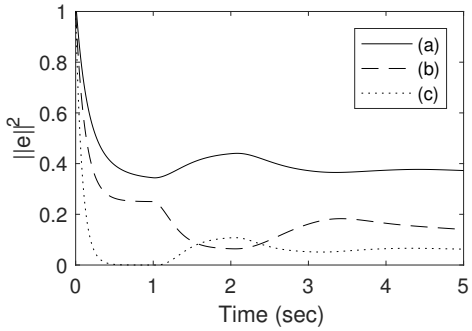


(iii) $k = 2$, $T = 1$ sec

Figure 4.5: Simulation results of the formation control with first-order dynamics

are used for the analysis, where the set of eigenvalues $\lambda(L)$ is given as $\{0, 0.382, 2.618\}$, $\{0, 1.5+0.866j, 1.5-0.866j\}$, and $\{0, 3, 3\}$, respectively for $N = 3$.

### 4.5.2 Simulation Results

The error between the output and reference input is shown in Fig. 4.5 and Fig. 4.6 with different control gain $k$ and accessing delay $T$. For the networked first-order system in Fig. 4.5, it is observed that the tracking performance of the fully connected network, (c), is better than the networks with smaller connectivity. This supports Remark 1 on the effect of network connectivity on the performance of the networked system. Also, comparing (i) and (ii) with different $k$, the steady state error is improved in case of higher control gain, validating the remark on the performance and agent dynamics in Remark 1. In (iii), a higher time delay $T = 1$ sec is applied to observe the stability. The response is stable regardless of the control gain and time delay as proven in Theorem 4.

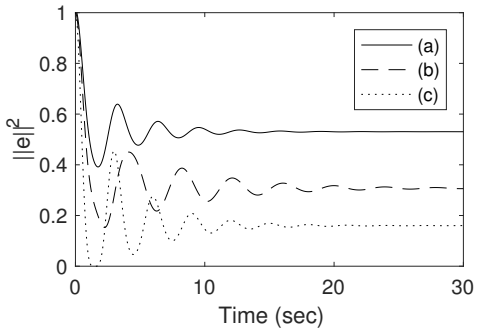


(i) $k = 1$, $T = 0.5$ sec

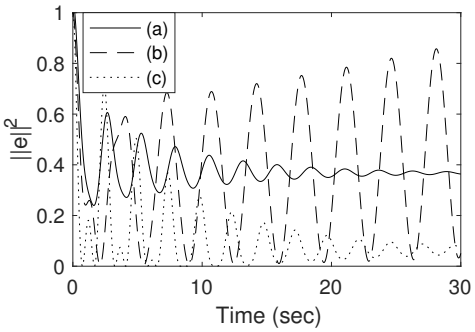


(ii) $k = 2$, $T = 0.5$ sec

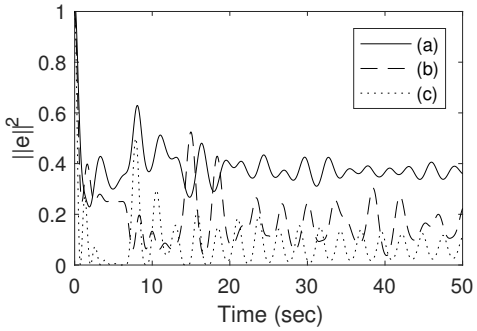


(iii) $k = 2$, $T = 6$ sec

Figure 4.6: Simulation results of the formation control with second-order dynamics

The result in Fig. 4.6 proves that the stability and performance of networked second-order system depends on the network topology, control gain, and time delay. In a similar manner with first-order system, the tracking performance of the system is improved with higher connectivity and control gain, as predicted in Remark 1. According to Theorem 6, the networked second-order system has a finite delay margin depending on the control gain and agent dynamics as opposed to the first-order system. The instability is observed with the network topology (b) in (i), and with all the topologies in (ii). This corresponds with Remark 2 in that the stability margin of the cyclic network is smaller than the networks with $\lambda_i = 0$.

## 4.6 Conclusions

In this chapter, a new stability analysis method for the networked multi-agent system has been proposed. The main idea is to model the networked system including the commu-

nication dynamics into a single MIMO transfer function and to utilise the analysis tools in linear control theory. The stability of the networked system is defined, and its robustness against gain/phase variation and accessing delay is evaluated with stability and delay margin. The analysis on first-, second- and higher order agent dynamics reveals the effect of network topology and agent dynamics on the robustness metrics defined. Also, the trade-off between the robustness and performance of the networked system is observed, suggesting the network topology and control gain to be designed in consideration of their balance. Numerical simulations with first- and second-order systems support the theoretical analysis.

The strength of the proposed method lies on that it can analyse any agent dynamics, controllers, and communication characteristics, if they could be modelled into a transfer function. By combining network and control theory, the properties of a graph have been explained in the view of controlling the agents. This research will provide an insight for designing the network or control considering their effects on the robustness and performance of the networked system.

For the future work, the analysis will be extended to physically coupled systems, e.g. slung-load system [71], which showed different patterns in our initial study. Intuitively, if the independently stable agents use others' uncertain information in their control, the robustness of stability should be degraded. However, in the physically coupled system where it is important to know others' information to maintain the stability, the larger connectivity of a network might improve the stability even though the received information is inaccurate. Also, for compensating the uncertainty and nonlinear dynamics, more complicated controllers including nonlinear controllers will be considered. Approximation of the stochastic packet dynamics into the deterministic transfer function will improve the feasibility of the proposed analysis.

# References

[14] J. P. Hespanha, P. Naghshtabrizi, and Y. Xu. "A survey of recent results in networked control systems". In: *Proc. of the IEEE* 95.1 (2007), pp. 138–162.

[15] J. D. Blight, R. Lane Dailey, and D. Gangsaas. "Practical control law design for aircraft using multivariable techniques". In: *International Journal of Control* 59.1 (1994), pp. 93–137.

[54] G. Walsh, H. Ye, and L. Bushnell. "Stability Analysis of Networked Control Systems". In: *IEEE Transactions on Control Systems Technology* 10.3 (2002), pp. 438–446.

[55] H. Lin, G. Zhai, and P. J. Antsaklis. "Robust stability and disturbance attenuation analysis of a class of networked control systems". In: *Decision and Control, 2003. Proceedings. 42nd IEEE Conference on* 2 (2003), pp. 1182–1187.

[56] Y. Cai, K. A. Hua, and A. Phillips. "Leveraging 1-hop neighborhood knowledge for efficient flooding in wireless ad hoc networks". In: *Proc. 24th IEEE International Performance, Computing, and Communications Conference IPCCC 2005* (2005), pp. 347–354.

[57] X. Liu, A. Goldsmith, S. S. Mahal, and J. K. Hedrick. "Effects of communication delay on string stability in vehicle platoons". In: *Intelligent Transportation Systems, 2001. Proceedings. 2001 IEEE* (2001), pp. 625–630.

[58] M. S. Branicky, S. M. Phillips, and W. Zhang. "Stability of networked control systems: Explicit analysis of delay". In: *American Control Conference, 2000. Proceedings of the 2000* 4 (2000), pp. 2352–2357.

[59] F.-L. Lian, J. Moyne, and D. Tilbury. "Analysis and modeling of networked control systems: MIMO case with multiple time delays". In: *Proceedings of the American Control Conference* (2001), pp. 4306–4312.

[60] C. Tan and G.-P. Liu. “Consensus of Discrete-Time Linear Networked Multi-Agent Systems With Communication Delays.” In: *IEEE Transactions on Automatic Control* 58.11 (2013), pp. 2962–2968.

[61] M. Schwager, N. Michael, V. Kumar, and D. Rus. “Time scales and stability in networked multi-robot systems”. In: *Robotics and Automation (ICRA), 2011 IEEE International Conference on* (2011), pp. 3855–3862.

[62] N. Michael, M. Schwager, V. Kumar, and D. Rus. “An experimental study of time scales and stability in networked multi-robot systems”. In: *Springer Tracts in Advanced Robotics* 79 (2014), pp. 631–643.

[63] Y. G. Sun and L. Wang. “Consensus of multi-agent systems in directed networks with nonuniform time-varying delays”. In: *IEEE Transactions on Automatic Control* 54.7 (2009), pp. 1607–1613.

[64] R. Olfati-Saber and R. M. Murray. “Consensus Problems in Networks of Agents with Switching Topology and Time-Delays”. In: *IEEE Transactions on Automatic Control* 49(9).9 (2004), pp. 1520–1533.

[65] Y. Kim. “On the Stability Margin of Networked Dynamical Systems”. In: *IEEE Transactions on Automatic Control* 62.10 (2017), pp. 5451–5456.

[66] I. S. Gradshteyn and I. M. Ryzhik. *Tables of Integrals, Series, and Products, 6th ed.: Routh-Hurwitz Theorem*. San Diego, CA: Academic Press, 2000.

[67] N. Lehtomaki, N. Sandell, and M. Athans. “Robustness results in linear-quadratic Gaussian based multivariable control designs”. In: *IEEE Transactions on Automatic Control* 26.1 (1981), pp. 75–93.

[68] R. Olfati-Saber, J. A. Fax, and R. M. Murray. “Consensus and cooperation in networked multi-agent systems”. In: *Proceedings of the IEEE* 95.1 (2007), pp. 215–233.

[69] A.-K. Schug, P. Seiler, and H. Pfifer. “Robustness Margins for Linear Parameter Varying Systems”. In: *AerospaceLab Journal* 13 (2017).

[70] A. Packard and J. Doyle. “The complex structured singular value”. In: *Automatica* 29.1 (1993), pp. 71–109.

[71] H.-I. Lee, D.-W. Yoo, B.-Y. Lee, G.-H. Moon, D.-Y. Lee, M.-J. Tahk, and H.-S. Shin. “Parameter-robust linear quadratic Gaussian technique for multi-agent slung load transportation”. In: *Aerospace Science and Technology* 71 (2017), pp. 119–127.

# Chapter 5

# Parameter-Robust Linear Quadratic Gaussian for Multi-Agent Slung-Load Transportation

## Abstract

This chapter copes with parameter-robust controller design for transportation system by multiple unmanned aerial vehicles. The transportation is designed in the form of string connection. Minimal state-space realisation of slung-load dynamics is obtained by Newtonian approach with spherical coordinates. Linear quadratic Gaussian / loop transfer recovery (LQG/LTR) is implemented to control the position and attitude of all the vehicles and payloads. The controller's robustness against variation of payload mass is improved using parameter-robust linear quadratic Gaussian (PRLQG) method. Numerical simulations are conducted with several transportation cases. The result verifies that LQG/LTR shows fast performance while PRLQG has its strong point in robustness against system variation.

## 5.1 Introduction

Recently, unmanned aerial vehicles (UAVs) are getting attention for both military and civilian uses. In the future, transportation using UAVs is also expected to be common, but a small light UAV generally does not have enough power to lift a heavy load. Rather than employing a larger UAV, cooperation of multiple UAVs can be an efficient approach for transporting various types of payload. Interconnection of multiple UAVs results in complicated equations of motion, as each UAV heavily affects the motion of the others. Importance and possibility of employing multiple UAVs in transportation has been mentioned in other previous studies [72]. Although there are many possible ways of cooperation, such as rigid gripping with clamps [73] and bar joint, string connection is chosen in this study to maintain the degree of freedom of each UAV as shown in Fig. 5.1.

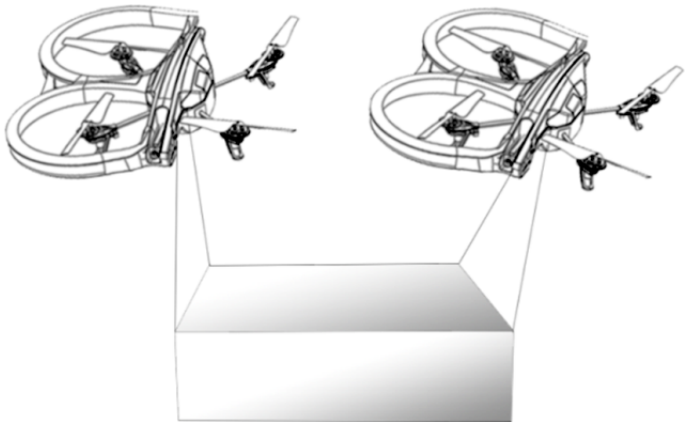

Figure 5.1: Slung-load system visualisation

In the previous studies, a single aircraft lifting one payload with a long string has been considered [74, 75]. As these cases assume a sufficiently long pendulum, coupling effects or aerodynamic disturbances on payload are negligible, and thus whole system does not have to be included in the model. To consider coupling effects into model, Maza *et al.* solved this problem using Kane method [76, 77, 78]. On the other hand, Bisgaard *et al.* [79, 80] employed Udwadia-Kalaba Equation (UKE), which is more efficient in expressing constrained dynamics. Existing modelling techniques, both Kane and UKE method, give the precise model of slung load transportation system, while state-space represen-

tations are not minimal. As one string connection reduces one degree of freedom, the minimum number of states is reduced by the number of strings. The existence of superficial states leads to a system model absent of controllability. Since the number of system variables is large and the model is complicated, model reduction is not easy. Our previous work [81] using UKE method, therefore, was not able to apply LQ-based controllers. To circumvent the controllability problem, it is suggested to utilise the combination of spherical coordinates and Cartesian coordinates [82]. The equation of motion is derived by Newtonian approach as it is easier to generalise the equation of motion compared to the Lagrangian approach. Unlike previous methods, tensile forces are computed by matrix inversion with inclusion of internal force into the state vector.

Stability analysis and control of the modelled system is another major issue in this chapter. Two approaches are possible for control design: control of each UAV with respect to external disturbance including the effect of tension and control design considering the whole system. Previously, studies in [74, 75] utilise the former and Michael *et al.* [83, 84] perform only stability analysis. In order to conduct aggressive control in response to pendulum motion, whole system states are required to be controlled at the same time. This research implements classical optimal control technique, linear quadratic Gaussian (LQG) technique [85]. LQG is useful to find gains for complicated transportation systems, while PID control, the most commonly used method, is hard to be implemented for large number of states. The tuning of PID gains is generally performed by trial-and-error and coupling between the longitudinal and lateral dynamics makes this tuning hard.

For practical use, it would be better to transport the payloads with various weights without changing the controller. Also, continuous loss of weight during transportation is common in agricultural uses. To improve the robustness of the LQG controller, loop transfer recovery (LTR) [16, 17] or parameter-robust linear quadratic Gaussian (PRLQG) [86, 87] can be employed. PRLQG is expected to provide better robustness then LQG/LTR. In addition to our previous work [82], frequency-domain analysis on stability proves the improvements in robustness.

This chapter is composed as follows. First, the mathematical modelling procedure of multi-UAV slung load transportation system using Newtonian approach is presented. Second, control design theory of LQG/LTR and PRLQG method is briefly reviewed, and the transportation system model is reformulated into a moderate form for controller design process. Third, numerical simulation using MATLAB is conducted to analyse the performance of LQG/LTR and PRLQG controller. Finally, conclusion is drawn from numerical results and future work is suggested.

## 5.2 Slung Load Transportation System Modelling

The following sub-sections suggest modelling procedure for transportation system with Newtonian approach, assuming no aerodynamic force or fluctuation in strings. Only gravitational force and lift force of UAVs are assumed to be significant in the model. The equation of motion is generalised with unspecified number and shape of UAVs. General equation of motion is then reduced to two cases: one point mass transportation system with one UAV, and one box payload transportation with four UAVs.

### 5.2.1 Derivation of General Equation of Motion

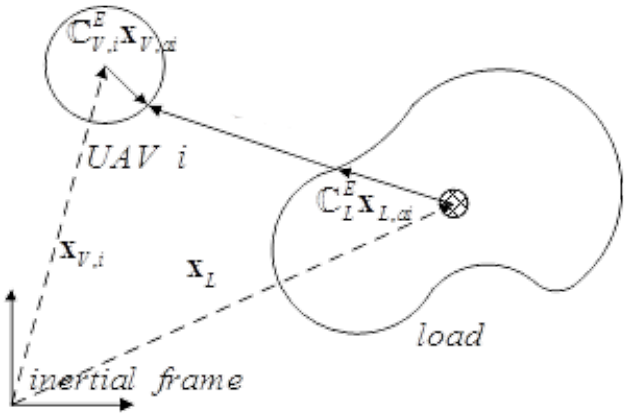


Figure 5.2: Slung-load system nomenclature

System variables of transportation system with unspecified number of UAVs and type of payloads are shown in Fig. 5.2. System variables chosen for modelling are position and attitude of the load ($\mathbf{x}_L = [x_L, y_L, z_L]^T$, $\boldsymbol{\theta}_L = [\phi_L, \theta_L, \psi_L]^T$), spherical coordinate angle of the strings ($\boldsymbol{\theta}_i = [\theta_i, \phi_i]^T$), and attitude of each UAV ($\boldsymbol{\theta}_{V,i} = [\phi_{V,i}, \theta_{V,i}, \psi_{V,i}]^T$), where attitude information is required for computing direction cosine matrices ($\mathbb{C}_{V,i}^E$, $\mathbb{C}_L^E$) and spherical coordinate ($C$) is used to describe the motion of strings for constrained length. The spherical coordinate is determined so that zero angles yield hovering condition as follows:

$$C(\boldsymbol{\theta}) = l \begin{bmatrix} \sin\phi \\ -\sin\theta\cos\phi \\ -\cos\theta\cos\phi \end{bmatrix} \tag{5.1}$$

Observing the geometric relationship in Fig. 5.2, position states of the UAVs ($\mathbf{x}_{V,i}$) are determined as follows.

$$\mathbf{x}_{V,i} = \mathbf{x}_L + \mathbb{C}_L^E \mathbf{x}_{L,ai} + C(\boldsymbol{\theta}_i) - \mathbb{C}_{V,i}^E \mathbf{x}_{V,ai} \tag{5.2}$$

where $\mathbf{x}_{v,ai}$ and $\mathbf{x}_{L,ai}$ stands for the vectors from the centre of mass of vehicle or load respectively to the attachment point of $i$-th string.

Applying Newton's 2nd law of motion and Euler equation, the following equation is the basic idea of modelling.

$$\begin{cases} \mathbf{M}_{V,i}\ddot{\mathbf{x}}_{V,i} &= \mathbf{F}_{V,i} - \sum T_i C(\boldsymbol{\theta}_i)/l_i \\ \mathbf{M}_L\ddot{\mathbf{x}}_L &= \mathbf{F}_L + \sum T_i C(\boldsymbol{\theta}_i)/l_i \\ \mathbf{I}_V\dot{\boldsymbol{\omega}}_{V,i} &= \boldsymbol{\tau}_{V,i} - \sum T_i(\mathbf{x}_{V,ai} \times \mathbb{C}_E^{V,i} C(\boldsymbol{\theta}_i))/l_i \\ \mathbf{I}_L\dot{\boldsymbol{\omega}}_L &= \sum T_i(\mathbf{x}_{L,ai} \times \mathbb{C}_E^L C(\boldsymbol{\theta}_i))/l_i \end{cases} \tag{5.3}$$

where $\mathbf{M}_L$ or $\mathbf{M}_{V,i}$ is a mass matrix with diagonal entries of mass $m_L$ or $m_{V,i}$, $\mathbf{I}$ is an inertial matrix, $T$ is a tensile force, $l$ is the length of a string, and $\boldsymbol{\omega}$ is the angular velocity in the

body frame. The forces $\mathbf{F}_{V,i}$ and $\mathbf{F}_L$ include the gravitational force as

$$\mathbf{F}_{V,i} = \mathbb{C}_{V,i}^{E}\mathbf{F}_{M,i} + \mathbf{M}_{V,i}\mathbf{g}, \quad \mathbf{F}_L = \mathbf{M}_L\mathbf{g}, \quad \mathbf{g} = [0,0,g]^T \tag{5.4}$$

The inputs of the system are given as external forces ($\mathbf{F}_{M,i}$) and moments ($\boldsymbol{\tau}_{V,i}$) regardless of UAV dynamics. This modelling is for general type and dynamics of UAV, and thus individual dynamics must be augmented separately.

Substitution of equation (5.2) into equation (5.3) yields relationship among system variables and tensile forces. Although values of tensile forces are not measured, second-derivative terms and tensile forces have linear relationship, and thus derivative terms can be computed as an inverse matrix form as follows.

$$\begin{bmatrix} \ddot{\mathbf{x}}_L^T & \ddot{\boldsymbol{\theta}}_i^T & \dot{\boldsymbol{\omega}}_L^T & \dot{\boldsymbol{\omega}}_{V,i}^T & T_i/l_i \end{bmatrix}^T = \\ \begin{bmatrix} \mathbf{M}_{V,i} & \mathbf{M}_{V,i}C'(\boldsymbol{\theta}_i) & \mathbf{M}_{V,i}\mathbb{C}_L'^{E}\mathbf{x}_{L,ai} & -\mathbf{M}_{V,i}\mathbb{C}_{V,i}'^{E}\mathbf{x}_{V,ai} & C(\boldsymbol{\theta}_i) \\ \mathbf{M}_L & \mathbf{0}_{3\times 2} & \mathbf{0}_{3\times 3} & \mathbf{0}_{3\times 3} & -C(\boldsymbol{\theta}_i) \\ \mathbf{0}_{3\times 3} & \mathbf{0}_{3\times 2} & \mathbf{0}_{3\times 3} & \mathbf{I}_{V,i} & \mathbf{x}_{V,ai}\times\mathbb{C}_E^{V,i}C(\boldsymbol{\theta}_i) \\ \mathbf{0}_{3\times 3} & \mathbf{0}_{3\times 2} & \mathbf{I}_L & \mathbf{0}_{3\times 3} & -\mathbf{x}_{L,ai}\times\mathbb{C}_E^{L}C(\boldsymbol{\theta}_i) \end{bmatrix}^{-1} \\ \begin{bmatrix} \mathbf{F}_{V,i} - \sum_i \mathbf{M}_{V,i}(G(\boldsymbol{\theta}_i,\dot{\boldsymbol{\theta}}_i) + \mathbb{G}_L^E\mathbf{x}_{L,ai} - \mathbb{G}_{V,i}^E\mathbf{x}_{V,ai}) \\ \mathbf{F}_L \\ \boldsymbol{\tau}_{V,i} \\ \mathbf{0}_{3\times 1} \end{bmatrix} \tag{5.5}$$

The prime mark notes for differentiation not along the time but along the spherical coordinate states of strings. To be specific, function $C'$ and matrix $\mathbb{C}'$ is computed as

$$C' \triangleq \begin{bmatrix} \dfrac{dC}{d\theta} & \dfrac{dC}{d\phi} \end{bmatrix}, \quad \mathbb{C}'\mathbf{x}_{ai} \triangleq \begin{bmatrix} \dfrac{d\mathbb{C}}{d\phi}\mathbf{x}_{ai} & \dfrac{d\mathbb{C}}{d\theta}\mathbf{x}_{ai} & \dfrac{d\mathbb{C}}{d\psi}\mathbf{x}_{ai} \end{bmatrix} \tag{5.6}$$

where the differentiated result is similar to the gradient in that the required form is an

augmented matrix.

Function $G$ and matrix is introduced to cope with first-derivative terms. For instance, function $G$, which is related to spherical coordinate transformation function $C$, is defined as

$$\begin{aligned} G(\boldsymbol{\theta}, \dot{\boldsymbol{\theta}}) &= \frac{d^2 C(\boldsymbol{\theta})}{dt^2} - C'(\boldsymbol{\theta})\ddot{\boldsymbol{\theta}}^T \\ &= -\begin{bmatrix} \dot{\phi}^2 \sin\phi \\ -(\dot{\theta}^2 + \dot{\phi}^2)\sin\theta\cos\phi \\ -(\dot{\theta}^2 + \dot{\phi}^2)\cos\theta\cos\phi \end{bmatrix} + 2\dot{\theta}\dot{\phi}\begin{bmatrix} 0 \\ \cos\theta\sin\phi \\ -\sin\theta\sin\phi \end{bmatrix} \end{aligned} \tag{5.7}$$

while $\mathbb{G}$ is computed similarly.

The size of the inverse matrix in equation (5.5) is thus $3n+3$ for two-dimensional case and $6n+6$ for three-dimensional case, when $n$ stands for the number of UAVs. It is the same as the summation of degree of freedom for $n+1$ agent, whereas the number of system variables reduces by $n$ as tensile forces do not belong to system variable. The number of reduced variables can be also interpreted as $n$ string constraints.

### 5.2.2 Equation of Motion for Sample Cases

The simplest transportation system is given with one UAV and a point mass load attached to the centre of UAV with a single string. General equation of motion given in equation (5.5) is reduced as follows:

$$\begin{aligned} &\begin{bmatrix} \ddot{\mathbf{x}}_L^T & \ddot{\boldsymbol{\theta}}^T & T/l \end{bmatrix}^T = \\ &\begin{bmatrix} \mathbf{M}_V & \mathbf{M}_V C'(\boldsymbol{\theta}) & C(\boldsymbol{\theta}) \\ \mathbf{M}_L & \mathbf{0}_{3\times 2} & -C(\boldsymbol{\theta}) \end{bmatrix}^{-1} \left( \begin{bmatrix} \mathbf{F}_V \\ \mathbf{F}_L \end{bmatrix} - \begin{bmatrix} \mathbf{M}_V G(\boldsymbol{\theta}, \dot{\boldsymbol{\theta}}) \\ \mathbf{0}_{3\times 1} \end{bmatrix} \right) \end{aligned} \tag{5.8}$$

As the string is connected to the centre of UAV, attitude of both load and UAV does not influence the whole system behaviour. However, in case of a quadrotor-type UAV, pitch and roll attitude can be determined by the relationship among external force vectors, as it

generates thrust mainly in $z$-axis direction.

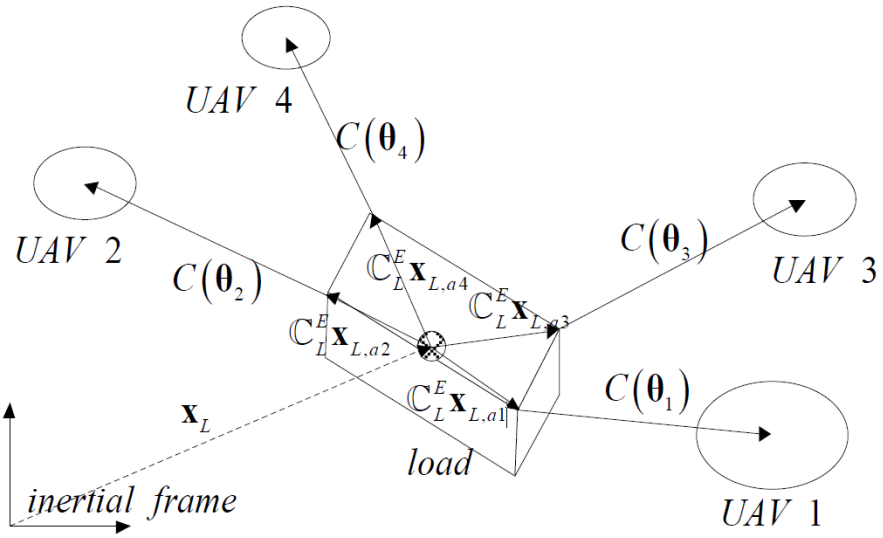


Figure 5.3: Slung-load system with four UAVs and a box payload

Expanding the modelling into four UAVs and a box, variables are determined as in Fig. 5.3. When setting connection points to the payload, one must be careful not to create uncontrollable mode. For instance, if all the strings are attached to a single point or divided to two points, the matrix in the equation (5.5) becomes singular and at least one mode of payload is not controllable. In this chapter, four UAVs are connected to the upper points of the box as shown in Fig. 5.3. Even though the attachment points are determined,

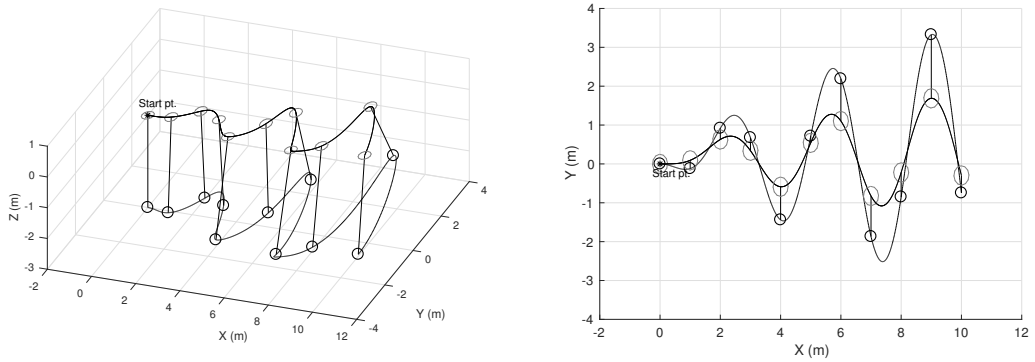


(i) 3D-plot (ii) 2D-plot

Figure 5.4: Verification of slung-load dynamics excited with natural frequency

$\mathbf{x}_{L,ai}$'s differ by the size of load. The resultant equation of motion is

$$\begin{bmatrix} \ddot{\mathbf{x}}_L^T & \ddot{\boldsymbol{\theta}}_1^T & \cdots & \dot{\boldsymbol{\omega}}_L^T & T_1/l_1 & \cdots \end{bmatrix}^T = \begin{bmatrix} \mathbf{M}_{V,1} & \mathbf{M}_{V,1}C'(\boldsymbol{\theta}_1) & \mathbf{0}_{3\times 2(n-1)} & \mathbf{M}_{V,1}\mathbb{C}_L'^E\mathbf{x}_{L,a1} & C(\boldsymbol{\theta}_1) & \mathbf{0}_{3\times(n-1)} \\ \vdots & \mathbf{0}_{3(n-1)\times 2} & \ddots & \vdots & \mathbf{0}_{3(n-1)\times 1} & \ddots \\ \mathbf{M}_L & \mathbf{0}_{3\times 2} & \mathbf{0}_{3\times 2(n-1)} & \mathbf{0}_{3\times 3} & -C(\boldsymbol{\theta}_1) & \cdots \\ \mathbf{0}_{3\times 3} & \mathbf{0}_{3\times 2} & \mathbf{0}_{3\times 2(n-1)} & I_L & \mathbf{x}_{L,a1}\times\mathbb{C}_E^L C(\boldsymbol{\theta}_1) & \cdots \end{bmatrix}^{-1} \begin{bmatrix} \mathbf{F}_{V,1} - \sum_i \mathbf{M}_{V,i}(G(\boldsymbol{\theta}_i,\dot{\boldsymbol{\theta}}_i) + \mathbb{G}_L^E\mathbf{x}_{L,ai}) \\ \vdots \\ \mathbf{F}_L \\ \mathbf{0}_{3\times 1} \end{bmatrix} \tag{5.9}$$

### 5.2.3 Verification with Udwadia-Kalaba Equation

To verify the modelling, comparison with UKE is suggested [9-10]. Among all the previous works, modelling using UKE considered the most general case when the strings are attached to the different point with centre of mass, and thus appropriate to be compared with the model suggested in this thesis. UKE enables explicit computation of internal

forces and moments with unconstrained states ($\mathbf{q}_u$), which is simply computed as

$$\ddot{\mathbf{q}}_u = \mathbf{M}^{-1}\begin{bmatrix}\mathbf{F}_{V,i}^T & \boldsymbol{\tau}_{V,i}^T & \mathbf{F}_L^T & \mathbf{0}_{1\times 3}\end{bmatrix}^T \tag{5.10}$$

where augmented mass matrix $\mathbf{M}$ consists of mass of all the states, and the states are composed of positions and attitudes of UAVs and payload. Utilizing the unconstrained states, constraint force and moments are computed as

$$F_c = \mathbf{M}^{\frac{1}{2}}(A_1\mathbf{M}^{-\frac{1}{2}})^{+}(A_2 - A_1\ddot{\mathbf{q}}_u) \tag{5.11}$$

where $F_C$ is different from tensile force as it includes forces and moments for all the state variables. Matrices $A_1$ and $A_2$ are defined in order to present string constraints as

$$A_1 = L_i^T\begin{bmatrix}\mathbb{C}_{V,i}^E & -\mathbb{C}_{V,i}^E\tilde{\mathbf{x}}_{V,ai} & -\mathbb{C}_L^E & \mathbb{C}_L^E\tilde{\mathbf{x}}_{L,ai}\end{bmatrix} \tag{5.12}$$

$$\begin{aligned}A_2 = {} & \dot{L}_i^T\dot{L}_i \\ & - L_i^T(\mathbb{C}_{V,i}^E\tilde{\omega}_{V,i}^2\mathbf{x}_{V,ai} + \mathbb{C}_{V,i}^E\tilde{\mathbf{x}}_{V,ai}I_V^{-1}\tilde{\omega}_{V,i}I_V\omega_{V,i} \\ & - \mathbb{C}_L^E\tilde{\omega}_L^2\mathbf{x}_{L,ai} - \mathbb{C}_L^E\tilde{\mathbf{x}}_{L,ai}I_L^{-1}\tilde{\omega}_L I_L\omega_L)\end{aligned} \tag{5.13}$$

where $L$ is a vector notation of strings as same as in Fig. 2. Using the equations from (5.12) to (5.13), result of equation (5.11) yields constrained states as follows.

$$\ddot{\mathbf{q}}_b = \ddot{\mathbf{q}}_u + \mathbf{M}^{-1}F_c \tag{5.14}$$

The UKE approach can be also represented by Newtonian approach similarly. Defining all the states the same, equation (5.11) and (5.14) can be unified in the form of equation

(5.5) as

$$\begin{bmatrix} \ddot{\mathbf{q}}_b \\ T \end{bmatrix} = \begin{bmatrix} \mathbf{M} & A_1^T \\ A_1 & 0 \end{bmatrix}^{-1} \begin{bmatrix} \mathbf{F}_{V,i} \\ \boldsymbol{\tau}_{V,i} \\ \mathbf{F}_L \\ \mathbf{0}_{3\times 1} \\ 0 \end{bmatrix} \tag{5.15}$$

In order to verify the modelling, simple case when one UAV is lifting one point mass payload is considered numerically. As two modelling methods have different choices of system states, spherical coordinates of Newtonian approach are converted to Cartesian coordinates for reference. The resultant second derivatives showed error less than the order of truncation error, and thus it can be concluded that the two modelling methods are correct. Also, when the lift is given with sinusoidal form in natural frequency $\sqrt{g/l}$, the pendulum motion enlarges as shown in Fig. 5.4. As swinging angle of the payload increases, coupling force on UAV enlarges the trajectory of UAV. Intuitively, it can be concluded that the moving pendulum dynamics and coupling effect is well-modelled.

## 5.3 Control Design

This section outlines design of controller. Classic control method LQG is implemented in more analytic perspective. Then, PRLQG is added in order to improve robustness along parameter variation. Finally, the modelled systems in section 2 are modified in an appropriate form for control techniques.

### 5.3.1 Linear Quadratic Gaussian / Loop Transfer Recovery Technique

LQG is to optimise the cost of state errors and input in linearised state-space form. Even though not all the states are observed, estimator is designed to compensate the error.

Formulation of controller and estimator is presented as follows.

$$\begin{aligned} &\dot{x} = Ax + Bu, \quad y = Cx \\ &u = -K_C\hat{x}, \quad \dot{\hat{x}} = (A - K_F C)\hat{x} + Bu + K_F y \end{aligned} \tag{5.16}$$

Here, the system dynamics is linearised from Section 5.2, with a trim point at the hovering state and non-oscillating payload.

Through optimisation method, gains are obtained by the solution of the following algebraic Riccati equation (ARE).

$$\begin{aligned} &K_C = R^{-1}B^T P_{C,},\ P_C A + A^T P_C + Q - P_C B R^{-1} B^T P_C = 0 \\ &K_F = P_F C^T W^{-1},\ P_F A^T + A P_F + V - P_F C^T W^{-1} C P_F = 0 \end{aligned} \tag{5.17}$$

Design parameters $Q$, $R$, $V$ and $W$ are determined by relative weighting among states, state and command, model accuracy, and sensor accuracy, respectively. As these design parameters have patterns, expanding the transportation system does not influence hardly on determining them, and it acts as a strong advantage compared to PID control technique.

As LQG may not have desirable robustness, LTR is augmented to recover open-loop gain. LTR is conducted by modifying the design parameters to get sensitivity recovery or robustness recovery as follows.

$$\begin{aligned} &\text{robustness recovery :} \quad Q = Q_0 + w_{C,LTR}^2 C^T C \\ &\text{sensitivity recovery:} \quad V = V_0 + w_{F,LTR}^2 B B^T \end{aligned} \tag{5.18}$$

While increasing the weight of LTR ($w_{LTR}^2$) improves robustness or sensitivity, the controller gains also increase along with the weight of LTR, resulting in the aggressive manoeuvre. Considering both robustness and performance, $w_{LTR}^2$, is selected to have the open-loop gain as close as possible to the target loop function at crossover frequency. The target loop function is defined as a transfer function to which the open-loop gain theoretically converges as $w_{LTR}^2$ approaches infinity. The LQG/LTR open-loop gain $G_2$

and the target loop function $G_1$ are computed by following equations.

$$\begin{aligned} G_1(s) &= K_C(sI-A)^{-1}B \\ G_2(s) &= K_C(sI-A+BK_C+K_FC)^{-1}K_FC(sI-A)^{-1}B \end{aligned} \tag{5.19}$$

Two important assumptions for applying LTR are that the system must be minimum phase and the number of measured states needs to be larger than that of control inputs. If the system has right half-plane closed-loop poles, the extra phase lead contributed by these poles is required for maintaining stability. Also, measurements should be sufficient for adding dummy columns to $B$ and zero rows to $K_C$ to make $C(sI-A)^{-1}B$ and $K_C(sI-A)^{-1}B$ square matrices. As $C(sI-A)^{-1}B$ must remain as a minimum phase system, enlarging $C$ matrix or using smaller number of measurements is inappropriate.

For simple transportation system with one UAV lifting a point mass payload, actual and target loop functions from equation (5.19) near the crossover frequency are given in Fig. 5.5. Weightings are given for robustness recovery, and transfer function is from $x$-axis to $x$-axis ($G_{xx}$) to show fluctuation control. Weighting value of 100 is expected to be most appropriate to make the transfer function closest to the target function. Resultant root locus is shown in Fig. 5.6. The system dynamics has two poles at the origin and another two poles on the imaginary axis as equation (5.20).

$$G_{xx} = \frac{\omega_n^2}{m_V s^2 (s^2 + \dfrac{m_V + m_L}{m_V}\omega_n^2)} \tag{5.20}$$

where $\omega_n$ is a natural frequency $\sqrt{g/l}$

Four poles and three zeros are added from LQG or LQG/LTR controller, and two zeros among them are located near to the system poles. It can be expected that the system changes might cause large change in root locus shape.

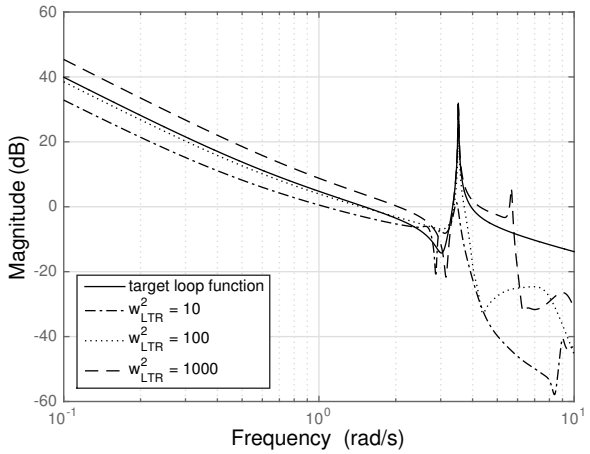


Figure 5.5: Bode plot of LQG/LTR with different weightings

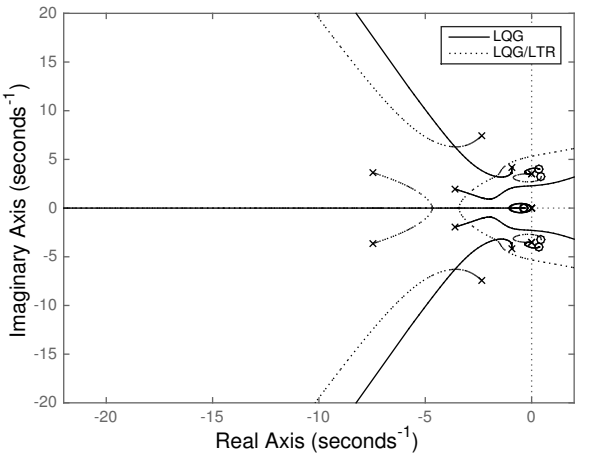


Figure 5.6: Root locus of LQG and LQG/LTR

### 5.3.2 Parameter-Robust Linear Quadratic Gaussian

PRLQG is applied to the system in which structure uncertainties such as parameter variation is expected. The estimated parameter change is reformulated in a fictitious loop called internal feedback loop (IFL), and then controller is designed to maintain robustness against the IFL. In order to implement PRLQG, perturbation of linearised system matrix $A$ caused by parameter variation is decomposed as follows.

$$\Delta A = M\varepsilon N \tag{5.21}$$

where matrix $M$ is column-similar to the system matrix $A$. Using the decomposed matrices $M$ and $N$, design parameters introduced in the previous session are modified with the following equations.

$$\begin{aligned} Q &= Q_0 + w_{C,PRLQG}^2 N^T N \\ V &= V_0 + w_{F,PRLQG}^2 M M^T \end{aligned} \tag{5.22}$$

where $w_{LTR}^2$ can still be added in case of losing controllability. The ratio between the weight of LTR and that of PRLQG is varied according to the design purpose. If robustness to the parameter variation is considered to be more significant than fast performance, the weight of PRLQG must be increased compared to that of LQG/LTR. When the mass of payload is exact enough, the weighting of PRLQG is not required to be large. Increasing the weight of PRLQG, the system's robustness function $G_2$ approaches to the target loop function $G_1$.

$$\begin{aligned} G_1(s) &= N(sI - A + BK_C)^{-1} M \\ G_2(s) &= N(sI - A)^{-1} M \\ &\quad - N(sI - A)^{-1} BK(I + GK)^{-1} C(sI - A)^{-1} M \end{aligned} \tag{5.23}$$

where function $K$ and $G$ is defined as

$$\begin{aligned} K(s) &= K_C(sI - A - BK_C + K_F C)^{-1} K_F \\ G(s) &= C(sI - A)^{-1} B \end{aligned} \tag{5.24}$$

As robustness function is the transfer function from parameter variation to output, gain is required to be similar throughout the range of interest.

Similar to the previous subsection, one UAV transportation system is considered for

instance. As system matrix $A$ is obtained as follows,

$$A = \begin{bmatrix} 0 & 0 & 0 & 0 & g \\ 0 & 0 & 0 & -g & 0 \\ 0 & 0 & 0 & 0 & 0 \\ 0 & 0 & 0 & -\frac{m_V+m_L}{m_V l}g & 0 \\ 0 & 0 & 0 & 0 & -\frac{m_V+m_L}{m_V l}g \end{bmatrix} \tag{5.25}$$

column-similar matrices $M$ and $N$ are defined as

$$\Delta A = M\varepsilon N = \begin{bmatrix} 0 & 0 \\ 0 & 0 \\ 0 & 0 \\ -\frac{g}{m_V l} & 0 \\ 0 & -\frac{g}{m_V l} \end{bmatrix} \Delta m_L \begin{bmatrix} 0 & 0 & 0 & 1 & 0 \\ 0 & 0 & 0 & 0 & 1 \end{bmatrix} \tag{5.26}$$

Bode plot of resultant transfer functions from mass variation is shown in Fig. 7. Compared with the result of LQG/LTR, PRLQG control shows relatively steady gain against parameter variations, whereas target function has more steady gain. As seen in the bode plot, the mass variation is magnified up to 42 dB with LQG/LTR, where the magnitude of the transfer function of PRLQG is upper bounded by -5 dB. Hence, less variation on performance along the parameter change is expected.

From the root locus of PRLQG in Fig. 8, zeros of the controller are placed near to the system poles at real axis. From the root locus shown in Fig. 6, it is clear that the system with LQG/LTR easily becomes non-minimum phase. On the other hand, Fig. 8 shows that parameter change does not cause large change in root locus trajectory of PRLQG. Therefore, improvements in robustness against parameter change is evident both from bode plot and root locus.

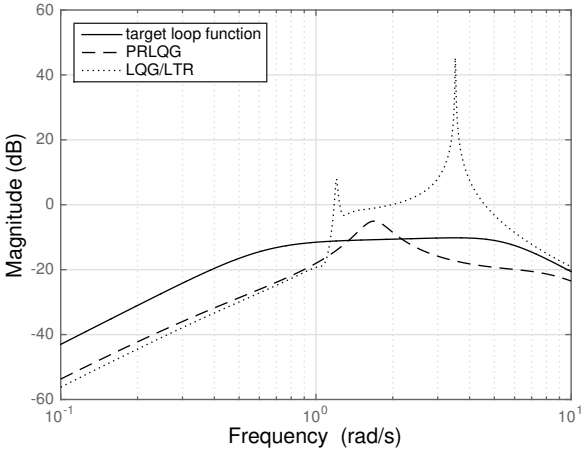


Figure 5.7: Bode plot of PRLQG

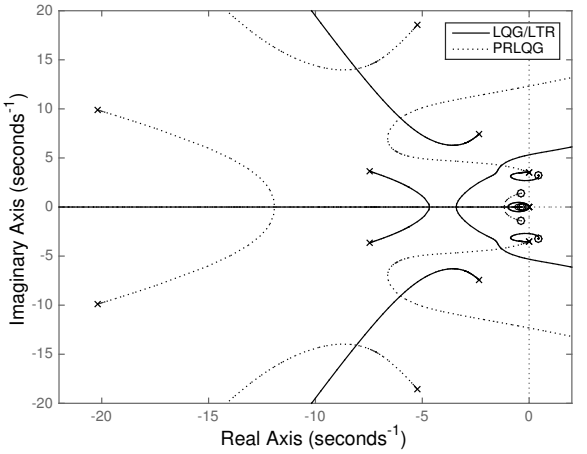


Figure 5.8: Root locus of PRLQG

## 5.4 Numerical Results

In this section, simulation setups and numerical results are presented. Specifications of UAVs and payload, and design parameters of controller introduced in previous sections are set. Then, result of applying the setups is presented.

### 5.4.1 Simulation Settings

The simulation is set with a single UAV and four-UAV transportation system. Specification of UAV and payload is given in Table 1. Size and weight of all the UAVs are set to

Table 5.1: Slung-load system specification

| | | **Case 1** | **Case 2** |
|---|---|---|---|
| UAV | Number | 1 | 4 |
| | Mass(kg) | 0.408 | |
| | Size(m) | $\phi$ 0.356 | |
| | Inertia(kg·m$^2$) | 2.2842·10-3 × 2.4451·10-3 × 4.4562·10-3 | |
| Payload | Type | Point mass | Box |
| | Mass(kg) | 0.1 | 0.4 |
| | Size(m) | None | 0.2 × 1.0 × 1.0 |
| String | Mass(kg) | None | |
| | Size(m) | 1.4 | |

be identical. The modelled mass of payload is set to be constant, and the mass or thickness of string is neglected. The type of UAV is selected as a small quad-rotor, AR. Drone 2.0 from Parrot, which shows the most stable hovering performance in its mass and size. Control allocation from rotational speed of rotors to force and moment of AR. Drone is defined as

$$\mathbf{F}_M = \begin{bmatrix} 0 \\ 0 \\ -4K_{t,0} - K_t(\Omega_1^2 + \Omega_2^2 + \Omega_3^2 + \Omega_4^2) \end{bmatrix} \tag{5.27}$$

$$\boldsymbol{\tau}_V = \begin{bmatrix} K_t(-\Omega_1^2 - \Omega_2^2 + \Omega_3^2 + \Omega_4^2)d + I_r q(\Omega_1 - \Omega_2 + \Omega_3 - \Omega_4) \\ K_t(\Omega_1^2 - \Omega_2^2 - \Omega_3^2 + \Omega_4^2)d - I_r p(\Omega_1 - \Omega_2 + \Omega_3 - \Omega_4) \\ 4K_{r,0} + K_r(\Omega_1^2 - \Omega_2^2 + \Omega_3^2 - \Omega_4^2) \end{bmatrix} \tag{5.28}$$

where $d$ is the distance from the center of UAV to rotors, $I_r$ is the inertia of UAV, and $p$ and $q$ are the roll and pitch rate, respectively. Also, $\Omega_i$'s are the rotational speed of each rotor, saturated by maximum of 4787.1 rpm, and the rotor coefficients for thrust computation

and torque are given as follows:

$$K_t = 8.1763 \cdot 10^{-6}, \quad K_{t,0} = 0.0562N \tag{5.29}$$

$$K_r = 2.1703 \cdot 10^{-7}, \quad K_{r,0} = 1.0950 \cdot 10^{-4} N \cdot m \tag{5.30}$$

For the details of quad-rotor dynamics, refer to [88].

In order to evaluate the controller's robustness against the mass variation, numerical simulations are conducted with four different cases: when the actual mass (1) is equivalent to the modelled mass, noted as the standard case, (2) has a constant mismatch with the modelled value with -20%, (3) has again a constant difference with +20%, and (4) is varying from +20% to -20% with a constant rate during the transportation. Also, to analyse the effect of time delay and maximum thrust, 0.1 sec of motor delay is applied, and maximum rotor speed is reduced by -20%. The effects are shown by the response in $x$-axis the same command (1, 1, -1) m, as the designed payload transportation system is symmetric in $x$-$y$ axis. Compared to $z$-axis performance, $x$- and $y$-axis response has more district changes, as perturbation of $A$ matrix in equation (5.26) lies in the string motion influencing mainly on $x$-$y$ motion of the load.

Design parameters for the LQG-based controllers are set as follows: $Q$ is 5 and 1, and $W$ is 0.1 and 1 for non-derivative terms and first derivative terms respectively. Diagonal terms of $R$ for all the states are set 10, and those of $V$ are 0.01. These rules are applied not only for the two cases we are dealing with, but also for further expansion of transportation system.

MATLAB simulation structure for one UAV and a point mass is given in Fig. 5.9, while larger transportation system is composed in similar sense. From dynamics, positions and attitudes of load and string is given, which is later used in calculating position of UAVs. Summation of input trim enables the linearised dynamics to be approximated to nonlinear dynamics. The command is given in feedforward structure with $\bar{N}$ matrix given

as

$$\bar{N} = N_u + K_C N_x, \quad \text{where} \begin{bmatrix} N_x \\ N_u \end{bmatrix} = \begin{bmatrix} A & B \\ C & D \end{bmatrix}^{-1} \begin{bmatrix} 0 \\ 1 \end{bmatrix} \tag{5.31}$$

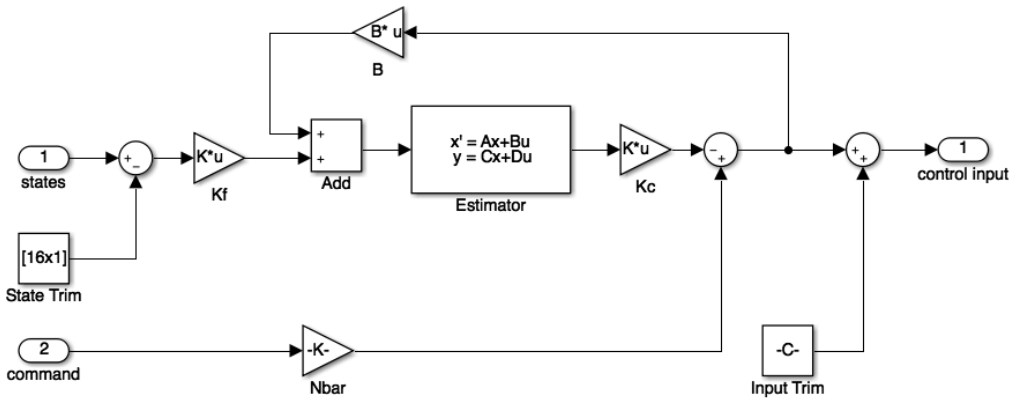


Figure 5.9: Simulation structure

### 5.4.2 Simulation Results

Simulation is first conducted for the single UAV slung load transportation system. The effect of variation in payload mass is demonstrated via the step responses of LQG/LTR and PRLQG in Fig. 5.10, and the trajectory of PRLQG-applied case is shown in Fig. 5.11 for reference. While the standard response of the LQG/LTR controller is fast and fluctuating, the system controlled by PRLQG has longer settling time but stable response. When there is a difference between the actual and modelled payload mass, the fluctuation in the LQG/LTR-controlled response is increased, resulting in instability for the cases with -20% and continuous variation. However, the responses of the PRLQG-controlled system remain similar in all cases. It is clearly shown that the PRLQG technique improves the robustness against the payload variation as expected from Section III.

The effect of time delay and motor thrust is shown in Fig. 5.12. Where the LQG/LTR controller shows unstable performance in the presence of time delay, the step response of the PRLQG control remains similar. The phase margin of the PRLQG is 69.5779 deg, whereas the phase margin of the LQG/LTR control is 11.0032 deg. The result implies

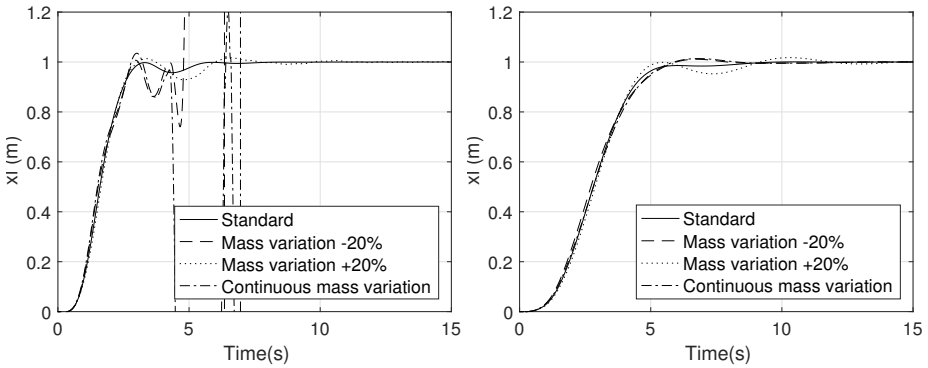


(i) LQG/LTR (ii) PRLQG

Figure 5.10: Simulation results: effect of payload variation in 1-UAV transportation system

that the PRLQG improves not only the robustness against parameter variation, but the phase margin. Reducing the maximum rotor speed seems to suppress the manoeuvre, which means that the LQG/LTR controller without saturation has aggressive manoeuvre. Increasing the PRLQG gain on the other hand smoothens the response. The problem of having higher gains of the LQG/LTR control can be resolved through applying the PRLQG.

Second, the step response of LQG/LTR and PRLQG of four-UAV slung load system is shown in Fig. 5.13. Similar to a single UAV system, the LQG/LTR controller shows a fluctuating, aggressive manoeuvre. In the presence of mass variation, the response further fluctuates and even becomes unstable. On the other hand, the PRLQG method shows stable performance, proving the improvements in the robustness against parameter variation. Although the root locus and bode plot are not analysed for the slung load system with more than one UAV, simulation results demonstrate enhanced robustness against the payload's mass variation with the PRLQG method.

The responses with time delay and reduction of motor thrust in four-UAV system is shown in Fig. 5.14 The LQG/LTR controller shows instability against the delay, implying that the phase margin is improved through the PRLQG method. Also, lower limit of saturation in the maximum thrust results in more suppression in the LQG/LTR-controlled system, while only the overshoot is suppressed in the PRLQG method. Similar to a single

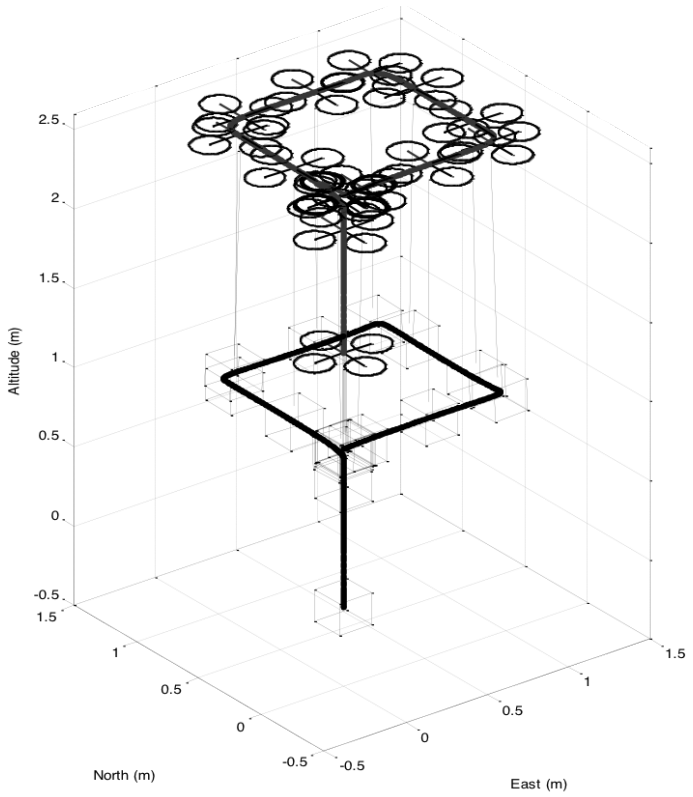


Figure 5.11: Simulation results: trajectory of PRLQG-controlled 1-UAV transportation system

UAV system, the PRLQG method does not result in aggressive manoeuvre.

## 5.5 Conclusions

In this chapter, transportation system with multiple UAVs and string connection is modelled and controlled. Modelling is conducted with Newtonian method, combining spherical coordinates with Cartesian coordinates and using matrix inversion to compute tensile force. The proposed modelling method uses less number of states compared to other previous methods, resulting in smaller size of matrix inversion. Therefore, the proposed method is expected to reduce the computational load. Moreover, the fact that LQG gains can be obtained implies that the linearised system is controllable. The corresponding controller is designed using PRLQG technique. While previous studies did not focus on controller or utilised simple PID controllers, applying analytic control technique is a

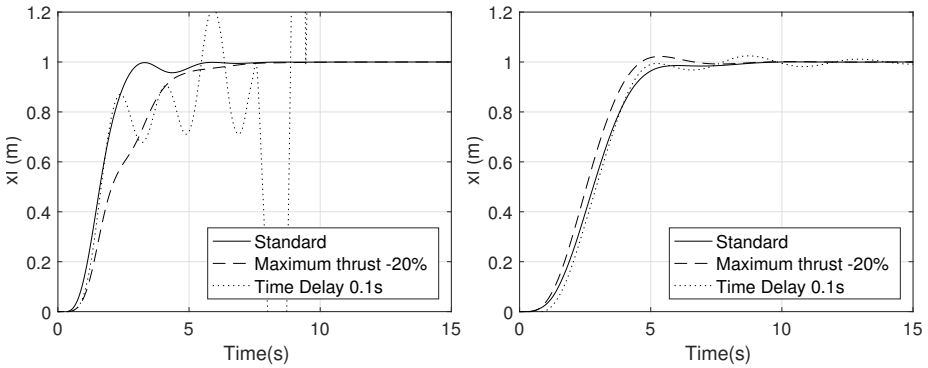


(i) LQG/LTR (ii) PRLQG

Figure 5.12: Simulation results: effect of system parameters in 1-UAV transportation system

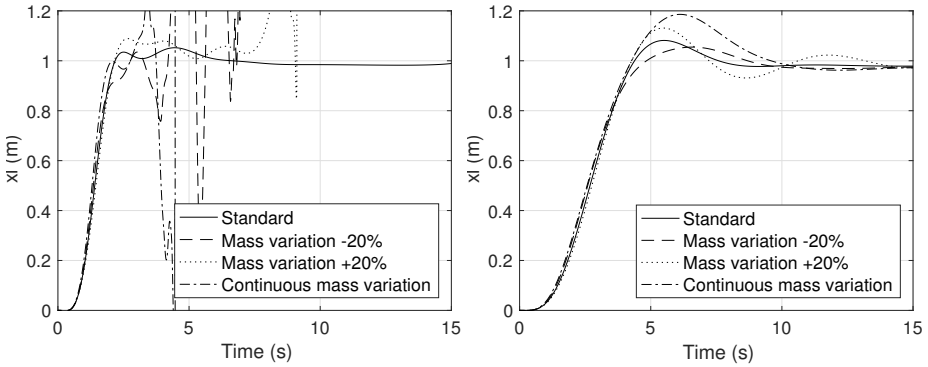


(i) LQG/LTR (ii) PRLQG

Figure 5.13: Simulation results: effect of payload variation in 4-UAV transportation system

significant idea of this research. Also, implementation of the PRLQG method, which is not well-known compared to classic controls like LQG/LTR, resulted in improvements in transporting varying mass of payload. Computer simulation shows simple verification of modelling and analysis of improvements not only in parameter robustness of controller, but also in phase margin and smooth performance.

Further studies are expected to include more details in cable modelling. Slackening of the wires or even loosing tension during the transportation would be a practically significant issue. Snapping of the cables would be modelled by excluding the corresponding UAVs from the constraint model, and adding on extra tension when it is first tightened.

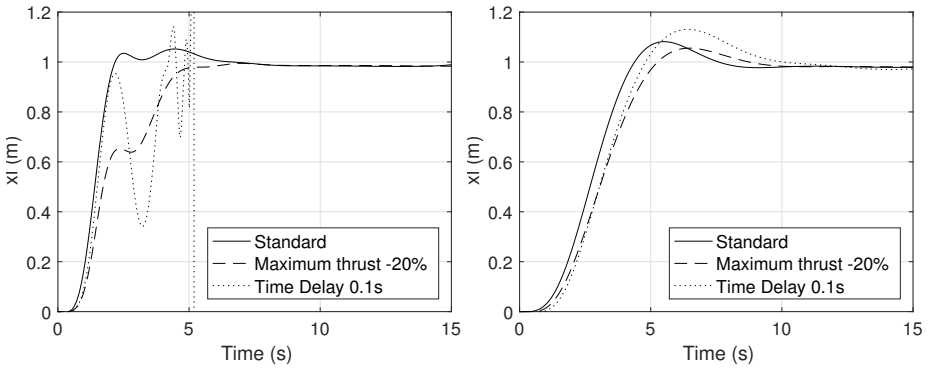


(i) LQG/LTR (ii) PRLQG

Figure 5.14: Simulation results: effect of system parameters in 4-UAV transportation system

Also, integration of unit length commonly used in architecture would be applied to model the elasticity of long wires. Consideration of aerodynamic forces would be another practical challenge. The effect of thrust of the UAV on the payloads might require further investigation, especially in consideration of oscillation, unpredicted behaviours, and even loss of stability. This issue, which is subject to future study, could be resolved either by refining the model to include the aerodynamic forces or by designing the controller robust to the wind disturbance. Experiments would be a valuable verification for the modelling.

Another important issue is rotor failures. In system matrices, partial reduction of performance due to the rotor failures are directly related to the variation in $B$ matrix, which can be covered by PRLQG method. It is expected to improve the robustness against the failures compared with the other linear controllers. Apart from linear controllers, applying adaptive controllers would be another interesting issue, as the parameter uncertainty can be structured.

# Acknowledgement

The authors would like to acknowledge support from Defense Acquisition Program Administration and Agency for Defense Development under the contract UE124026JD.

# References

[16] J. Doyle and G. Stein. “Multivariable feedback design: Concepts for a classical/modern synthesis”. In: *Automatic Control, IEEE Transactions on* 26.1 (1981), pp. 4–16.

[17] G. Stein and M. Athans. “The LQG / LTR Procedure for Multivariable Feedback Control Design”. In: *IEEE Transactions on Automatic Control* 32.2 (1987), pp. 105–114.

[72] Y. Feng, C. A. Rabbath, and C.-Y. Su. “Modeling of a Micro UAV with Slung Payload”. In: *Handbook of Unmanned Aerial Vehicles*. 2015, pp. 2787–2811.

[73] D. Mellinger, Q. Lindsey, M. Shomin, and V. Kumar. “Design, modeling, estimation and control for aerial grasping and manipulation”. In: *IEEE International Conference on Intelligent Robots and Systems* (2011).

[74] R. A. Stuckey. “Mathematical Modelling of Helicopter Slung-Load Systems”. In: *DSTO Aeronautical and Maritime Research Laboratory* (2001).

[75] I. Palunko, R. Fierro, and P. Cruz. “Trajectory Generation for Swing-Free Maneuvers of a Quadrotor with Suspended Payload : A Dynamic Programming Approach”. In: *IEEE International Conference on Robotics and Automation* (2012).

[76] M. Bernard and K. Kondak. “Generic Slung Load Transportation System Using Small Size Helicopters”. In: *IEEE International Conference on Robotics and Automation* (2009).

[77] M. Bernard, K. Kondak, I. Maza, and A. Ollero. “Autonomous Transportation and Deployment with”. In: *Journal of Field Robot* 28.6 (2011), pp. 914–931.

[78] I. Maza, K. Kondak, M. Bernard, and A. Ollero. “Multi-UAV cooperation and control for load transportation and deployment The original publication is available at www.springerlink.com in this link :” in: *Journal of Intelligent Robot Systems* 57 (2010), pp. 417–449.

[79] M. Bisgaard. “Modeling, Estimation, and Control of Helicopter Slung Load System”. PhD thesis. Aalborg University, 2007.

[80] M. Bisgaard, J. D. Bendtsen, and A. Cour-harbo. “Modeling of Generic Slung Load System”. In: *Journal of Guidance, Control, and Dynamics* 32.2 (2009), pp. 573–585.

[81] B. Y. Lee, H. I. Lee, D. W. Yoo, G. H. Moon, D. Y. Lee, Y. Y. Kim, and M. J. Tahk. “Study on payload stabilization method with the slung-load transportation system using a quad-rotor”. In: *2015 European Control Conference, ECC 2015* (2015), pp. 2097–2102.

[82] H.-I. Lee, B.-Y. Lee, D.-W. Yoo, G.-H. Moon, and M.-J. Tahk. “Dynamics Modeling and Robust Controller Design of the Multi-Uav Transportation System”. In: *29th Congress of the International Council of the Aeronautical Sciences* (2014).

[83] N. Michael, S. Kim, J. Fink, and V. Kumar. “Kinematics and Statics of Cooperative Multi-Robot Manipulation with Cables”. In: *Proceedings of the International Design Engineering Technical Conferences* 8 (2009), pp. 83–91.

[84] N. Michael, J. Fink, and V. Kumar. “Cooperative manipulation and transportation with aerial robots”. In: *Autonomous Robots* September 2010 (2010), pp. 1–14.

[85] K. Morris. *Introduction to Feedback Control*. Harcourt/Academic Press, 2001, pp. 163, 198.

[86] M.-J. Tahk and J. L. Speyer. “Modeling of Parameter Variations and Asymptotic LQG Synthesis”. In: *IEEE Transactions on Automatic Control* 32.9 (1987), pp. 793–801.

[87] M.-J. Tahk and J. L. Speyer. “Parameter Robust Linear- Quadratic-Gaussian Design Synthesis with Flexible Structure Control Applications”. In: *Journal of Guidance, Control, and Dynamics,* 12.4 (1988), pp. 460–468.

[88] V. Ghadiok. “Autonomous Aerial Manipulation Using a Quadrotor”. Utah State University, 2011.

# Chapter 6

# Control Synthesis for Multi-UAV Slung-Load Systems with Uncertainties


## Abstract

This chapter develops a new control synthesis for the slung-load transportation system by multiple unmanned aerial vehicles. Effects of the unmatched uncertainties that cannot be directly controlled by the adaptive control are suppressed using the parameter-robust linear quadratic Gaussian method. The stability condition of the tracking and parameter estimation error is proven with Lyapunov analysis. The numerical simulations support the enhancement of robustness and system performance in the presence of both the unmatched and matched uncertainties in the slung-load system.


## 6.1 Introduction

The large scale of unmanned aerial vehicle (UAV) applications has proliferated vastly within the last few years. The operational experience of UAVs has proven that their technology can bring a dramatic impact to military and civilian areas. This includes, but is not limited to: obtaining real-time, relevant situational awareness; helping human operators;

and reducing risk to the mission and operation. Potential applications of UAVs under consideration are quite wide, e.g. border patrol [89, 90, 91], airborne surveillance [92, 93, 94], police law enforcement [95, 96], and forest-fire localisation [97]. One important application that has been attracting an increasing attention is logistics.

This chapter addresses a logistics problem using a group of small UAVs. While small UAVs are advantageous in their accessibility and convenience, their payload is limited. This implies that cooperation of multiple UAVs is inevitable to relieve payload constraints. There could be a few ways to enable a group of small UAVs to cooperate for the logistics. One of the most obvious approaches is to utilise a slung-load system in which the vehicles are connected to the payload with suspended cables. Hence, this research considers the slung-load system as the approach for UAV cooperation in logistics.

Dynamics model of the slung-load system may contain both unmatched and matched uncertainties. Note that the matched and unmatched uncertainties are the uncertainties that lie in the span and the null space of the control input matrix, respectively. UAVs are most likely to deliver various masses of the load. Mass of the load could not be exactly known prior to the operation or could change during the operation. The issue with such uncertainty on the mass is that it generates unmatched uncertainty to the system. The dynamics of the slung-load system is highly coupled and encompasses highly nonlinear terms. This means that a dynamics model of the slung-load system typically contains modelling uncertainty, which also generates matched uncertainties to the system.

Control of a slung-load system is challenging. The motion of each UAV in the slung-load system could be constrained due to the cables connected to the UAV. Oscillation of a vehicle or payload is transmitted through the connected strings to the other vehicles with constrained motion, potentially resulting in instability. The existence of both unmatched and matched uncertainties makes control of a slung-load system even much more challenging.

To this end, this chapter aims to develop a control synthesis to tackle the challenge in the slung-load system control under the presence of unmatched and matched uncer-

tainty. The model reference adaptive control (MRAC) method is an option for being a well known parameter-robust controller. However, most MRAC methods are limited to cancel out the effect of the matched uncertainties. The unmatched uncertainties can be neither estimated, nor cancelled out by common MRAC methods.

While the majority of the previous works focused on the matched uncertainties, there have been some studies specifically on the unmatched uncertainties. As controlling the unmatched uncertainties directly in the MRAC formulation is not possible, the bound of the unmatched uncertainties has been investigated by [98]. The detailed effects on the robustness are analysed with linear matrix inequality in [99]. Under the assumption that the unmatched uncertainties are bounded, modifications on the MRAC, such as $\mathscr{L}_1$ adaptive and bi-objective control, have been proposed in [100, 101]. The modifications are focused mainly on preventing the tracking error from drifting. To suppress the specific effect of unmatched uncertainties, adaptive sliding mode control is suggested by [102], and later extended to multiple sliding surfaces in [103] and to cope with time delays in [104]. The adaptive sliding mode control, unlike the MRAC, pursues the states to converge on the sliding surfaces regardless of the reference model. In [105], the concurrent learning MRAC method is used to fully utilise the reference model and to control the unmatched uncertainties by switching the baseline control gain after estimating the unmatched uncertainties. In the actual implementation, however, it is difficult to know the correct values of the unmatched uncertainties and thus the gain switching time remains illusive.

This chapter proposes a new adaptive approach to cope with both matched and unmatched uncertainties by using the parameter-robust linear quadratic Gaussian method. The approach consists of two parts: the baseline control is designed to be robust to the unmatched uncertainties using the PRLQG method, and the adaptive control cancels out the matched uncertainties with nonlinear basis from the reference model of the baseline control. The previous works [82, 71] have suggested to use the PRLQG method to handle the uncertainties in the payload. The PRLQG method determines the controller gain to increase the stability margin against the parameter variation in the system state matrix [86,

87]. The uncertainty in the system state matrix is assumed to be a function of the system parameter only, implying that the robustness enhancement is limited to the uncertainties with linear basis of states. The remaining uncertainties with nonlinear basis is estimated and cancelled out by the adaptive control.

For the validation of the proposed control synthesis, the convergence of the tracking and parameter estimation error are theoretically investigated using Lyapunov analysis. The performance of the control synthesis is also demonstrated through numerical simulations. The simulation results for the slung-load systems with 1, 2, and 4 quadrotors confirm the robustness of the proposed control synthesis against both unmatched and matched uncertainty.

The rest of this chapter is composed as follows: in section 6.2, the problem formulation is given. In section 6.3, the control synthesis method is proposed and analysed. In section 6.5, the settings and results of numerical simulation is given. The chapter is finalised with conclusion.

## 6.2 Problem Formulation

Consider a state-space representation containing the uncertainty as

$$\dot{x}(t) = Ax(t) + B(u(t) + \Delta(x)) + B_u\Delta_u(x) \tag{6.1}$$

where $x(t) \in \mathbb{R}^n$ and $u(t) \in \mathbb{R}^m$ stand for state, input, and uncertainty vector, respectively. The matched uncertainty $\Delta(x) \in \mathbb{R}^m$ includes all the uncertainties that lie in the span of the control input matrix $B \in \mathbb{R}^{n\times m}$, and the unmatched uncertainty $\Delta_u(x) \in \mathbb{R}^{n-m}$ lies in the span of $B_u \in \mathbb{R}^{n\times(n-m)}$, which is the null space of the control input matrix. The state-space representation is minimal and the system matrices $(A,B)$ are constant and controllable.

The uncertainty $\Delta(t)$ is assumed to be linearly parametrised as

$$\Delta(t) = W^{*T}(t)\Phi(x(t)) \tag{6.2}$$

where $W^*(t) \in \mathbb{R}^{p\times m}$ is the unknown true parameter matrix, and $\Phi(x(t)) \in \mathbb{R}^p$ is the basis vector.

The unmatched uncertainty is assumed to have a basis linear to $x(t)$ as

$$\Delta_u(x) = N^{*T}x(t) \tag{6.3}$$

where $N^* \in \mathbb{R}^{n\times(n-m)}$ is a weight matrix.

The control input is denoted as

$$u(t) = [u_1(t), u_2(t), \cdots, u_N(t)]^T, \qquad y_i(t) = C_i x(t) \tag{6.4}$$

where $N$ is the number of agents, $y_i(t) \in \mathbb{R}^{l/N}$ is the output for each agent, and $u_i(t) \in \mathbb{R}^{m/N}$ is the control of each agent which is a function of $y_i(t) \in \mathbb{R}^l$ from the connected agents.

## 6.3 Control Design

The proposed control use the structure of the MRAC method as

$$u(t) = u_{base}(t) + u_{ad}(t) \tag{6.5}$$

where the baseline control $u_{base}(t)$ determines the reference model with the desired performance, and the adaptive control $u_{ad}(t)$ cancels out the effect of matched uncertainty to track the reference model. The baseline control improves the robustness against the unmatched uncertainty by using the PRLQG method, and the $\sigma$-mod adaptive law is used to estimate the matched uncertainty. The stability of the controller is analysed with the Lyapunov analysis.

### 6.3.1 Parameter-Robust Linear Quadratic Gaussian

The unmatched uncertainty $\Delta_u(x)$ is converted to the perturbation of the system matrix as

$$\Delta A = B_u N^{*T} \tag{6.6}$$

where the perturbation matrix $\Delta A \in \mathbb{R}^{n\times n}$ is implemented as

$$\dot{x}(t) = (A + \Delta A)x(t) + B(u(t) + \Delta(x)) \tag{6.7}$$

The PRLQG method is applicable for the case that the variation in the system matrix can be decomposed as

$$\Delta A = M_{PR}\varepsilon N_{PR}^T \tag{6.8}$$

where $\varepsilon \in \mathbb{R}^{q\times q}$ is the system parameter variation, and $M_{PR} \in \mathbb{R}^{n\times q}$ and $N_{PR} \in \mathbb{R}^{n\times q}$ are constant matrices. Noting that $N_{PR}$ is row-similar to $N^*$, the PRLQG gain is designed with respect to $N_{PR}$ to enhance the robustness against $N^*$.

The baseline PRLQG controller is designed as

$$u_{base}(t) = -Kx(t) \tag{6.9}$$

The gain of the baseline controller $K = R^{-1}B^T P$ is obtained by the following algebraic Riccati equation:

$$PA + A^T P + Q + w_{PR}N_{PR}N_{PR}^T - PBR^{-1}B^T P = 0 \tag{6.10}$$

where $Q \in \mathbb{R}^{n\times n}$ and $R \in \mathbb{R}^{m\times m}$ are positive definite weight matrices for states and inputs respectively, and $w_{PR} \in \mathbb{R}$ is a positive weight for the PRLQG method.

The reference model with the desired performance is designed with the baseline PRLQG

control as

$$\dot{x}_r(t) = A_r x_r(t) - B_r r(t) \tag{6.11}$$

where $x_r(t) \in \mathbb{R}^n$ is the reference state, $r(t) \in \mathbb{R}^m$ is the external reference command, and the system matrix $A_r = A - BK$ is Hurwitz stable.

Defining the tracking error between the reference model and the actual system as $e(t) \triangleq x_r(t) - x(t)$, the tracking dynamics is expressed as

$$\dot{e}(t) = A_r e(t) - B(u_{ad}(t) + \Delta(x)) - B_u \Delta_u(x) \tag{6.12}$$

If $N_{PR}(sI - A)^{-1}B$ is minimum phase, it is proven that as $w_{PR} \to \infty$, the transfer function from $\Delta_u(x)$ to $e(t)$ approaches 0, i.e.

$$\dot{e}(t) \to A_r e(t) - B(u_{ad}(t) + \Delta(x)) \tag{6.13}$$

The details of the proof are given in [87], and for the bode plot analysis of the slung-load system, refer to our previous work [71].

### 6.3.2 Adaptive Law

The matched uncertainty $\Delta(x)$ is cancelled out by the adaptive control as

$$u_{ad} = -\hat{W}(t)^T \Phi(x) \tag{6.14}$$

where $\hat{W}(t) \in \mathbb{R}^{p \times m}$ is the estimate of the parameter $W^*$.

The parameter is estimated with the following $\sigma$-mod adaptive law:

$$\dot{\hat{W}}(t) = -\Gamma \left( \Phi(x) e(t)^T P_r B + \sigma(\hat{W}(t) - W_{guess}) \right) \tag{6.15}$$

where $\Gamma \in \mathbb{R}^{p \times p}$ is the adaptation gain, $\sigma \in \mathbb{R}^{p \times p}$ is the $\sigma$-mod gain, and $P_r \in \mathbb{R}^{n \times n}$ is a

positive definite matrix defined by the following algebraic Riccati equation:

$$P_r A_r + A_r^T P_r + Q_r = 0, \quad Q_r > 0 \tag{6.16}$$

The $\sigma$-mod is applied with respect to $W_{guess} \in \mathbb{R}^{p \times m}$ which is a constant guess of the estimate of the parameter.

## 6.4 Lyapunov Stability Analysis

The stability of the tracking and parameter estimation error is analysed by Lyapunov function. The following conditions for stability can be obtained:

**Theorem 7.**

1. *If $N_{PR}(sI - A)^{-1}B$ and $w_{PR} \to \infty$, the tracking and parameter estimation error is Lyapunov stable with respect to $e(t) = 0$ and $\tilde{W}(t) = W_{guess} - W^*$.*

2. *If the condition 1) is satisfied and the signal is persistently excited, i.e. $\int e(t)e^T(t)dt > 0$, the tracking and parameter estimation error is asymptotically stable.*

3. *If the condition 2) is satisfied and $W_{guess} = W^*$, the tracking and parameter estimation error is exponentially stable with respect to $e(t) = 0$ and $\tilde{W}(t) = 0$.*

*Proof.* Consider the following continuously differentiable, positive definite Lyapunov function:

$$V(e, \tilde{W}) = \frac{1}{2} e^T(t) P_r e(t) + \frac{1}{2} tr(\tilde{W}^T(t) \Gamma^{-1} \tilde{W}(t)) \tag{6.17}$$

where $\tilde{W}(t) \triangleq \hat{W}(t) - W^*$ is the parameter estimation error. Defining $\xi(t) \triangleq [e^T(t), \tilde{W}^T(t)]^T$, the lower and upper bounds of the Lyapunov function are given as

$$\frac{1}{2} \min\left(\lambda(P_r), \lambda(\Gamma^{-1})\right) ||\xi||^2 \leq V(e, \tilde{W}) \leq \frac{1}{2} \max\left(\lambda(P_r), \lambda(\Gamma^{-1})\right) ||\xi||^2 \tag{6.18}$$

The Lie derivative of the Lyapunov function is computed as

$$\dot{V}(e,\tilde{W}) = e^T(t)P_r\dot{e}(t) + tr(\tilde{W}^T(t)\Gamma^{-1}\dot{\hat{W}}(t)) \tag{6.19}$$

Substituting the tracking error dynamics in Eqn. (6.12) and the adaptive law in Eqn. (6.15) gives

$$\dot{V}(e,\tilde{W}) = -\frac{1}{2}e^T(t)Q_re(t) + e^T(t)P_rB_u\Delta_u(x) - tr(\tilde{W}^T(t)\sigma(\hat{W}(t) - W_{guess})) \tag{6.20}$$

The Lyapunov is negative definite except $e(t) = 0$ and $\tilde{W}(t) = W_{guess} - W^*$ if

$$\frac{1}{2}\lambda_{min}(Q)||e(t)|| > ||P_rB_u\Delta_u(x)|| \tag{6.21}$$

If $N_{PR}(sI - A)^{-1}B$ is minimum phase, increasing the weight of PRLQG to infinity leads to $||e(t)|| \gg ||B_u\Delta_u(x)||$, approximating the Lyapunov function as

$$\dot{V}(e,\tilde{W}) \to -\frac{1}{2}e^T(t)Q_re(t) - tr(\tilde{W}^T(t)\sigma(\hat{W}(t) - W_{guess})) \tag{6.22}$$

The approximated Lyapunov function is bounded as

$$\dot{V}(e,\tilde{W}) \leq -\frac{1}{2}\lambda_{min}(Q_r)||e(t)||^2 - \sigma||\tilde{W} - W_{guess} + W^*||^2 \tag{6.23}$$

Using the bounds of the Lyapunov function in Eqn. (6.18):

$$\dot{V}(e,\tilde{W}) \leq -\frac{\min(\lambda(Q_r), 2\sigma)}{\max(\lambda(P_r), \lambda(\Gamma^{-1}))}V(e,\tilde{W}) \tag{6.24}$$

□

## 6.5 Numerical Simulations

The slung-load transportation system in Chapter 5 is considered for the numerical simulation. The dynamics is briefly summarised, and then the simulation settings and results are presented.

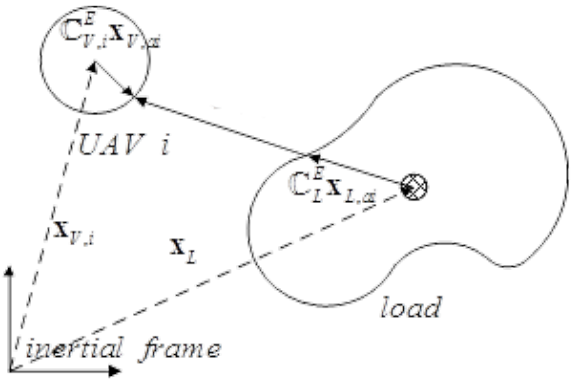


Figure 6.1: Slung-load system nomenclature

### 6.5.1 Slung-Load Dynamics

The system variables of the slung-load system are shown in Fig. 6.1. Note that bold fonts are used for the vectors and matrices in this section in order to prevent the confusion with the scalar variables. The subscripts $V$, $L$, and $E$ stand for vehicle, load, and inertial frame, respectively. The position of each vehicle and the load is denoted by $\mathbf{x}_{V,i} \in \mathbb{R}^3$ and $\mathbf{x}_L \in \mathbb{R}^3$ in the inertial frame, and the vector from the centre of mass to the point that the string is attached is $\mathbf{x}_{ai} \in \mathbb{R}^3$ in the body frame. The vector in the body frame is multiplied by a direction cosine matrix $\mathbb{C}_{V,i}^{E} \in \mathbb{R}^{3\times3}$ or $\mathbb{C}_{L}^{E} \in \mathbb{R}^{3\times3}$ to present in the inertial frame, which is a function of the attitude of each vehicle or the load, $\boldsymbol{\theta}_{V,i} \in \mathbb{R}^3$ and $\boldsymbol{\theta}_L \in \mathbb{R}^3$ respectively.

From the geometric relationship, the string vector is expressed as

$$\begin{aligned} C(\boldsymbol{\theta}_i) &= \mathbf{x}_{V,i} - \mathbf{x}_L - \mathbb{C}_L^E \mathbf{x}_{L,ai} + \mathbb{C}_{V,i}^E \mathbf{x}_{V,ai} \\ &= l_i \begin{bmatrix} \sin\phi_i \\ -\sin\theta_i \cos\phi_i \\ -\cos\theta_i \cos\phi_i \end{bmatrix}, \end{aligned} \tag{6.25}$$

where $l_i \in \mathbb{R}$ is the length of the $i$-th string and $\boldsymbol{\theta}_i = [\theta_i, \phi_i]^T \in \mathbb{R}^2$ is the string vector in the spherical coordinate.

The equation of motion of the slung-load system is

$$\begin{aligned} &\begin{bmatrix} \ddot{\boldsymbol{\theta}}_i^T & \ddot{\mathbf{x}}_L^T & \dot{\boldsymbol{\omega}}_{V,i}^T & \dot{\boldsymbol{\omega}}_L^T & T_i/l_i \end{bmatrix}^T = \\ &\begin{bmatrix} \mathbf{M}_{V,i} C'(\boldsymbol{\theta}_i) & \mathbf{M}_{V,i} & \mathbf{0}_{3\times3} & \mathbf{0}_{3\times3} & C(\boldsymbol{\theta}_i) \\ \mathbf{0}_{3\times2} & \mathbf{M}_L & \mathbf{0}_{3\times3} & \mathbf{0}_{3\times3} & -C(\boldsymbol{\theta}_i) \\ \mathbf{0}_{3\times2} & \mathbf{0}_{3\times3} & \mathbf{I}_{V,i} & \mathbf{0}_{3\times3} & \mathbf{x}_{V,ai} \times \mathbb{C}_E^{V,i} C(\boldsymbol{\theta}_i) \\ \mathbf{0}_{3\times2} & \mathbf{0}_{3\times3} & \mathbf{0}_{3\times3} & \mathbf{I}_L & -\mathbf{x}_{L,ai} \times \mathbb{C}_E^L C(\boldsymbol{\theta}_i) \end{bmatrix}^{-1} \\ &\begin{bmatrix} \mathbf{F}_{V,i} - \sum_i \mathbf{M}_{V,i} (G(\boldsymbol{\theta}_i, \dot{\boldsymbol{\theta}}_i) + \mathbb{G}_L^E \mathbf{x}_{L,ai} - \mathbb{G}_{V,i}^E \mathbf{x}_{V,ai}) \\ \mathbf{F}_L \\ \boldsymbol{\tau}_{V,i} \\ \mathbf{0}_{3\times1} \end{bmatrix}, \end{aligned} \tag{6.26}$$

where $\boldsymbol{\omega} \in \mathbb{R}^3$ is the angular rate in the body frame, $T_i \in \mathbb{R}$ the tensile force, $\mathbf{M} \in \mathbb{R}^{3\times3}$ the mass matrix, and $\mathbf{I} \in \mathbb{R}^{3\times3}$ the inertia. The functions $G(\boldsymbol{\theta}, \dot{\boldsymbol{\theta}}) \in \mathbb{R}^3$, and $\mathbb{G}^E \in \mathbb{R}^{3\times3}$ are defined as

$$\begin{aligned} G(\boldsymbol{\theta}, \dot{\boldsymbol{\theta}}) &= \begin{bmatrix} -\dot{\phi}^2 \sin\phi \\ (\dot{\theta}^2 + \dot{\phi}^2)\sin\theta\cos\phi + 2\dot{\theta}\dot{\phi}\cos\theta\sin\phi \\ (\dot{\theta}^2 + \dot{\phi}^2)\cos\theta\cos\phi - 2\dot{\theta}\dot{\phi}\sin\theta\sin\phi \end{bmatrix}, \\ \mathbb{G}^E &= (\mathbb{C}^E \times \boldsymbol{\omega}) \times \boldsymbol{\omega}. \end{aligned} \tag{6.27}$$

The external forces, $\mathbf{F}_{V,i} \in \mathbb{R}^3$ and $\mathbf{F}_L \in \mathbb{R}^3$, include gravitational force as

$$\begin{aligned} \mathbf{F}_{V,i} &= \mathbb{C}_{V,i}^{E} \mathbf{F}_{M,i} + \mathbf{M}_{V,i}\mathbf{g}, \\ \mathbf{F}_L &= \mathbf{M}_L \mathbf{g}, \end{aligned} \tag{6.28}$$

where $\mathbf{g} = [0,0,g]^T$ is the gravitational acceleration vector. The force and moment generated by the vehicle, $\mathbf{F}_{M,i} \in \mathbb{R}^3$ and $\boldsymbol{\tau}_{V,i} \in \mathbb{R}^3$, are obtained with respect to the quadrotor dynamics as

$$\begin{aligned} \mathbf{F}_{M,i} &= \begin{bmatrix} 0 \\ 0 \\ -4K_{t,0} - K_t(\Omega_1^2 + \Omega_2^2 + \Omega_3^2 + \Omega_4^2) \end{bmatrix}, \\ \boldsymbol{\tau}_{V,i} &= \begin{bmatrix} K_t(-\Omega_1^2 - \Omega_2^2 + \Omega_3^2 + \Omega_4^2)d \\ K_t(\Omega_1^2 - \Omega_2^2 - \Omega_3^2 + \Omega_4^2)d \\ 4K_{r,0} + K_r(\Omega_1^2 - \Omega_2^2 + \Omega_3^2 - \Omega_4^2) \end{bmatrix} \\ &+ \begin{bmatrix} I_{r_i} q_i(\Omega_1 - \Omega_2 + \Omega_3 - \Omega_4) \\ -I_{r_i} p_i(\Omega_1 - \Omega_2 + \Omega_3 - \Omega_4) \\ 0 \end{bmatrix}, \end{aligned} \tag{6.29}$$

where $K_t$ is the thrust coefficient, $K_r$ the torque coefficient, $d$ the distance between the rotors, $\Omega$ the rotational speed of each rotor, and $\omega_{V,i} = [p_i, q_i, r_i]^T$ the angular rate of the vehicle.

The control allocation of the quadrotor vehicle from the roll, pitch, yaw, and thrust commands to the rotor speeds is

$$\begin{bmatrix} \Omega_1 \\ \Omega_2 \\ \Omega_3 \\ \Omega_4 \end{bmatrix} = K_{c,0} + K_c \begin{bmatrix} 0.5 & 0.5 & -1 & 1 \\ -0.5 & 0.5 & 1 & 1 \\ -0.5 & -0.5 & -1 & 1 \\ 0.5 & -0.5 & 1 & 1 \end{bmatrix} \begin{bmatrix} u_{roll} \\ u_{pitch} \\ u_{yaw} \\ u_{thrust} \end{bmatrix}, \tag{6.30}$$

where $K_c$ is the control allocation coefficient.

For the linearised dynamics, the state and control input vector of the slung-load dynamics are defined as

$$\begin{aligned} x(t) = [&\boldsymbol{\theta}_i^T(t), \boldsymbol{\theta}_{V,i}^T(t), \mathbf{x}_L^T(t), \boldsymbol{\theta}_L^T(t), \\ &\dot{\boldsymbol{\theta}}_i^T(t), \boldsymbol{\omega}_{V,i}^T(t), \dot{\mathbf{x}}_L^T(t), \boldsymbol{\omega}_L(t)^T]^T \in \mathbb{R}^n, \\ u(t) = [&u_{roll}(t), u_{pitch}(t), u_{yaw}(t), u_{thrust}(t)]^T \in \mathbb{R}.^m, \end{aligned} \tag{6.31}$$

where the number of the states $n$ equals to $10N+12$ and the number of the control inputs $m$ is $4N$, where $N$ is the number of the UAVs.

### 6.5.2 Simulation Settings

Table 6.1: Slung-load system specification

| | | **Case 1** | **Case 2** | **Case 3** |
|---|---|---|---|---|
| Quadrotor | Number | 1 | 2 | 4 |
| | Mass (kg) | 0.408 | | |
| | Size (m) | $\phi$ 0.356 | | |
| | Inertia (kg·m$^2$) | 2.2842·10-3 × 2.4451·10-3 × 4.4562·10-3 | | |
| | Thrust Coefficient (N) | $K_t = 8.1763 \cdot 10^{-6}, \quad K_{t,0} = 0.0562$ | | |
| | Torque Coefficient (N·m) | $K_r = 2.1703 \cdot 10^{-7}, \quad K_{r,0} = 1.0950 \cdot 10^{-4}$ | | |
| | Control Allocation Coefficient (rad/s) | $K_c = 0.7326, \quad K_{c,0} = 1.2694 \cdot 10^2$ | | |
| Payload | Nominal Mass (kg) | 0.1 | 0.2 | 0.4 |
| | Size (m) | 0.2 × 0.2 × 0.2 | 0.2 × 0.2 × 1.0 | 0.2 × 1.0 × 1.0 |
| String | Mass (kg) | None | | |
| | Size (m) | 1.4 | | |

The numerical simulation is set with uncertainty in the mass of payload and nonlinear dynamics on the quadrotor dynamics. The tracking performance and parameter estimation of the proposed control synthesis method are evaluated in three slung-load systems: 1-, 2-, and 4-quadorotor systems.

The dynamic coefficients of the quadrotor, and the dimension of the payload and string are specified in the Table 6.1. The strings are attached on the top surface of the payload, and below each quadrotor with a distance of $||\mathbf{x}_{V,ai}|| = 0.1$ m from the centre of mass.

The actual mass of payload is considered as 120% of the nominal mass, i.e. $\Delta m_L =$

$0.2m_{L,nominal}$, creating the variation on the system matrix $A$ as

$$\begin{aligned}\Delta A &= \mathbf{U}_1 \left(\mathbf{I}_{N\times N} \otimes \Delta A_i\right) \mathbf{U}_2 \\ \Delta A_i &= -\frac{\Delta m_L g}{N} \begin{bmatrix} \mathbf{U}_3 \mathbf{M}_{V,i}^{-1} \mathbf{U}_4 \\ ||\mathbf{x}_{V,ai}|| \mathbf{I}_{V,i}^{-1} \mathbf{U}_4 \end{bmatrix}\end{aligned} \tag{6.32}$$

where the unit permutation matrices $\mathbf{U}$'s are

$$\begin{aligned}\mathbf{U}_1 &= [\mathbf{I}_{5N\times 5N} \quad \mathbf{0}_{5N\times(5N+12)}]^T \\ \mathbf{U}_2 &= [\mathbf{0}_{5N\times(5N+6)} \quad \mathbf{I}_{5N\times 5N} \quad \mathbf{0}_{5N\times 6}] \\ \mathbf{U}_3 &= [\mathbf{I}_{2\times 2} \quad \mathbf{0}_{2\times 1}] \\ \mathbf{U}_4 &= \begin{bmatrix} \mathbf{I}_{2\times 2} & \mathbf{I}_{2\times 2} & \mathbf{0}_{2\times 1} \\ \mathbf{0}_{1\times 2} & \mathbf{0}_{1\times 2} & 0 \end{bmatrix}\end{aligned} \tag{6.33}$$

The variation $\Delta A$ leads to the unmatched uncertainty as

$$N^* = -\mathbf{U}_2^T \left( \mathbf{I}_{N\times N} \otimes \frac{\Delta m_L g}{N} \mathbf{U}_3 \mathbf{M}_{V,i}^{-1} \mathbf{U}_4 \right)^T \tag{6.34}$$

The nonlinear uncertainty is considered on the dynamics of a quadrotor as

$$\begin{aligned} W^* &= \mathbf{I}_{N\times N} \otimes [1 \quad 0 \quad 0 \quad -0.8] \\ \Phi(x) &= [x_3^2 \quad x_8^2 \quad \cdots \quad x_{5(N-1)+3}^2]^T \end{aligned} \tag{6.35}$$

where $x_{5(i-1)+3}$ is the roll rate of each quadrotor as defined in Eqn. (6.31).

The external reference command $r(t)$ is applied on the position of each quadrotor with

the change in every 10s as

$$\begin{aligned} r(t) &= [x_{cmd}, y_{cmd}, z_{cmd}]^T \\ &= \begin{bmatrix} 1 \\ 1 - h(t-10) - h(t-20) + h(t-30) \\ -h(t-10) \end{bmatrix} \end{aligned} \tag{6.36}$$

where $h(t)$ is the unit step function.

The gains of PRLQG are designed as $Q = 1$ for the position and attitude states, $Q = 0.5$ for their derivatives, and $R = 10$ for the control inputs. The weight of PRLQG is chosen as $w_{PR} = 10$. The adaptation gains are set as $\Gamma = 10^3$ and $\sigma = 10^{-5}$.

### 6.5.3 Simulation Results

The tracking error $||e(t)||_2$, parameter estimation error $||\tilde{W}^T(t)\tilde{W}(t)||_2$, and thrust control input of a quadrotor are shown in Fig. 6.2. The figures (a), (b), and (c) show the response of the slung-load system with 1, 2, and 4 quadrotors, respectively.

The simulation is conducted with three different controls for the reference: the proposed control synthesis method, the PRLQG method without adaptation, and the adaptive control on the baseline controller with LQG gain. The three control schemes are applied in all the scenario cases, but the diverging responses are not shown in the figure. Note that only the responses of the proposed control remain stable and are able to be plotted on all the cases. The PRLQG method diverges on the point $t = 30$ s in Case 1, and has rapid oscillations in the quadrotor attitude with the strictly large tracking errors compared with the control synthesis method. The adaptive control is stable when the number of quadrotor is large and the effect of the variation of the payload's mass is smaller than the other cases. Whereas the matched parameter is estimated similarly with the adaptive PRLQG, the tracking error shows undesirable response for the presence of unmatched uncertainties. The matched and unmatched uncertainties are successfully suppressed only by the control synthesis among the three control schemes.

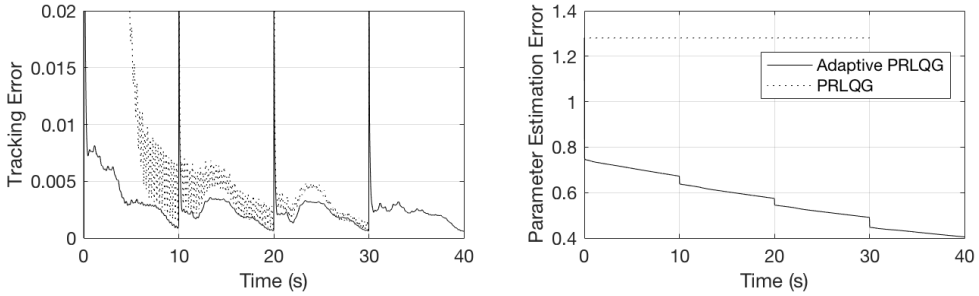


(i) Case 1: Single quadrotor transportation system

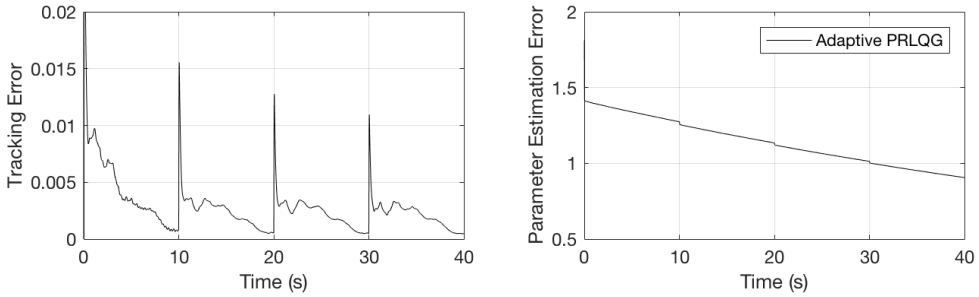


(ii) Case 2: 2-quadrotor transportation system

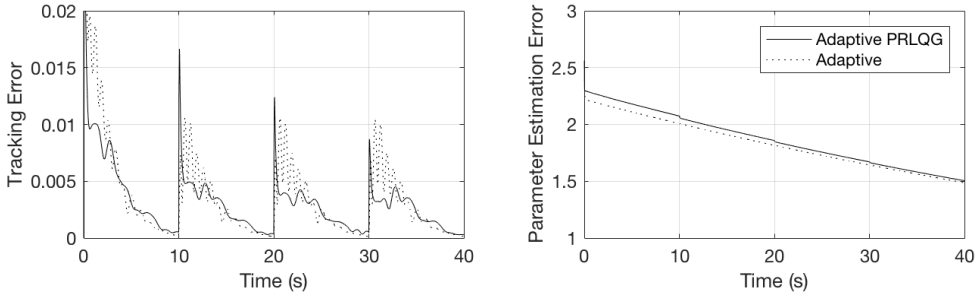


(iii) Case 3: 4-quadrotor transportation system

Figure 6.2: Simulation results of tracking and parameter estimation error

The tracking error of the control synthesis is not only stable, but also shows similarities with respect to different slung-load systems: the sudden increase of tracking error at the signal excitation gradually diminishes as the parameter estimation converges, and the scale of the peak error is bounded. This implies that the proposed control method can be applied for the slung-load system with general number of UAVs.

## 6.6 Conclusions

In this chapter, we proposed an control synthesis to effectively suppress the effect of uncertainty of the multi-UAV slung-load system. The rationale behind the idea was that although the slung-load system has considerable unmatched uncertainties which are neither estimated or controlled with common adaptive controls, the baseline controller can be designed to be robust to the unmatched uncertainties through the PRLQG method. The stability conditions of the proposed control method were obtained through Lyapunov analysis. The numerical simulations demonstrate that the proposed adaptive PRLQG approach effectively cancels out the effect of both unmatched and matched uncertainties in three different slung-load systems with a potential to be extended to incorporate more UAVs.

# References

[71] H.-I. Lee, D.-W. Yoo, B.-Y. Lee, G.-H. Moon, D.-Y. Lee, M.-J. Tahk, and H.-S. Shin. “Parameter-robust linear quadratic Gaussian technique for multi-agent slung load transportation”. In: *Aerospace Science and Technology* 71 (2017), pp. 119–127.

[82] H.-I. Lee, B.-Y. Lee, D.-W. Yoo, G.-H. Moon, and M.-J. Tahk. “Dynamics Modeling and Robust Controller Design of the Multi-Uav Transportation System”. In: *29th Congress of the International Council of the Aeronautical Sciences* (2014).

[86] M.-J. Tahk and J. L. Speyer. “Modeling of Parameter Variations and Asymptotic LQG Synthesis”. In: *IEEE Transactions on Automatic Control* 32.9 (1987), pp. 793–801.

[87] M.-J. Tahk and J. L. Speyer. “Parameter Robust Linear- Quadratic-Gaussian Design Synthesis with Flexible Structure Control Applications”. In: *Journal of Guidance, Control, and Dynamics,* 12.4 (1988), pp. 460–468.

[89] D. Kingston, R. Beard, and R. Holt. “Decentralized Perimeter Surveillance Using a Team of UAVs”. In: *IEEE Transactions on Robotics* 24.6 (2008), pp. 1394–1404.

[90] D. Bein, W. Bein, A. Karki, and B. Madan. “Optimizing Border Patrol Operations Using Unmanned Aerial Vehicles”. In: 2015, pp. 479–484.

[91] S. Minaeian, J. Liu, and Y.-J. Son. “Vision-Based Target Detection and Localization via a Team of Cooperative UAV and UGVs”. In: *IEEE Transactions on Systems, Man, and Cybernetics: Systems* 46.7 (2016), pp. 1005–1016.

[92] R. Pitre, X. Li, and R. Delbalzo. “UAV Route Planning for Joint Search and Track Mission - An Informative-Value Approach”. In: *IEEE Transactions on Aerospace and Electronic Systems* 48.3 (2012), pp. 2551–2565.

[93] B. Lim, J. Kim, S. Ha, and Y. Moon. “Development of software platform for monitoring of multiple small UAVs”. In: vol. 2016-December. 2016.

[94] P. Li and H. Duan. “A potential game approach to multiple UAV cooperative search and surveillance”. In: *Aerospace Science and Technology* 68 (2017), pp. 403–415.

[95] A. Puri. *A survey of Unmanned Aerial Vehicles (UAV) for Traffic Surveillance*. Tech. rep. Department of Computer Science and Engineering, University of South Florida, 2004.

[96] E. Carapezza and D. Law. “Sensors, C3I, Information, and Training Technologies for Law Enforcement”. In: *Proc. SPIE*. 1999.

[97] A. Belbachir and J.-A. Escareno. “Autonomous decisional high-level planning for UAVs-based forest-fire localization”. In: vol. 1. 2016, pp. 153–159.

[98] B. R. Barmish and G. Leitmann. “On Ultimate Boundedness Control of Uncertain Systems in the Absence of Matching Assumptions”. In: *IEEE Transactions on Automatic Control* 116.1 (1982), pp. 153–155.

[99] B.-j. Yang, T. Yucelen, and J.-y. Shin. “An LMI-based Analysis of an Adaptive Flight Control”. In: *AIAA Infotech@Aerospace 2010* (2010).

[100] C. Cao and N. Hovakimyan. “Design and Analysis of a Novel L1 Adaptive Control”. In: *IEEE Transactions on Automatic Control* 53.2 (2008), pp. 586–591.

[101] N. T. Nguyen and S. N. Balakrishnan. “Bi-objective optimal control modification adaptive control for systems with input uncertainty”. In: *IEEE/CAA Journal of Automatica Sinica* 1.4 (2014), pp. 423–434.

[102] T. I. Fossen and S. I. Sagatun. “Adaptive control of nonlinear systems: A case study of underwater robotic systems”. In: *Journal of Robotic Systems* 8.3 (1991), pp. 393–412.

[103] A. C. Huang and Y. C. Chen. “Adaptive sliding control for single-link flexible-joint robot with mismatched uncertainties”. In: *IEEE Transactions on Control Systems Technology* 12.5 (2004), pp. 770–775.

[104] B. Meng, C. Gao, S. Tang, and Y. Liu. “Adaptive Variable Structure Control for Linear Systems with Time-varying Multi-delays and Mismatching Uncertainties”. In: *Physics Procedia* 33.60974025 (2012), pp. 1753–1761.

[105] J. F. Quindlen, G. Chowdhary, and J. P. How. “Hybrid model reference adaptive control for unmatched uncertainties”. In: *2015 American Control Conference (ACC)* (2015), pp. 1125–1130.

# Chapter 7

# Concurrent Learning Adaptive Control with Directional Forgetting

## Abstract

This chapter proposes a new concurrent learning based adaptive control algorithm. The main objective behind our proposition is to relax the persistent excitation requirement for the stability guarantee, while providing the ability to identify time-varying parameters. To achieve the objective, this chapter designs a directional forgetting algorithm, which is then integrated with the adaptive law. The theoretical stability analysis shows that the tracking and parameter estimation error is exponentially stable with the signal only finitely excited, not persistently excited. The analysis also shows that the proposed algorithm can guarantee the stability under time-varying parameters. Moreover, the necessary and sufficient conditions for the stability given the time-varying parameters are derived. The results of numerical simulations confirm the validity of the theoretical analysis results and demonstrate the performance of the proposed algorithm.

## 7.1 Introduction

model reference adaptive control (MRAC) has been widely used for estimating the uncertainty and canceling out its effect from the system to achieve the nominal designed performance [106]. One of the main issues of the MRAC is that the persistence of excitation (PE) is required for the parameter estimation to be converged. The PE corresponds to the continuous change in the states, which is undesirable for the control performance as it contradicts with obtaining the steady-state, and may contribute to the waste of energy.

There have been great efforts made to relax the PE requirement. Earlier studies on the relaxation of the PE requirement for parameter convergence include the concurrent learning (CL) based method [107, 108] and its modifications [109, 110, 111]. Conceptually, the PE condition is required since the adaptive law is rank-1 and thus the inputs are required to be persistently excited in every direction to span the parameter estimation error. The common principle to relax the dependence on PE in CL based methods is to use the stored data containing information from the Finite Excitation (FE) in the past together with the current data. In this way, the rank deficiency of an information matrix is expected to be solved after sufficient accumulation of data, and this is the key of relaxation.

The issue with these methods is that the parameter convergence is difficult to be guaranteed if parameters are time varying. The information accumulated before a parameter change contains only the information about the previous parameters. After the parameter change, the information about the parameters changed starts to be accumulated. Roughly speaking, since the information matrix contains both the previous parameters and those changed, utilising this information matrix is difficult to guarantee the convergence to time-varying parameters. Especially when the information about previous parameters is rich, the convergence issue could be exacerbated. The CL based methods thus may not guarantee the stability of parameter estimation for the systems with time-varying parameters, such as the control of strip temperature for heating furnaces, automation of the heavy duty vehicles, and self-tuning cruise control [112, 113, 114].

Forgetting the previous information could address convergence issue under the time-

varying parameters: various forgetting algorithms have been used in the online parameter estimation [115] to cope with the time-varying parameters. Note that an adaptive control architecture for uncertain dynamic system consists of two principal components: one is the adaptive element in the control law and the other is the adaptation law. The adaptive element in the control law is usually a function approximator to cancel out the effect of uncertainty from the tracking error dynamics. The adaptation law is in principle a regression algorithm working for better approximation of uncertainty. Therefore, it is clear that the forgetting methods can be applied to the adaptation law and thus integrated to CL methods.

Cho *et al.* [111] developed a composite MRAC algorithm to relax the PE requirement. Based on the filtered regressor, they integrated the exponential forgetting method in the composite MRAC. The potential issue is that their proposed algorithm requires PE condition for the forgetting algorithm. To avoid the PE requirement in the typical exponential forgetting methods for the stability guarantee [116, 117], they applied the exponential forgetting only when the minimum eigenvalue of the stacked data increases. However, the forgetting is not working in the modified forgetting algorithm when the signal is not persistently exited. Therefore, the PE condition is again crucial either for the convergence of parameter estimation or for the forgetting of past information.

This chapter proposes a new CL adaptive control algorithm to relax the PE requirement and also to handle the convergence issue under time-varying parameters. The key idea of the proposed adaptive control algorithm is to integrate directional forgetting to the adaptation law. Note that the directional forgetting method [118, 119, 120] was intended to avoid the estimator windup – zero eigenvalue of the information matrix – by forgetting the old data only in the direction of new data. In this chapter, its objective is extended to guarantee the stability of the both tracking and parameter estimation error. To achieve this objective, we modify the directional forgetting proposed in [120] and apply it to the adaptation law. As the modified directional forgetting accumulates the data and maintains the stacked data, the PE condition can be directly relaxed. Moreover, since it discounts

the information in the direction of new data, forgetting is always working on the non-zero signals after FE. This could relax the PE condition for forgetting the past data and consequently provide the convergence of time-varying parameters.

The characteristics of the new CL adaptive are analytically and empirically investigated. The stacked data is first proven to be always lower bounded by a positive value and thus full-rank. Then, this chapter shows that the past information is consistently forgotten but maintains its ability to estimate parameter uncertainty without requiring the PE condition. The stability of tracking and parameter estimation under the presence of parameter change is also theoretically analysed by assuming the discrete changes in parameters. The stability conditions depend on the size of parameter change and forgetting rate, providing the design trade-offs of forgetting rate. The numerical results on the wingrock dynamics confirm the stability analysis results and demonstrate the effect of forgetting rate.

The rest of the chapter is organised as follows. In Section 7.2, mathematical preliminaries with definitions and lemmas are given for later proofs. The control problem with the parameterised uncertainty is formulated in Section 7.3. In Section 7.5, the adaptive control with directional forgetting is suggested, and the bounds of the information and the stability conditions are examined. The numerical simulations in Section 7.6 show the performance of the proposed control and support the theoretic stability conditions. The chapter is concluded in Section 7.7.

## 7.2 Preliminaries

The PE condition is crucial for the common MRAC methods and the parameter estimation with exponential forgetting. This research intends to relax the PE condition to FE which requires exciting signals only for a finite time interval. The PE and FE conditions are defined as in [121].

**Definition 3** (Persistence of Excitation (PE))**.** *A bounded vector signal $q(t)$ is persistently*

*exciting if there exist* $T > 0$ *and* $\gamma > 0$ *such that*

$$\int_t^{t+T} q(\tau)q(\tau)^T d\tau \geq \gamma I, \qquad \forall t \geq t_0 \tag{7.1}$$

**Definition 4** (Finite Excitation (FE))**.** *A bounded vector signal* $q(t)$ *is finitely exciting over a time set* $[t_s, t_s + T]$ *if there exist* $t_s \geq t_0$*,* $T > 0$ *and* $\gamma > 0$ *such that*

$$\int_{t_s}^{t_s+T} q(\tau)q(\tau)^T d\tau \geq \gamma I \tag{7.2}$$

The following Lemmas utilise the characteristics of spectral radius, determinant, and trace to obtain the bound of a matrix. These Lemmas are used in Theorem 8 and 9 to prove the lower and upper bounds of the information.

**Lemma 4.** *For a Hermitian positive semi-definite matrix* $A \in \mathbb{R}^{n\times n}$*,* $A \leq I$ *if and only if* $\rho(A) \leq 1$*, where the spectral radius* $\rho(\cdot)$ *is defined as the largest absolute value of the eigenvalues of a matrix.*

*Proof.* Refer to Appendix A and Theorem 7.7.3 in [122]. □

**Lemma 5.** *For any square matrix* $A \in \mathbb{R}^{n\times n}$*,*

$$\det(\exp(A)) = \exp(tr(A)) \tag{7.3}$$

*Proof.* Refer to Appendix A and Section 8.3 in [123]. □

**Lemma 6.** *If a matrix* $A \in \mathbb{R}^{n\times n}$ *is positive-definite,*

$$\det(A) \leq \left(\frac{tr(A)}{n}\right)^n \tag{7.4}$$

## 7.3 Problem Formulation

Consider a state-space representation as:

$$\dot{x}(t) = Ax(t) + B(u(t) + \Delta(t)), \tag{7.5}$$

where $x(t) \in \mathbb{R}^n$, $u(t) \in \mathbb{R}^m$, and $\Delta(t) \in \mathbb{R}^m$ stand for state, input, and uncertainty vector, respectively. The system matrices $A \in \mathbb{R}^{n\times n}$ and $B \in \mathbb{R}^{n\times m}$ are assumed to be constant and controllable.

The uncertainty $\Delta(t)$ is assumed to be linearly parametrised as:

$$\Delta(t) = W^{*T}(t)\Phi(x(t)), \tag{7.6}$$

where $W^*(t) \in \mathbb{R}^{p\times m}$ is the unknown true parameter matrix, and $\Phi(x(t)) \in \mathbb{R}^p$ is the basis vector.

## 7.4 Control Design

The controller is designed in two parts as:

$$u(t) = u_{base}(t) - u_{ad}(t) \tag{7.7}$$

where the baseline control $u_{base}(t)$ determines the nominal performance of the control and the adaptive control $u_{ad}(t)$ alleviates the effect of uncertainty.

### 7.4.1 Baseline Controller

The baseline controller is designed as $u_{base}(t) = -Kx(t) + K_r r(t)$ such that the system is stable and tracks the reference input $r(t) \in \mathbb{R}^m$. The reference model, the model without

any parameter uncertainty, is obtainted as

$$\dot{x}_r = A_r x_r(t) + B_r r(t) \tag{7.8}$$

where $x_r(t) \in \mathbb{R}^n$ is the reference state. The input matrix of the reference model is defined with respect to the reference input matrix $K_r \in \mathbb{R}^{m\times m}$ as $B_r = BK_r$. The control gain $K \in \mathbb{R}^{m\times n}$ is determined such that the system matrix of the reference model, $A_r = A - BK$, is Hurwitz stable. Then, there exists a positive definite symmetric matrix $P \in \mathbb{R}^{n\times n}$ satisfying the following Lyapunov equation:

$$A_r^T P + PA_r = Q \tag{7.9}$$

Defining the tracking error as $e(t) = x_r(t) - x(t)$, the tracking error dynamics is given by

$$\dot{e}(t) = A_r e(t) + B\varepsilon(t) \tag{7.10}$$

where $\varepsilon(t) \triangleq u_{ad}(t) - \Delta(t)$ is the adaptation error.

Assuming that the uncertainty lies in the span of the input matrix $B$, the uncertainty is accessed as:

$$\Delta(t) = B^+(\dot{e}(t) - A_r e(t)) + u_{ad}(t), \tag{7.11}$$

where $B^+$ is a pseudoinverse of $B$.

Note that the derivative of the tracking error, $\dot{e}(t)$ in Eqn. (7.11), cannot be perfectly known and should be approximated. To alleviate this issue, various filters, such as fixed-point smoother [109] and a low-pass filter [111], can be used. Using one of the filters, the filtered vector of $\Delta(t)$ is obtained and denoted as $c(t)$. For instance, using a low-pass

filter, the Laplace transform of Eqn. (7.11) is expressed in the $s$-domain as:

$$\begin{aligned} c(s) \triangleq \Delta_f(s) &= \frac{1}{\tau s+1} \cdot \left(B^+(sI-A_r)e(s)+u_{ad}(s)\right) \\ &= B^+\left(\frac{1}{\tau}e(s)-\left(\frac{1}{\tau}I+A_r\right)e_f(s)\right)+u_{ad,f}(s) \end{aligned} \tag{7.12}$$

where $\tau$ is the time-constant of a low-pass filter $1/(\tau s+1)$, and the subscript $f$ denotes for the filtered vectors. The inverse Laplace transform yields in the filtered system dynamics in the $t$-domain as:

$$\begin{aligned} c(t) &\triangleq \xi(t)-\frac{1}{\tau}B^+e(t) = W^{*T}q(t) \\ \dot{\xi}(t) &= \frac{1}{\tau}\left(-B^+\left(\frac{1}{\tau}I+A_r\right)e(t)+u_{ad}(t)-\xi(t)\right) \end{aligned} \tag{7.13}$$

where $q(t)$ denotes the filtered vector of $\Phi(x(t))$, and $\xi(t)$ is an auxiliary variable to compute $c(t)$.

### 7.4.2 Adaptive Law

The adaptive control is designed to cancel out the effect of uncertainty from the tracking error dynamics in Eqn. (7.8) by estimating the parameter as

$$u_{ad}(t) = \hat{W}^T(t)\Phi(x(t)) \tag{7.14}$$

Here, the estimated parameter vector $\hat{W}(t) \in \mathbb{R}^{l\times m}$ is determined by an adaptive law. The adaptive law used in this research is the summation of gradient descent method and the information-based parameter estimation as:

$$\dot{\hat{W}}(t) = \Gamma\left(\underbrace{\Phi(x)e^T(t)PB}_{\text{gradient descent}} - \underbrace{\gamma_b(\Omega(t)\hat{W}(t)-M(t))}_{\text{information architecture}}\right) \tag{7.15}$$

where $\Gamma \in \mathbb{R}^{p\times p}$, and $\gamma_b \in \mathbb{R}^{p\times p}$ are the adaptive gains for gradient descent and information architecture, respectively. Also, $\Omega(t) \in \mathbb{R}^{p\times p}$, and $M(t) \in \mathbb{R}^{p\times p}$ are the information

matrix and auxiliary matrix, respectively.

The information matrix is the accumulation of measured basis vectors, and the auxiliary matrix is that of the filtered uncertainty. Once the FE condition is satisfied, both the information and auxiliary matrices are forgotten with the directional forgetting method. The dynamics of the accumulation and forgetting method is expressed as

$$\dot{\Omega}(t) = \begin{cases} q(t)q^T(t) & \text{if } rank(\Omega(t)) < rank(\Omega(t)+q(t)q^T(t)) \\ -k\dfrac{\Omega(t)q(t)q^T(t)}{q^T(t)\Omega(t)q(t)}\Omega(t)+q(t)q^T(t) & \text{otherwise} \end{cases}$$
$$\dot{M}(t) = \begin{cases} q(t)c^T(t) & \text{if } rank(\Omega(t)) < rank(\Omega(t)+q(t)q^T(t)) \\ -k\dfrac{\Omega(t)q(t)q^T(t)}{q^T(t)\Omega(t)q(t)}M(t)+q(t)c^T(t) & \text{otherwise} \end{cases} \tag{7.16}$$

where $k \in \mathbb{R}$ is a positive constant.

## 7.5 Lyapunov Stability Analysis

### 7.5.1 Lower and Upper Bounds of the Information Matrix

The value of the information matrix is directly related to the convergence rate of the parameter estimation as in Eqn. (6.15), and thus the bounds of the information matrix are inferred to be crucial for proving the stability of parameter estimation and for finding the convergence rate. The following theorems give the lower and upper bounds of the information matrix.

**Theorem 8** (Lower bound of the information matrix)**.** *If there exist a constant* $\gamma > 0$ *and* $t_1 > t_0$ *such that*

$$\Omega(t_1) \geq \gamma I, \tag{7.17}$$

*there exists a constant* $\alpha > 0$ *such that*

$$\Omega(t) \geq \alpha I, \qquad \forall t \geq t_1 \tag{7.18}$$

*Proof.* Let the subspace which is excited by $q(t)$ as $\phi$ with its dimension $m$, and the unexcited subspace as $\phi^{\perp}$. The information matrix can be decomposed as

$$\Omega(t) = \Omega_o(t) + \Omega_p(t), \qquad \Omega_o(t)q(t) = 0 \tag{7.19}$$

where each part $\Omega_o(t)$ and $\Omega_p(t)$ satisfies the following equations:

$$\begin{aligned} \dot{\Omega}_o(t) &= 0 \\ \dot{\Omega}_p(t) &= -k\frac{\Omega_p(t)q(t)q^T(t)}{q^T(t)\Omega_p(t)q(t)}\Omega_p(t) + q(t)q^T(t) \end{aligned} \tag{7.20}$$

Defining an orthogonal matrix $U = [U_1 \quad U_2]$ where the columns of $U_1 \in \mathbb{R}^{n\times m}$ are the orthogonal basis for $\phi$ and those of $U_2 \in \mathbb{R}^{n\times(n-m)}$ are the orthogonal basis for $\phi^{\perp}$, the following equation is obtained.

$$U^T\dot{\Omega}(t)U \geq \begin{bmatrix} \left(-kU_1^T\dfrac{\Omega_p(t)q(t)q^T(t)}{q^T(t)\Omega_p(t)q(t)}U_1\right)U_1^T\Omega_p(t)U_1 + U_1^Tq(t)q^T(t)U_1 & 0 \\ 0 & 0 \end{bmatrix} \tag{7.21}$$

Here, the forgetting part, $U_1^T\Omega_p(t)U_1$ is structured as

$$U_1^T\Omega_p(t)U_1 = \Psi(t,t_1)U_1^T\Omega_p(t_1)U_1 + \int_{t_1}^{t}\Psi(t,\tau)U_1^Tq(\tau)q^T(\tau)U_1 d\tau \tag{7.22}$$

where $\Psi(t,t_1) \in \mathbb{R}^{l\times l}$ is the transition matrix from time $t_1$ to $t$. The lower bound of the

transition matrix is obtained using Lemma 4 as

$$\Psi(t,t_1) = \exp\left(-k\int_{t_1}^{t} U_1^T \frac{\Omega_p(\tau)q(\tau)q^T(\tau)}{q^T(\tau)\Omega_p(\tau)q(\tau)}U_1 d\tau\right) \geq e^{-k(t-t_1)}I \tag{7.23}$$

As a matrix $U_1^T q(\tau)q^T(\tau)U_1 > 0$ acts as the persistent excitation, there exists a constant $\alpha > 0$ such that

$$U_1^T \Omega_p(t)U_1 \geq e^{-k(t-t_1)}U_1^T \Omega_p(t_1)U_1 + \alpha I \tag{7.24}$$

The non-forgetting part, $U_2^T \Omega_o(t)U_2$, is obtained as

$$U_2^T \Omega_o(t)U_2 = U_2^T \Omega_o(t_1)U_2 \tag{7.25}$$

Assuming $\Omega(t_1) \geq \gamma I$, the solution of the equation (7.21) is thus lower-bounded as

$$U^T \Omega(t)U \geq \min(\gamma e^{-k(t-t_1)} + \alpha, \gamma)I \tag{7.26}$$

As the matrix $U$ is an orthogonal matrix and the positive value $\alpha$ can be chosen to be $\gamma$, the lower bound of the information matrix is obtained as

$$\Omega(t) \geq \alpha I \tag{7.27}$$

□

**Theorem 9** (Upper bound of the information matrix)**.** *If there exist a constant $\gamma > 0$ and $t_1 > t_0$ such that*

$$\Omega(t_1) \geq \gamma I, \tag{7.28}$$

*and the signal is bounded, i.e. $|q(t)| < c$, there exists a constant $\beta > 0$ such that*

$$\Omega(t) \leq \beta I, \qquad \forall t > t_1 \tag{7.29}$$

*Proof.* The forgetting dynamics of the information matrix results in

$$\Omega(t) = \Psi(t,t_1)\Omega(t_1) + \int_{t_1}^{t} \Psi(t,\tau)q(\tau)q^T(\tau)d\tau \tag{7.30}$$

where the transition matrix is defined as

$$\Psi(t,t_1) = \exp\left(-k\int_{t_1}^{t} \frac{\Omega(\tau)q(\tau)q^T(\tau)}{q^T(\tau)\Omega(\tau)q(\tau)}d\tau\right) \tag{7.31}$$

Using Lemma 5, the determinant of the information matrix is computed as

$$\det(\Omega(t)) = \exp^{-k(t-t_1)}\det(\Omega(t_1)) + \int_{t_1}^{t} \exp^{-k(t-\tau)}\det(q(\tau)q^T(\tau))d\tau \tag{7.32}$$

If the signal is bounded, i.e. $|q(t)| < c$, the determinant of the matrix $q(\tau)q^T(\tau)$ is also bounded by Lemma 6.

$$\det(q(\tau)q^T(\tau)) \leq \left(\frac{q^T(\tau)q(\tau)}{p}\right)^p \leq \left(\frac{c^2}{l}\right)^p \triangleq C \tag{7.33}$$

Therefore, the determinant of the information matrix is upper-bounded as

$$\det(\Omega(t)) \leq \exp^{-k(t-t_1)}\det(\Omega(t_1)) + \frac{C}{k}\left(1-\exp^{-k(t-t_1)}\right) \tag{7.34}$$

As the information matrix is positive definite by Theorem 8, the upper bound of the information matrix is obtained with a constant $\beta > 0$ as

$$\Omega(t) \leq \beta I \tag{7.35}$$

□

### 7.5.2 Stability Analysis

Using that the information matrix is lower-bounded to be positive definite even without the persistent excitation, the tracking error and the parameter estimation error can be proved to be stable by the following theorem.

**Theorem 10** (Stability in $(e,\tilde{W})$)**.** *If there exists $t_1 > t_0$ such that*

$$\Omega(t_1) \geq \gamma I, \tag{7.36}$$

*the tracking error e and the parameter estimation error $\tilde{W}$ are globally uniformly exponentially stable for $t > t_1$.*

*Proof.* The explicit forms of the information matrix and the auxiliary matrix are expressed as

$$\begin{cases} \Omega(t) = \Psi(t,t_0)\Omega(t_0) + \int_{t_0}^{t} \Psi(t,\tau)q(\tau)q^T(\tau)d\tau \\ M(t) = \Psi(t,t_0)M(t_0) + \int_{t_0}^{t} \Psi(t,\tau)q(\tau)c^T(\tau)d\tau \end{cases} \tag{7.37}$$

Assuming that the initial values of the information and auxiliary matrix are zero, the following equation is obtained:

$$\Omega(t)\hat{W}(t) - M(t) = \Omega(t)\tilde{W}(t) \tag{7.38}$$

The Lyapunov function is defined as

$$V(e,\tilde{W}) = \frac{1}{2}e^T(t)Pe(t) + \frac{1}{2}tr(\tilde{W}^T(t)\Gamma^{-1}\tilde{W}(t)), \tag{7.39}$$

where $\tilde{W}(t) \triangleq \hat{W}(t) - W^*(t)$ is the parameter estimation error. Defining an augmented vector $\xi(t) \triangleq [e^T(t), \tilde{W}^T(t)]$, the upper bound of the Lyapunov function is given as

$$V(e,\tilde{W}) \leq \frac{1}{2}\max(\lambda(P), \lambda(\Gamma^{-1}))||\xi(t)||^2 \tag{7.40}$$

where $\lambda(\cdot)$ is a set of eigenvalues of a matrix.

Substituting the tracking dynamics in Eqn. (7.10) and the adaptive law in Eqn. (7.15) to the derivative of Eqn. (7.39), the derivative of the Lyapunov function is obtained as

$$\dot{V}(e,\tilde{W}) = -\frac{1}{2}e^T(t)Qe(t) - tr(\tilde{W}^T(t)\gamma_b\Omega(t)\tilde{W}(t)) \tag{7.41}$$

From the Theorem 8, the information matrix is lower bounded, and thus the derivative of the Lyapunov function is upper bounded as

$$\dot{V}(e,\tilde{W}) \leq -\frac{1}{2}\min(\lambda(Q),\alpha)||\xi||^2 \tag{7.42}$$

Using the upper bound of the Lyapunov function in Eqn. (7.40),

$$\dot{V}(e,\tilde{W}) \leq -\frac{\min(\lambda(Q),\alpha)}{\max(\lambda(P),\lambda(\Gamma^{-1}))}V(e,\tilde{W}) \tag{7.43}$$

As $V(e,\tilde{W}) > 0$ for all $(e,\tilde{W})$ except the origin, and the lower bound of the information matrix is positive, i.e. $\alpha > 0$, by Theorem 8, $(e,\tilde{W})$ are globally uniformly exponentially stable. □

The main objective of the forgetting algorithms is to cope with the parameter changes. Assume the parameter change with the size of $\Delta W_i^*$ at $t = t_i$ as

$$W^*(t) = W_0^* + \sum_i \Delta W_i^* h(t - t_i) \tag{7.44}$$

where $h(t)$ is the step function.

The sufficient and necessary stability condition under the presence of parameter change is derived in the following theorem.

**Theorem 11** (Stability in $(e,\tilde{W})$ with parameter changes)**.** *The tracking error e and the*

*parameter estimation error $\tilde{W}$ are Lyapunov stable for $t \in [t_i \quad t_{i+1}]$ if and only if*

$$f(e,\tilde{W}) \geq 0, \quad \Omega(t_i) > \gamma I \tag{7.45}$$

*where the function $f(e,\tilde{W})$ is defined as*

$$f(e,\tilde{W}) = \frac{1}{2}e^T(t)Qe(t)I + \Omega(t)\tilde{W}(t)\tilde{W}^T(t) + \sum_{j=1}^{i}\Psi(t,t_j)\Omega(t_j)\Delta W_j^*\tilde{W}^T(t) \tag{7.46}$$

*and the transition matrix $\Psi(t,t_j)$ is*

$$\Psi(t,t_j) = \exp\left(-k\int_{t_j}^{t}\frac{\Omega(\tau)q(\tau)q^T(\tau)}{q^T(\tau)\Omega(\tau)q(\tau)}d\tau\right) \tag{7.47}$$

*Proof.* For the time span $t \in [t_i \quad t_{i+1}]$, the information matrix and the auxiliary matrix are expressed as

$$\begin{cases} \Omega(t) = \Psi(t,t_i)\Omega(t_i) + \int_{t_i}^{t}\Psi(t,\tau)q(\tau)q^T(\tau)d\tau \\ M(t) = \Psi(t,t_i)M(t_i) + \int_{t_i}^{t}\Psi(t,\tau)q(\tau)c^T(\tau)d\tau \end{cases} \tag{7.48}$$

As the values of both information and auxiliary matrices are continuous at the parameter jumps, the following equation is satisfied.

$$\Omega(t)\hat{W}(t) - M(t) = \Omega(t)\tilde{W}(t) + \sum_{j=1}^{i}\Psi(t,t_j)\Omega(t_j)\Delta W_j^* \tag{7.49}$$

Substituting the equation into the same Lyapunov function as the equation (7.39), the derivative of the Lyapunov function is computed as

$$\begin{aligned} \dot{V}(e,\tilde{W}) = &-\frac{1}{2}e^T(t)Qe(t) - tr(\tilde{W}^T(t)\gamma_b\Omega(t)\tilde{W}(t)) \\ &- \sum_{j=1}^{i}tr(\tilde{W}^T(t)\gamma_b\Psi(t,t_j)\Omega(t_j)\Delta W_j^*) \end{aligned} \tag{7.50}$$

The necessary and sufficient condition for $\dot{V}(e,\tilde{W}) \leq 0$ for all $(e,\tilde{W})$ except the origin is

$$\frac{1}{2}e^T(t)Qe(t)I + \Omega(t)\tilde{W}(t)\tilde{W}^T(t) + \sum_{j=1}^{i}\Psi(t,t_j)\Omega(t_j)\Delta W_j^*\tilde{W}^T(t) \geq 0 \tag{7.51}$$

□

In the Theorem 11, the sufficient and necessary condition $f(e,\tilde{W})$ is not deterministic as the transition matrix $\Psi(t,t_j)$ for the time-varying system is almost impossible to obtain. Instead, the following theorem separates the sufficient condition $f_1(e,\tilde{W})$ and the necessary condition $f_2(e,\tilde{W})$, of which the bounds are conservative, but can be computed deterministically.

**Theorem 12.**

1. *The tracking error e and the parameter estimation error $\tilde{W}$ are exponentially stable if $\Delta W_j^*\tilde{W}^T(t_j) \geq 0$ for all $t_j$.*

2. *The tracking error e and the parameter estimation error $\tilde{W}$ are Lyapunov stable if $f_1(e,\tilde{W}) \geq 0$ for $t \in [t_i,t_{i+1}]$, where the function $f_1(e,\tilde{W})$ is defined as*

$$f_1(e,\tilde{W}) = \frac{1}{2}e^T(t)Qe(t)I + \alpha\tilde{W}(t)\tilde{W}^T(t) + \beta\sum_{j=1}^{i}\Delta W_j^*\tilde{W}^T(t) \tag{7.52}$$

3. *The tracking error e and the parameter estimation error $\tilde{W}$ are Lyapunov stable, $f_2(e,\tilde{W}) \geq 0$ for $t \in [t_i,t_{i+1}]$, where the function $f_2(e,\tilde{W})$ is defined as*

$$f_2(e,\tilde{W}) = \frac{1}{2}e^T(t)Qe(t)I + \beta\tilde{W}(t)\tilde{W}^T(t) + \alpha\sum_{j=1}^{i}e^{-k(t-t_j)}\Delta W_j^*\tilde{W}^T(t) \tag{7.53}$$

*Proof.*

1. If $\Delta W_j^* \tilde{W}^T(t) \geq 0$, the derivative of the Lyapunov function under the presence of parameter change in the equation (7.50) is less than or equal to that without the parameter change in the equation (7.41). Converging faster than the exponentially stable case, $(e, \tilde{W})$ is also exponentially stable.

2. If $\Delta W_j^* \tilde{W}^T(t) < 0$, from the bounds of the information matrix and the upper bound of the transition matrix as

$$\alpha I \leq \Omega(t) \leq \beta I, \qquad \Psi(t, t_j) \leq I, \tag{7.54}$$

the following inequality is satisfied.

$$f_1(e, \tilde{W}) \leq f(e, \tilde{W}) \tag{7.55}$$

It follows that if $f_1(e, \tilde{W})$ is positive semi-definite, the stability condition in Theorem 11 is satisfied, i.e. $f(e, \tilde{W}) \geq 0$. If $\Delta W_j^* \tilde{W}^T(t) \geq 0$, $f_1(e, \tilde{W})$ is always positive semi-definite and from the first statement of Theorem 12, the Lyapunov stability is guaranteed. Therefore, $f_1(e, \tilde{W}) \geq 0$ is the sufficient condition for the Lyapunov stability of $(e, \tilde{W})$.

3. If $\Delta W_j^* \tilde{W}^T(t) < 0$, from the bounds of the information matrix and the lower bound of the transition matrix in Eqn. (7.23), the following equation is satisfied.

$$f(e, \tilde{W}) \leq f_2(e, \tilde{W}) \tag{7.56}$$

If the stability condition in Theorem 11 is satisfied, the function $f_2(e, \tilde{W})$ is positive semi-definite. If $\Delta W_j^* \tilde{W}^T(t) \geq 0$, $f_2(e, \tilde{W})$ is always positive semi-definite and is satisfied regardless of the stability of $(e, \tilde{W})$. Therefore, $f_2(e, \tilde{W}) \geq 0$ is the necessary condition for the Lyapunov stability of $(e, \tilde{W})$.

□

Summarising the Theorem 8, 10, and 12, the effect of the parameter change $\Delta W_i^*$ and the forgetting factor $k$ is interpreted in the following remark.

**Remark 3.**

1. *The parameter change $\Delta W_i^*$ in the direction of making $\Delta W_j^* \tilde{W}(t)^T \geq 0$ does not effect on the stability condition.*

2. *If the parameter change $\Delta W_i^*$ lies in the direction of $\Delta W_j^* \tilde{W}^T(t) < 0$, increase in the size of $\Delta W_i^*$ reduces both $f_1(e,\tilde{W})$ and $f_2(e,\tilde{W})$, narrowing down both the necessary and sufficient stability condition.*

3. *When $\Delta W_j^* \tilde{W}^T(t) < 0$, large forgetting factor $k$ increases $f_2(e,\tilde{W})$, enlarging the region for satisfying the necessary condtion.*

4. *Large forgetting factor $k$ results in smaller lower bound of the information matrix, reducing the convergence rate of parameter estimation.*

The value of the forgetting factor $k$ needs to be chosen accordingly, considering the expected change of parameter, its effect on the stability conditions, and the desired convergence rate.

## 7.6 Numerical Simulations

### 7.6.1 Simulation Settings

The wing rock roll dynamics, a common application example of adaptive control for its nonlinearity, is considered. The dynamics is modelled as in [124].

$$\begin{aligned} \dot{\phi} &= p \\ \dot{p} &= I_{xx}^{-1} \frac{1}{2} \rho U_\infty^2 Sb(C_l + C_{l_{\delta_a}} \delta_a) = \Delta(x) + L_{\delta_a} \delta_a, \end{aligned} \tag{7.57}$$

where $\phi$ and $p$ are the roll angle and its rate, and $\delta_a$ and $C_{l_{\delta_a}}$ are the aileron deflection and its nondimensional effectiveness.

Defining the state vector as $x = [\phi \quad p]^T$, the basis vector and the time-varying parameter are modelled as:

$$\begin{cases} \Phi(x) = [1, \phi, p, |\phi|p, |p|, \phi^3]^T \\ W_0^* = [.8, .2314, .6918, -.0624, .0095, .0215]^T \\ \Delta W_1^* = [.8, -.5 \cdot .2314, -.9 \cdot .6918, \\ \qquad -9 \cdot .0624, 2 \cdot .0095, -.3 \cdot .0215]^T \\ t_1 = 50s \end{cases} \tag{7.58}$$

The reference input is given as:

$$\begin{aligned} r(t) = g(t,15) + g(t,55) + g(t,75) \\ + g(t,95) + g(t,115) + g(t,135) \end{aligned} \tag{7.59}$$

where the split square function $g(t,t_i)$ is defined as:

$$g(t,t_i) = \begin{cases} 4 & \text{for } t_i < t \leq t_i + 2 \\ 0 & \text{for } t_i + 2 < t \leq t_i + 10 \\ -4 & \text{for } t_i + 10 < t \leq t_i + 12 \end{cases} \tag{7.60}$$

For the reference, the performance of the proposed adaptive control with the directional forgetting (DF) is compared with that of the integral based concurrent learning (CL) algorithm without forgetting algorithm and the exponential forgetting (EF).

Without any forgetting, the CL method results in infinitely large information matrix, and thus requires an stack-manager algorithm. The stack-manager algorithm used in this

research is given as:

$$\begin{aligned}
&\Omega(t+\Delta t) \\
&= \begin{cases} q(t)q^T(t), & \text{if rank}(\Omega(t))<\text{rank}(\Omega(t)+q(t)q^T(t)) \\ & \text{or } ||\Phi(z(t))-\Phi_{last}||/||\Phi(z(t))||\geq tol \\ \Omega(t), & \text{otherwise} \end{cases} \\
&M(t+\Delta t) \\
&= \begin{cases} q(t)c^T(t), & \text{if rank}(\Omega(t))<\text{rank}(\Omega(t)+q(t)q^T(t)) \\ & \text{or } ||\Phi(z(t))-\Phi_{last}||/||\Phi(z(t))||\geq tol \\ M(t), & \text{otherwise} \end{cases}
\end{aligned} \tag{7.61}$$

The EF method is a forgetting method in uniform directions. The discrete dynamics of the EF method is given as:

$$\begin{aligned}
&\Omega(t+\Delta t) \\
&= \begin{cases} q(t)q^T(t), \text{ if rank}(\Omega(t)) < \text{rank}(\Omega(t)+q(t)q^T(t)) \\ \mu\Omega(t)+q(t)q^T(t), \text{ otherwise} \end{cases} \\
&M(t+\Delta t) \\
&= \begin{cases} q(t)c^T(t), \text{ if rank}(\Omega(t)) < \text{rank}(\Omega(t)+q(t)q^T(t)) \\ \mu M(t)+q(t)c^T(t), \text{ otherwise} \end{cases}
\end{aligned} \tag{7.62}$$

Likewise, the discrete dynamics of the DF method is

$$\begin{aligned}
&\Omega(t+\Delta t) \\
&= \begin{cases} q(t)q^T(t), \text{ if } \operatorname{rank}(\Omega(t)) < \operatorname{rank}(\Omega(t)+q(t)q^T(t)) \\ \mu\dfrac{\Omega(t)q(t)q^T(t)}{q^T(t)\Omega(t)q(t)}\Omega(t)+q(t)q^T(t), \text{ otherwise} \end{cases} \\
&M(t+\Delta t) \\
&= \begin{cases} q(t)c^T(t), \text{ if } \operatorname{rank}(\Omega(t)) < \operatorname{rank}(\Omega(t)+q(t)q^T(t)) \\ \mu\dfrac{\Omega(t)q(t)q^T(t)}{q^T(t)\Omega(t)q(t)}M(t)+q(t)c^T(t), \text{ otherwise} \end{cases}
\end{aligned} \tag{7.63}$$

where the forgetting factor $0 < \mu \leq 1$ corresponds to $e^{-k}$ of the continuous dynamics. Considering that $\mu$ is usually selected between 0.95 – 0.99 and the forgetting of the EF is much faster than the DF, the value of $\mu$ is chosen differently on EF and DF for similar performance.

$$\mu = \begin{cases} 0.99 & \text{for EF} \\ 0.95 & \text{for DF} \end{cases} \tag{7.64}$$

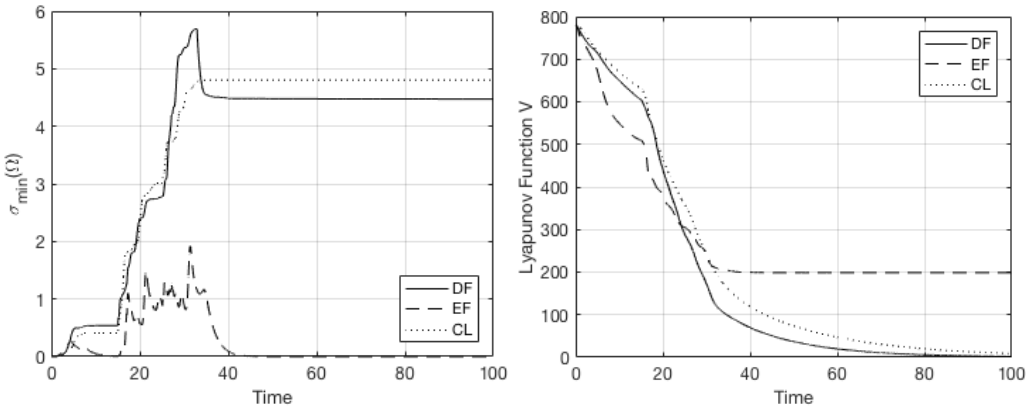


(i) Minimum eigenvalue of $\Omega(t)$ (ii) Lyapunov function $V(t)$

Figure 7.1: Simulation results without parameter jump or excitation after 50s

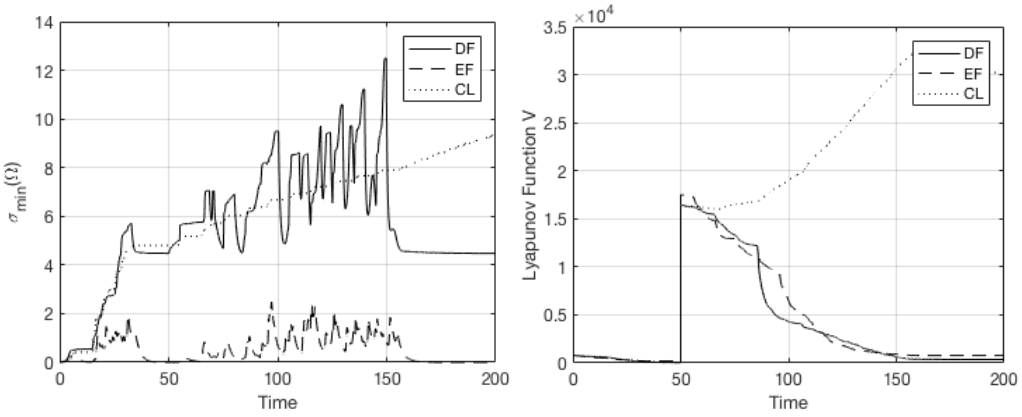


(i) Minimum eigenvalue of $\Omega(t)$ (ii) Lyapunov function $V(t)$

Figure 7.2: Simulation results with parameter jump at 50s

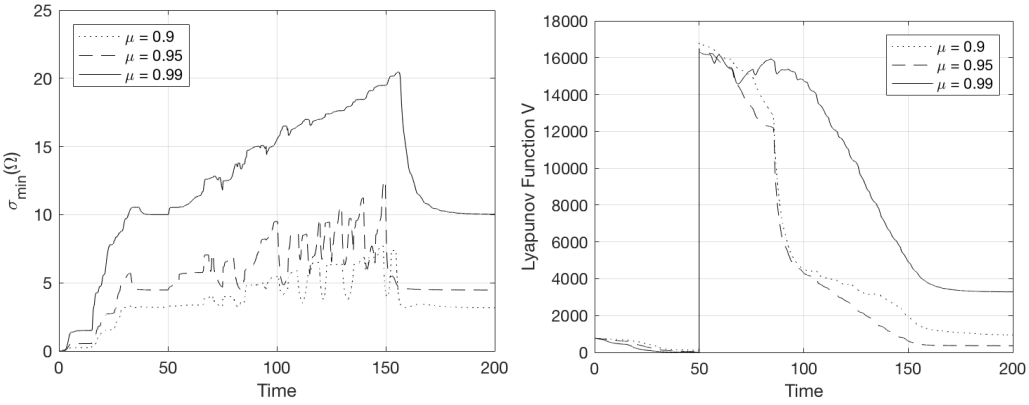


(i) Minimum eigenvalue of $\Omega(t)$ (ii) Lyapunov function $V(t)$

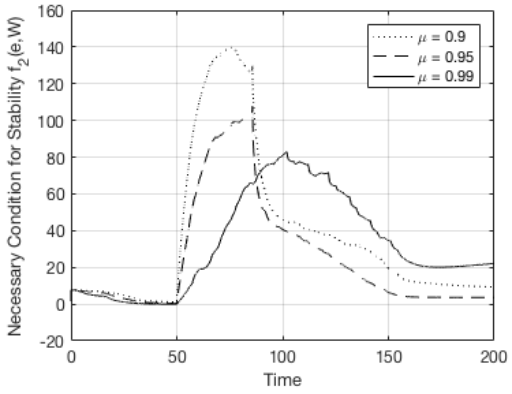


(iii) Necessary condition for stability $F_2(e,\tilde{W})$

Figure 7.3: Simulation results with parameter jump at 50s and different forgetting rates

### 7.6.2 Simulation Results

First, assume there is no parameter change or reference inputs after 50s. The lower bound of the information matrix, i.e. the minimum singular value, and the Lyapunov function are shown in Fig. 7.1. The information matrix of DF is lower bounded, and both the tracking and parameter estimation error converge to zero without PE, while the information matrix of EF converges to zero resulting in the stagnation of the parameter estimation. The result clearly supports the Theorem 8 and 10.

If there is a parameter jump at 50s, the lower bound of the information matrix and the Lyapunov function are shown in Fig. 7.2. The information matrix of DF is lower bounded with a non-zero value as proven in Theorem 8, and upper bounded to a finite value as in Theorem 9. While the parameter error increases in CL, both forgetting algorithms show Lyapunov stability.

The result of the same simulation with different $\mu$'s is shown in Fig. 7.3, where the necessary condition for stability $F_2(e,\tilde{W})$ is given from Theorem 12. As the lower and upper bounds of the information matrix are not determined, worst-case values for reducing the $F_2(e,\tilde{W})$, i.e. $\alpha = \beta$, are chosen. The Lyapunov function is stable, and the necessary condition is met with positive semi-definiteness. Increase in $k$, or alternatively decrease in $\mu$, results in large $F_2(e,\tilde{W})$ in the first part as the positive terms decay fast. In the later part, the parameter estimation is stagnated as the information matrix is lower bounded by a smaller value, which mainly determines the convergence rate

## 7.7 Conclusions

In this chapter, a directional forgetting based concurrent learning adaptive control has been proposed. The theoretical studies have shown that the information matrix is bounded, and both the tracking and parameter error converges to zero without the PE requirement under the assumption that there is no parameter change. The conditions for the convergence with the existence of parameter jumps have been obtained. The theoretical studies

are supported by the numerical simulations on wingrock model. The proposed method is expected to be applicable to many adaptive control problems with time-varying parameters for its simplicity and convergence guarantee.

# References

[106] K. Astrom and B. Wittenmark. *Adaptive control (2nd ed.)* Reading, MA: Addsion-Wesley, 1995.

[107] G. Chowdhary, T. Yucelen, M. Muhlegg, and E. N. Johnson. "Concurrent Learning Adaptive Control of Linear Systems with Exponentially Convergent Bounds". In: *International Journal of Adaptive Control and Signal Processing* 22.4 (2011), pp. 325–343.

[108] G. Chowdhary, M. Mühlegg, and E. Johnson. "Exponential parameter and tracking error convergence guarantees for adaptive controllers without persistency of excitation". In: *International Journal of Control* 87.8 (2014), pp. 1583–1603.

[109] A. Parikh, R. Kamalapurkar, and W. E. Dixon. "Integral Concurrent Learning: Adaptive Control with Parameter Convergence without PE or State Derivatives". In: *submitted to Automatica, see at arXiv:1512.03464* (2017).

[110] N. Cho and Y. Kim. "Basis Integral Concurrent-Learning Model Reference Adaptive Control". In: *2016 European Control Conference* (2016).

[111] N. Cho, H.-S. Shin, Y. Kim, and A. Tsourdos. "Composite Model Reference Adaptive Control with Parameter Convergence under Finite Excitation". In: *IEEE Transactions on Automatic Control* (2017), pp. 1–1.

[112] K. Oda, H. Takeuchi, M. Tsujii, and M. Ohba. "Practical Estimator for Self-Tuning Automotive Cruise Control". In: *1991 American Control Conference* (1991), pp. 2066–2071.

[113] N. Yoshitani and A. Hasegawa. “Model-based control of strip temperature for the heating furnace in continuous annealing”. In: *IEEE Transactions on Control Systems Technology* 6.2 (1998), pp. 146–156.

[114] A. Vahidi, A. Stefanopoulou, and H. Peng. “Recursive least squares with forgetting for online estimation of vehicle mass and road grade: theory and experiments”. In: *Vehicle System Dynamics* 43.1 (2005), pp. 31–55.

[115] F. Fraccaroli, A. Peruffo, and M. Zorzi. “A new recursive least squares method with multiple forgetting schemes”. In: *Proceedings of the IEEE Conference on Decision and Control* 2016-Febru (2016), pp. 3367–3372. arXiv: 1503.07338.

[116] R. M. Johnstone, C. Richard Johnson, R. R. Bitmead, and B. D. Anderson. “Exponential convergence of recursive least squares with exponential forgetting factor”. In: *Systems and Control Letters* 2.2 (1982), pp. 77–82.

[117] Q. Zhang and A. Clavel. “Adaptive observer with exponential forgetting factor for linear time varying systems”. In: *IEEE Conference on Decision and Control (CDC)* 4.December (2001), pp. 3886–3891.

[118] S. Bittanti, P. Bolzern, and M. Campi. “Convergence and exponential convergence of identification algorithms with directional forgetting factor”. In: *Automatica* 26.5 (1990), pp. 929–932.

[119] L. Cao and H. Schwartz. “Directional forgetting algorithm based on the decomposition of the information matrix”. In: *Mediterranean Conference on Control and Automation (MED09)* (1999), pp. 1635–1644.

[120] L. Cao and H. Schwartz. “Directional forgetting algorithm based on the decomposition of the information matrix”. In: *Automatica* 36.11 (2000), pp. 1725–1731.

[121] G. Tao. *Adaptive control design and analysis*. New York NY: Wiley, 2003.

[122] R. A. Horn and C. R. Johnson. *Matrix Analysis*. Cambridge: Cambridge University Press, 1985.

[123] J. R. Magnus and H. Neudecker. “The Differential of a Determinant”. In: *Matrix Differential Calculus with Applications in Statistics and Econometrics*. Wiley, 1999.

[124] P. Ghorawat. “Adaptive, Neural and Robust Control of Wing-Rock and Aeroelastic System”. In: May (2015).

# Chapter 8

# General Discussion

In this chapter, the proposed analysis and control design frameworks in Chapters 2 to 7 are discussed with respect to two main application examples: formation control and slung-load system. Both of the application examples are the networked control system, to which the extended analysis from Chapter 4 is applicable.

## 8.1 Formation Control

Formation control is a typical example of multi-UAV system without physical interconnections between them. The UAVs are controlled to track the reference trajectory while maintaining the spatial distance. Different UAV dynamics and network topology are considered to show how the proposed analysis framework can be applied and the network parameters influence on robustness and performance of the networked control system. Assuming that the dynamics of the UAVs are identical, the analysis and numerical simulation results of the case studies in Chapter 4 are directly applicable. The proposed control methods in Chapters 5 to 7 are not considered in this application, as there are not specific structured uncertainties on the unmatched or time-varying parameters.

Consider a formation control problem where the distance between UAVs is controlled with a P-gain control, i.e. $K(s) = kL$. Approximating the UAV dynamics and capturing only the dominant characteristics, individual UAV's dynamics can be modelled as

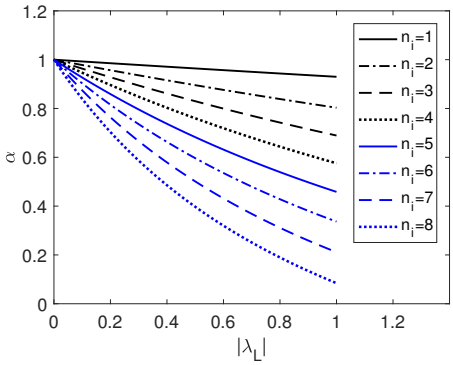


(i) Stability margin with different $|\lambda_L|$

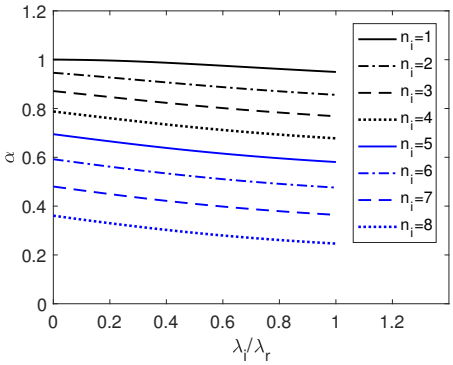


(ii) Stability margin with different $\lambda_i/\lambda_r$

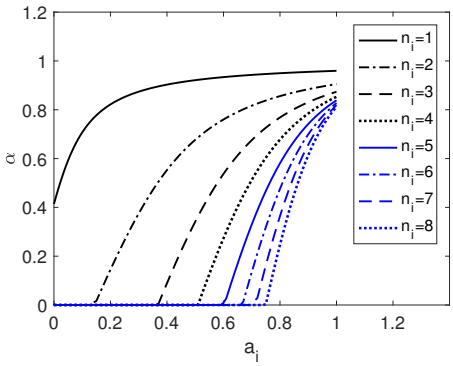


(iii) Stability margin with different $a_i$

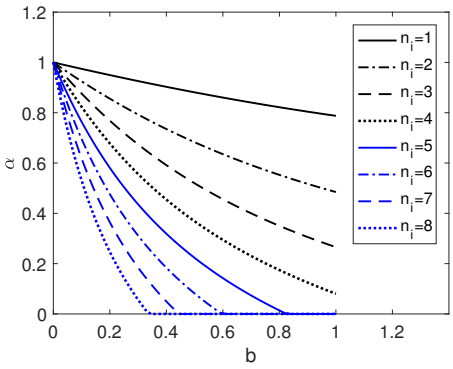


(iv) Stability margin with different $b$

Figure 8.1: Stability margin with different network topologies & system dynamics

$G_I(s) = bk/\prod_{i=0}^{n_i}(s+a_i)$. Since the UAVs are not physically interconnected, the open-loop transfer function of the networked control system is obtained as:

$$G^*_{OL} = \frac{bkL \circ H(s)}{\prod_{i=0}^{n_i}(s+a_i)}. \tag{8.1}$$

Then, the main results of the robustness analysis are revisited in Fig. 8.1. The effect of network topology and agent dynamics on the control robustness of a whole network can be summarised as:

- Effect of network topology: From (i) and (ii), the increase of $|\lambda_L|$ and $\lambda_i/\lambda_r$ deteriorates the stability margin. It is known that $|\lambda_L|$ is relevant with the connectivity of a graph, and $\lambda_i/\lambda_r$ with the cyclic network. Also, even though it is not directly considered in the analysis, increase in the accessing delay has a similar effect on

increasing $\lambda_i$ as a cyclic network, deteriorating the stability margin.

- Effect of agent dynamics: From (iii) and (iv), the increase of $a_i$'s and decrease of $b$ or $k$ improves the stability margin. The conclusion coincides with physical intuition: dependence more on the agent's own states than on the others' is beneficial for the stability margin.

With the analysis results on the performance, there is a trade-off between the robustness and performance metrics. The effect of cyclic network or accessing delay is obscure in the performance metric, but the network connectivity and agent dynamics has a conflicting effect on the networked control system. When the connectivity of a graph is increased, the robustness is degraded while the performance is improved. Also, the increase of $a_i$'s compared with $b$ or $k$ implies that the agents are more dependent on their own states, increasing the robustness and losing the tracking performance of the whole system. Therefore, the network or control gain should be designed not to achieve both the robustness and performance, but to find a balance between them.

Note that in the formation control, the stability may refer to the convergence of UAV positions to the reference formation in other literature. In this thesis, the stability is defined as the convergence of the UAV's states to the equilibrium point, and the robustness is the maximum gain and phase variations of the uncertainties that do not lead to the loss of stability. Hence the notion of the stability with respect to the reference input is similar to the performance metrics in this paper. For the main objective of the formation control lies in the tracking of the formation, the network and control gain would be designed with more emphasis on the performance.

## 8.2 Slung-Load System

The slung-load transportation system is a challenging application for its physical coupling between the UAVs. The strings connected to the payload, and the movements of

the payload is affected by those of the UAVs and vice versa. For the analysis, the characteristic equation is not expressed explicitly as Eqn. (4.10), and consequently the margins are obtained only numerically. For the control design, the control techniques proposed in Chapters 5 to 7 are applied to cope with the uncertainties and recover the nominal controller response.

The robustness analysis results with respect to different network topologies are shown in Fig. 8.2 and Fig. 8.3. The $x$-axes are the second largest eigenvalue of $L$ and the largest one of $A$ respectively, both of which are positive real number. These eigenvalues correspond to the effect of $|\lambda_L|$ and $\tau_{ij}$, respectively. The $y$-axes are gain margin obtained from the disk margin, meaning that the phase margin is also increased with the increase of gain margin.

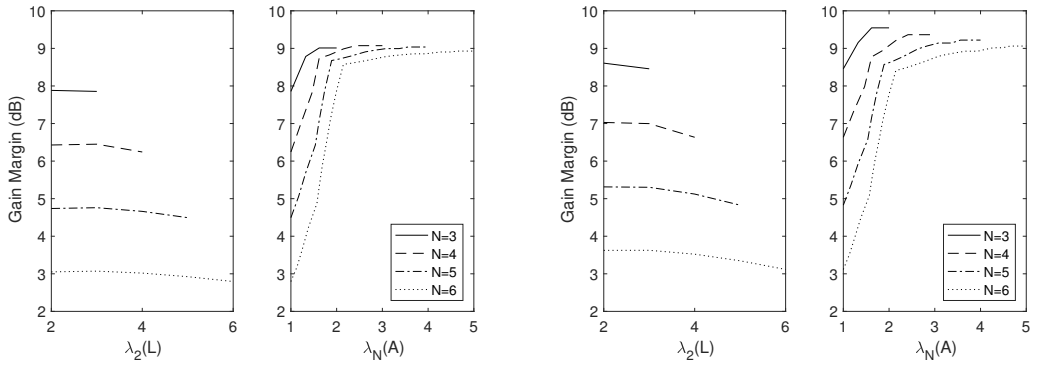


(i) Stability margin with LQR (ii) Stability margin with PRLQR

Figure 8.2: Stability margin with different full-state feedback control techniques

In Fig. 8.2, the margins are analysed with full-state feedback controllers, the LQR controller and the parameter-robust LQR. A notable effect of the network topology on the stability margin is that the more the network is connected, the stability margin decreases. The tendency is the same as the discussions on the formation control, where the agent dynamics is not coupled with each other. However, the difference lies on that the tendency depends on the number of vehicles. The larger the number of vehicles, the more sensitive the stability of the system to the uncertainties or disturbances. Once the network is fully spanned, increase of connectivity leads to the decrease of multi-hop delay $\tau_{ij}$, and thus to

the increase of stability. Comparing the LQR technique with the parameter-robust LQR, the overall scale of the gain margin is increased with parameter-robust technique. Note that the PRLQG method is suggested to improve the robustness of the observer-based controller, not the full-state feedback control.

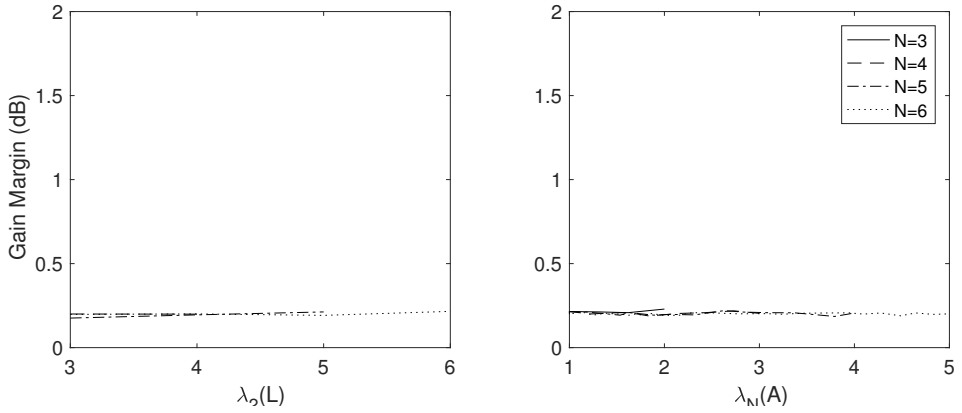


(i) Stability margin with LQG

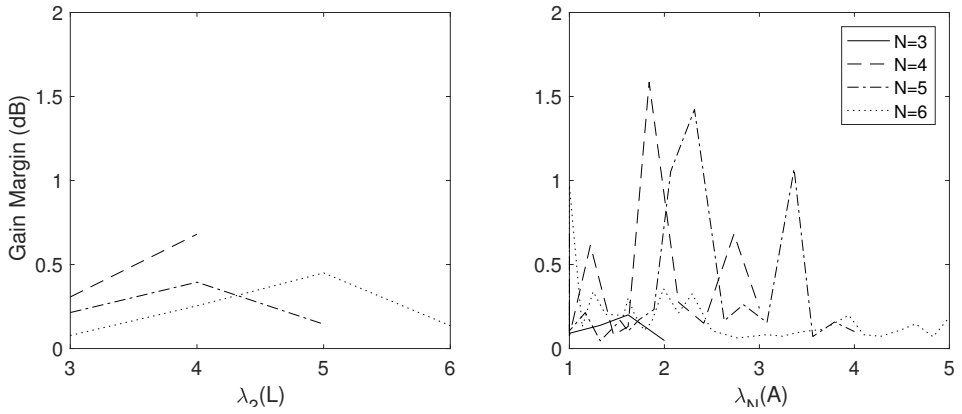


(ii) Stability margin with PRLQG

Figure 8.3: Stability margin with different observer-based control techniques

In Fig. 8.3, the margins are analysed with respect to the LQG and PRLQG method, where only the positions of the vehicles are observed. When it comes to observer-based control, it is difficult to find the distinct relationship between the stability margin and the network topology. While obtaining the disk margin, the value of $\alpha(\omega)$ is sensitive to the variation of the frequency $\omega$. The resultant stability margin, $\alpha^*$ is therefore also sensitive, showing an irregular pattern with respect to the network topology. However, the overall scale of the gain margin is increased around 1.1 dB, using the PRLQG method.

Comparing with the formation control, the physical interconnections between the vehicles deteriorate the system robustness in a significant degree, but the proposed control technique recovers the stability margin.

Note that the robustness analysis only covers the linear dynamics and controller. Considering the nonlinear part, the numerical simulations in Chapter 6 suggest that the adaptive terms play a crucial role in stabilising the tracking and parameter estimation error, but the analysis of its robustness is illusive. Although the main objective of the proposed adaptive control methods is not to improve the general stability margin but to cancel out the structured uncertainties, the analysis of its robustness as a future work could improve the quality of the research.

# Chapter 9

# Conclusions and Future Work

## 9.1 Conclusions

In this thesis, a systematic approach to analyse and design the networked control system with multiple UAVs has been proposed. The approach includes analysis method of a simple network and networked control system, adaptive control design concerning the potential issues, and application examples to validate the approach. The conclusions of each objectives can be summarised as follows:

- **Analysis on networked system** The design of scale free core-periphery networks is formulated into a single parameter problem, and the network properties are optimised using the evolutionary game based MOO method. Numerical simulation is conducted with different average degrees, which are relevant to the size of network by the transmission power or coverage. The parameter of the network structure is given by the optimal exponent of the degree distribution. This part is expected to suggest a guide for designing a topology in the various fields including multi-agent or sensor network design.

- **Analysis on networked control system** A new stability analysis method for the networked multi-agent system has been proposed. The main idea is to model the networked system including the communication dynamics into a single MIMO

transfer function and to utilise the analysis tools in linear control theory. The stability of the networked system is defined, and its robustness against gain/phase variation and accessing delay is evaluated with stability and delay margin. The strength of the proposed analysis method lies on that it can analyse any agent dynamics, controllers, and communication characteristics, if they could be modelled into a transfer function. By combining network and control theory, the properties of a graph have been explained in the view of controlling the agents. This research will provide an insight for designing the network or control considering their effects on the robustness and performance of the networked system.

- **Adaptive control design for unmatched uncertainties** An control synthesis to effectively suppress the effect of uncertainty of the multi-UAV slung-load system is proposed. The rationale behind the idea is that although the slung-load system has considerable unmatched uncertainties which are neither estimated or controlled with common adaptive controls, the baseline controller can be designed to be robust to the unmatched uncertainties through the PRLQG method. The stability conditions of the proposed control method are obtained through Lyapunov analysis.

- **Adaptive control design for time-varying uncertainties** A directional forgetting based concurrent learning adaptive control has been proposed. The theoretical studies have shown that the information matrix is bounded, and both the tracking and parameter error converges to zero without the PE requirement under the assumption that there is no parameter change. The conditions for the convergence with the existence of parameter jumps have been obtained. The proposed method is expected to be applicable to many adaptive control problems with time-varying parameters for its simplicity and convergence guarantee.

- **Application** Two application examples are chosen to validate the analysis framework and the proposed control: formation control and slung-load system. For formation control, considering the dominant agent dynamics reveals the effect of net-

work topology and agent dynamics on the robustness metrics defined. Also, the trade-off between the robustness and performance of the networked system is observed, suggesting the network topology and control gain to be designed in consideration of their balance. Numerical simulations with first- and second-order systems support the theoretical analysis.

For slung-load system, the stability and its robustness is also analysed with numerical support. The numerical simulations demonstrate that the proposed control approach effectively cancels out the effect of both unmatched and matched uncertainties in three different slung-load systems with a potential to be extended to incorporate more UAVs.

## 9.2 Future work

There are several points that must be followed to support and develop this research in the future.

- **Nonlinear analysis in slung-load system.** The effect of communication between the agents has been analysed for the linearised dynamics and control only, and the nonlinear part has been dealt with in the numerical simulation. A systematic scheme for analysing the robustness and performance of the nonlinear system would improve the research.

- **Effect of data rate.** Although the analysis framework has been proposed to consider general communication dynamics, the effect of delay has been mainly discussed in this research. Another important aspect of the communication network is the data rate. The amount of data transferred between the agents can be modelled as an information theory, and using the information theory, the stability bounds for the system could be obtained [125].

# Appendix A

# Proofs on Lemmas

## Proof of Lemma 4

For a positive semi-definite matrix $A \in \mathbb{R}^{n\times n}$, the maximum eigenvalue is the same as the spectral radius, which is expressed as the following equation:

$$\rho(A) = \lambda_{max} = \max_{x\neq 0} \frac{x^T A x}{x^T x} \tag{A.1}$$

For any non-zero vector $x \in \mathbb{R}^n$, the following inequality is hold.

$$x^T (A - \rho(A) I) x = x^T A x - \rho(A) x^T x \geq 0 \tag{A.2}$$

Thus, the matrix $(A - \rho(A)I)$ being positive semi-definite, the following equation is satisfied.

$$A \leq \rho(A) I \tag{A.3}$$

The inequality $A \leq I$ is satisfied if and only if $\rho(A) \leq 1$.

## Proof of Lemma 5

Determinant of a matrix $F$ is expressed as the summation of cofactors and its corresponding vectors as

$$\det(F) = \sum_{i=1}^{m} c_{ij} f_{ij} \tag{A.4}$$

where $c_{ij}$ is the cofactor and $F = (f_{ij})$. As the cofactors and the corresponding vectors are independent, the partial differential is obtained as

$$\frac{\partial \det(F)}{\partial f_{ij}} = c_{ij} \tag{A.5}$$

The differential of the determinant is thus obtained as follows:

$$d\det(F) = \sum_{i=1}^{m} \sum_{j=1}^{m} c_{ij} df_{ij} = trF^{\sharp} dF \tag{A.6}$$

where $F^{\sharp}$ is the adjoint matrix. Substituting $F^{\sharp} = \det(F)F^{-1}$,

$$d\det(F) = \det(F) trF^{-1} dF \tag{A.7}$$

Integrating the both sides, the following equation is obtained for a positive definite matrix $F$:

$$\det(F) = \exp(tr(\log(F))) \tag{A.8}$$

Substituting $F = \exp(A)$, the Lemma 5 is obtained as

$$\det(\exp(A)) = \exp(tr(A)) \tag{A.9}$$

**Proof of Lemma 6**

The determinant and trace of a matrix $A$ is known as the product and summation of its eigenvalues, respectively, as

$$\det(A) = \prod_i \lambda_i, \qquad tr(A) = \sum_i \lambda_i \tag{A.10}$$

If the matrix is positive semi-definite, the eigenvalues satisfy $\lambda_i \geq 0$. From Arithmetic Mean-Geometric Mean Inequality, the Lemma 6 is obtained as

$$\det(A) \leq \left( \frac{tr(A)}{n} \right)^n \tag{A.11}$$

# Complete Bibliography


[1] H. S. Shin. “UAV Swarms : Decision Making Paradigms”. In: *Encyclopedia of Aerospace Engineering*. John Wiley: Chichester, 2014, pp. 1–34.

[2] I. Akyildiz, W. Su, Y. Sankarasubramaniam, and E. Cayirci. “Wireless sensor networks: a survey”. In: *Computer Networks* 38.4 (2002), pp. 393–422.

[3] T. Samad, J. S. Bay, and D. Godbole. “Network-centric systems for military operations in urban terrain: The role of UAVs”. In: *Proceedings of the IEEE* 95.1 (2007), pp. 92–107.

[4] M. Hauge, L. Landmark, and M. Amanowicz. “Selected Issues of QoS Provision in Heterogenous Military Networks”. In: *International Journal of Electronics and Telecommunications* 60.1 (2014), pp. 7–13.

[5] G. Pau and R. Tse. “Challenges and opportunities in immersive vehicular sensing: Lessons from urban deployments”. In: *Signal Processing: Image Communication* 27.8 (2012), pp. 900–908.

[6] P. Carvalhal, C. Santos, M. Ferreira, L. Silva, and J. Afonso. “Design and Development of a Fly-by-Wireless UAV Platform”. In: *Aerial Vehicles* (2009), pp. 1–12.

[7] F. Ciucu and J. Schmitt. “Perspectives on network calculus: no free lunch, but still good value”. In: *SIGCOMM Comput. Commun. Rev.* 42.4 (2012), pp. 311–322.

[8] M. Fidler. “Survey of deterministic and stochastic service curve models in the network calculus”. In: *IEEE Communications Surveys & Tutorials* 12.1 (2010), pp. 59–86.

[9] M. Fidler and A. Rizk. “A Guide to the Stochastic Network Calculus”. In: *IEEE Communications Surveys & Tutorials* PP.99 (2014), pp. 1–1.

[10] Y. Jiang and Y. Liu. *Stochastic Network Calculus*. Springer Berlin Heidelberg, 2008.

[11] C. Lin, Y. Deng, and Y. Jiang. “On applying stochastic network calculus”. In: *Frontiers of Computer Science* 7.6 (2013), pp. 924–942.

[12] S. Y. Park and A. Sahai. “Network Coding meets Decentralized Control: Network Linearization and Capacity-Stabilizablilty Equivalence”. In: *arXiv* (2013), pp. 4817–4822. arXiv: 1308.5045.

[13] M. E. J. Newman. “Networks. An introduction”. In: *Oxford University Press* (2010), p. 772.

[14] J. P. Hespanha, P. Naghshtabrizi, and Y. Xu. “A survey of recent results in networked control systems”. In: *Proc. of the IEEE* 95.1 (2007), pp. 138–162.

[15] J. D. Blight, R. Lane Dailey, and D. Gangsaas. “Practical control law design for aircraft using multivariable techniques”. In: *International Journal of Control* 59.1 (1994), pp. 93–137.

[16] J. Doyle and G. Stein. “Multivariable feedback design: Concepts for a classical/modern synthesis”. In: *Automatic Control, IEEE Transactions on* 26.1 (1981), pp. 4–16.

[17] G. Stein and M. Athans. “The LQG / LTR Procedure for Multivariable Feedback Control Design”. In: *IEEE Transactions on Automatic Control* 32.2 (1987), pp. 105–114.

[18] A. E. Motter, C. Zhou, and J. Kurths. “Network synchronization, diffusion, and the paradox of heterogeneity”. In: *Physical Review E - Statistical, Nonlinear, and Soft Matter Physics* 71.1 (2005), pp. 1–10.

[19] B. Wang, H. Tang, C. Guo, Z. Xiu, and T. Zhou. “Optimization of network structure to random failures”. In: *Physica A: Statistical Mechanics and its Applications* 368.2 (2006), pp. 607–614.

[20] T. P. Peixoto and S. Bornholdt. “Evolution of robust network topologies: Emergence of central backbones”. In: *Physical Review Letters* 109.11 (2012), pp. 1–5.

[21] C. Leboucher, H. S. Shin, S. Le Menec, A. Tsourdos, A. Kotenkoff, P. Siarry, and R. Chelouah. “Novel Evolutionary Game Based Multi-Objective Optimisation for Dynamic Weapon Target Assignment”. In: *the 19th World Congress The International Federation of Automatic Control* 2010 (2014), pp. 3936–3941.

[22] P. Holme. “Core-periphery organization of complex networks”. In: *Physical Review E - Statistical, Nonlinear, and Soft Matter Physics* 72.4 (2005).

[23] V. Batagelj and A. Mrvar. “Pajek – program for large network analysis”. In: *Connections* (1999), pp. 47–57.

[24] K. Deb. *Multi-objective optimization using evolutionary algorithms: an introduction*. John Wiley & Sons, LTD., 2011.

[25] M. Kok. “A Note on the Pay-off Matrix in Multiple Objective Programming”. In: *European Journal of Operational Research* 26.1 (1986), pp. 96–107.

[26] J. Hofbauer and K. Sigmund. “Evolutionary Game Dynamics”. In: *Bulletin of the Anerican Mathematical Society* 40.4 (2003), pp. 479–519.

[27] M. M. Zavlanos and G. J. Pappas. “Potential fields for maintaining connectivity of mobile networks”. In: *IEEE Transactions on Robotics* 23.4 (2007), pp. 812–816.

[28] R. T. Marler and J. S. Arora. “Survey of multi-objective optimization methods for engineering”. In: *Structural and Multidisciplinary Optimization* 26.6 (2004), pp. 369–395.

[29] T. Stewart, O. Bandte, H. Braun, N. Chakraborti, M. Ehrgott, M. Göbelt, Y. Jin, H. Nakayama, S. Poles, and D. Di Stefano. “Real-world applications of multiobjective optimization”. In: *Multiobjective Optimization: Interactive and Evolutionary Approaches*. Springer, 2008, pp. 285–327.

[30] P. Korhonen. “Multiple objective programming support”. In: *Encyclopedia of optimization* (2009), pp. 2503–2511.

[31] Y. Collette and P. Siarry. *Multiobjective Optimization: Principles and Case Studies*. Springer, 2003, p. 315.

[32] C.-L. Hwang and A. S. M. Masud. *Multiple Objective Decision Making - Methods and Applications*. Springer Berlin Heidelberg, 1979, p. 357.

[33] V. Changkong and Y. Y. Haimes. *Multiobjective decision making theory and methodology*. New York: Elsevier Science Publishing Co., Inc., 1983.

[34] K. Deb. “Classical Methods”. In: *Multi-objective optimization using evolutionary algorithms*. John Wiley & Sons, LTD., 2011, pp. 47–75.

[35] T. W. Athan and P. Y. Papalambros. “A note on weighted criteria methods for compromise solutions in multi-objective optimization”. In: *Engineering Optimization* 27.2 (1996), pp. 155–176.

[36] A. Messac. “From dubious construction of objective functions to the application of physical programming”. In: *AIAA Journal* 38.1 (2000), pp. 155–163.

[37] S. Opricovic and G. H. Tzeng. “Compromise solution by MCDM methods: A comparative analysis of VIKOR and TOPSIS”. In: *European Journal of Operational Research* 156.2 (2004), pp. 445–455.

[38] H. Mausser. “Normalization and Other Topics in Multi Objective Optimization”. In: *Proceedings of the Fields-MITACS Industrial Problems Workshop* (2006), pp. 89–101.

[39] K. Miettinen. *Nonlinear multiobjective optimization*. Vol. 12. Springer US, 1999, p. 320.

[40] S. Zionts. “The Interactive Surrogate Worth Trade-Off (ISWT) Method for Multiobjective Decision-Making”. In: *Lecture Notes in Economics and Mathematical Systems*. Springer Berlin Heidelberg, 1978, pp. 42–47.

[41] M. Sakawa. “Interactive Multiobjective Optimization by the Sequential Proxy Optimization Technique (SPOT)”. In: *IEEE Transactions on Reliability* R-31.5 (1982), pp. 386–396.

[42] J.-B. Yang. “Gradient projection and local region search for multiobjective optimisation”. In: *European Journal of Operational Research* 112.2 (1999), pp. 432–459.

[43] M. Sakawa and H. Yano. “Trade-off rates in the hyperplane method for multiobjective optimization problems”. In: *European Journal of Operational Research* 44.1 (1990), pp. 105–118.

[44] P. Eskelinen and K. Miettinen. “Trade-off analysis approach for interactive nonlinear multiobjective optimization”. In: *OR Spectrum* 34.4 (2011), pp. 803–816.

[45] I. Kaliszewski and W. Michalowski. “Efficient Solutions and Bounds on Tradeoffs 1,2”. In: *Optimization* 94.2 (1997), pp. 381–394.

[46] S. Zionts. “A multiple criteria method for choosing among discrete alternatives”. In: *European Journal of Operational Research* 7.2 (1981), pp. 143–147.

[47] I. Kaliszewski. “Using trade-off information in decision-making algorithms”. In: *Computers & Operations Research* 27.May 1998 (2000), pp. 161–182.

[48] M. Pelillo. “Replicator equations, maximal cliques, and graph isomorphism.” In: *Neural computation* 11.8 (1999), pp. 1933–1955.

[49] H. Ohtsuki and M. Nowak. “The replicator equation on graphs”. In: *Journal of Theoretical Biology* 243.1 (2006), pp. 86–97.

[50] K. Deb. “Salient Issues of Multi-Objective Evolutionary Algorithms”. In: *Multi-objective optimization using evolutionary algorithms*. John Wiley & Sons, LTD., 2011, pp. 324–370.

[51] J. Pang and J. Liang. “Evaluation of the results of multi-attribute group decision-making with linguistic information”. In: *Omega* 40.3 (2012), pp. 294–301.

[52] K. Deb, L. Thiele, M. Laumanns, and E. Zitzler. “Scalable Multi-Objective Optimization Test Problems”. In: *Proceedings of the Congress on Evolutionary Computation (CEC-2002)* 2 (2002), pp. 825–830.

[53] M. Farina, K. Deb, and P. Amato. “Dynamic Multiobjective Optimization Problems: Test Cases Approximation and Applications”. In: *IEEE Transactions on Evolutionary Computation* 8.5 (2004), pp. 311–326.

[54] G. Walsh, H. Ye, and L. Bushnell. “Stability Analysis of Networked Control Systems”. In: *IEEE Transactions on Control Systems Technology* 10.3 (2002), pp. 438–446.

[55] H. Lin, G. Zhai, and P. J. Antsaklis. “Robust stability and disturbance attenuation analysis of a class of networked control systems”. In: *Decision and Control, 2003. Proceedings. 42nd IEEE Conference on* 2 (2003), pp. 1182–1187.

[56] Y. Cai, K. A. Hua, and A. Phillips. “Leveraging 1-hop neighborhood knowledge for efficient flooding in wireless ad hoc networks”. In: *Proc. 24th IEEE International Performance, Computing, and Communications Conference IPCCC 2005* (2005), pp. 347–354.

[57] X. Liu, A. Goldsmith, S. S. Mahal, and J. K. Hedrick. “Effects of communication delay on string stability in vehicle platoons”. In: *Intelligent Transportation Systems, 2001. Proceedings. 2001 IEEE* (2001), pp. 625–630.

[58] M. S. Branicky, S. M. Phillips, and W. Zhang. “Stability of networked control systems: Explicit analysis of delay”. In: *American Control Conference, 2000. Proceedings of the 2000* 4 (2000), pp. 2352–2357.

[59] F.-L. Lian, J. Moyne, and D. Tilbury. “Analysis and modeling of networked control systems: MIMO case with multiple time delays”. In: *Proceedings of the American Control Conference* (2001), pp. 4306–4312.

[60] C. Tan and G.-P. Liu. “Consensus of Discrete-Time Linear Networked Multi-Agent Systems With Communication Delays.” In: *IEEE Transactions on Automatic Control* 58.11 (2013), pp. 2962–2968.

[61] M. Schwager, N. Michael, V. Kumar, and D. Rus. “Time scales and stability in networked multi-robot systems”. In: *Robotics and Automation (ICRA), 2011 IEEE International Conference on* (2011), pp. 3855–3862.

[62] N. Michael, M. Schwager, V. Kumar, and D. Rus. “An experimental study of time scales and stability in networked multi-robot systems”. In: *Springer Tracts in Advanced Robotics* 79 (2014), pp. 631–643.

[63] Y. G. Sun and L. Wang. “Consensus of multi-agent systems in directed networks with nonuniform time-varying delays”. In: *IEEE Transactions on Automatic Control* 54.7 (2009), pp. 1607–1613.

[64] R. Olfati-Saber and R. M. Murray. “Consensus Problems in Networks of Agents with Switching Topology and Time-Delays”. In: *IEEE Transactions on Automatic Control* 49(9).9 (2004), pp. 1520–1533.

[65] Y. Kim. “On the Stability Margin of Networked Dynamical Systems”. In: *IEEE Transactions on Automatic Control* 62.10 (2017), pp. 5451–5456.

[66] I. S. Gradshteyn and I. M. Ryzhik. *Tables of Integrals, Series, and Products, 6th ed.: Routh-Hurwitz Theorem*. San Diego, CA: Academic Press, 2000.

[67] N. Lehtomaki, N. Sandell, and M. Athans. "Robustness results in linear-quadratic Gaussian based multivariable control designs". In: *IEEE Transactions on Automatic Control* 26.1 (1981), pp. 75–93.

[68] R. Olfati-Saber, J. A. Fax, and R. M. Murray. "Consensus and cooperation in networked multi-agent systems". In: *Proceedings of the IEEE* 95.1 (2007), pp. 215–233.

[69] A.-K. Schug, P. Seiler, and H. Pfifer. "Robustness Margins for Linear Parameter Varying Systems". In: *AerospaceLab Journal* 13 (2017).

[70] A. Packard and J. Doyle. "The complex structured singular value". In: *Automatica* 29.1 (1993), pp. 71–109.

[71] H.-I. Lee, D.-W. Yoo, B.-Y. Lee, G.-H. Moon, D.-Y. Lee, M.-J. Tahk, and H.-S. Shin. "Parameter-robust linear quadratic Gaussian technique for multi-agent slung load transportation". In: *Aerospace Science and Technology* 71 (2017), pp. 119–127.

[72] Y. Feng, C. A. Rabbath, and C.-Y. Su. "Modeling of a Micro UAV with Slung Payload". In: *Handbook of Unmanned Aerial Vehicles*. 2015, pp. 2787–2811.

[73] D. Mellinger, Q. Lindsey, M. Shomin, and V. Kumar. "Design, modeling, estimation and control for aerial grasping and manipulation". In: *IEEE International Conference on Intelligent Robots and Systems* (2011).

[74] R. A. Stuckey. "Mathematical Modelling of Helicopter Slung-Load Systems". In: *DSTO Aeronautical and Maritime Research Laboratory* (2001).

[75] I. Palunko, R. Fierro, and P. Cruz. "Trajectory Generation for Swing-Free Maneuvers of a Quadrotor with Suspended Payload : A Dynamic Programming Approach". In: *IEEE International Conference on Robotics and Automation* (2012).

[76] M. Bernard and K. Kondak. “Generic Slung Load Transportation System Using Small Size Helicopters”. In: *IEEE International Conference on Robotics and Automation* (2009).

[77] M. Bernard, K. Kondak, I. Maza, and A. Ollero. “Autonomous Transportation and Deployment with”. In: *Journal of Field Robot* 28.6 (2011), pp. 914–931.

[78] I. Maza, K. Kondak, M. Bernard, and A. Ollero. “Multi-UAV cooperation and control for load transportation and deployment The original publication is available at www.springerlink.com in this link :” in: *Journal of Intelligent Robot Systems* 57 (2010), pp. 417–449.

[79] M. Bisgaard. “Modeling, Estimation, and Control of Helicopter Slung Load System”. PhD thesis. Aalborg University, 2007.

[80] M. Bisgaard, J. D. Bendtsen, and A. Cour-harbo. “Modeling of Generic Slung Load System”. In: *Journal of Guidance, Control, and Dynamics* 32.2 (2009), pp. 573–585.

[81] B. Y. Lee, H. I. Lee, D. W. Yoo, G. H. Moon, D. Y. Lee, Y. Y. Kim, and M. J. Tahk. “Study on payload stabilization method with the slung-load transportation system using a quad-rotor”. In: *2015 European Control Conference, ECC 2015* (2015), pp. 2097–2102.

[82] H.-I. Lee, B.-Y. Lee, D.-W. Yoo, G.-H. Moon, and M.-J. Tahk. “Dynamics Modeling and Robust Controller Design of the Multi-Uav Transportation System”. In: *29th Congress of the International Council of the Aeronautical Sciences* (2014).

[83] N. Michael, S. Kim, J. Fink, and V. Kumar. “Kinematics and Statics of Cooperative Multi-Robot Manipulation with Cables”. In: *Proceedings of the International Design Engineering Technical Conferences* 8 (2009), pp. 83–91.

[84] N. Michael, J. Fink, and V. Kumar. “Cooperative manipulation and transportation with aerial robots”. In: *Autonomous Robots* September 2010 (2010), pp. 1–14.

[85] K. Morris. *Introduction to Feedback Control*. Harcourt/Academic Press, 2001, pp. 163, 198.

[86] M.-J. Tahk and J. L. Speyer. "Modeling of Parameter Variations and Asymptotic LQG Synthesis". In: *IEEE Transactions on Automatic Control* 32.9 (1987), pp. 793–801.

[87] M.-J. Tahk and J. L. Speyer. "Parameter Robust Linear- Quadratic-Gaussian Design Synthesis with Flexible Structure Control Applications". In: *Journal of Guidance, Control, and Dynamics,* 12.4 (1988), pp. 460–468.

[88] V. Ghadiok. "Autonomous Aerial Manipulation Using a Quadrotor". Utah State University, 2011.

[89] D. Kingston, R. Beard, and R. Holt. "Decentralized Perimeter Surveillance Using a Team of UAVs". In: *IEEE Transactions on Robotics* 24.6 (2008), pp. 1394–1404.

[90] D. Bein, W. Bein, A. Karki, and B. Madan. "Optimizing Border Patrol Operations Using Unmanned Aerial Vehicles". In: 2015, pp. 479–484.

[91] S. Minaeian, J. Liu, and Y.-J. Son. "Vision-Based Target Detection and Localization via a Team of Cooperative UAV and UGVs". In: *IEEE Transactions on Systems, Man, and Cybernetics: Systems* 46.7 (2016), pp. 1005–1016.

[92] R. Pitre, X. Li, and R. Delbalzo. "UAV Route Planning for Joint Search and Track Mission - An Informative-Value Approach". In: *IEEE Transactions on Aerospace and Electronic Systems* 48.3 (2012), pp. 2551–2565.

[93] B. Lim, J. Kim, S. Ha, and Y. Moon. "Development of software platform for monitoring of multiple small UAVs". In: vol. 2016-December. 2016.

[94] P. Li and H. Duan. "A potential game approach to multiple UAV cooperative search and surveillance". In: *Aerospace Science and Technology* 68 (2017), pp. 403–415.

[95] A. Puri. *A survey of Unmanned Aerial Vehicles (UAV) for Traffic Surveillance*. Tech. rep. Department of Computer Science and Engineering, University of South Florida, 2004.

[96] E. Carapezza and D. Law. "Sensors, C3I, Information, and Training Technologies for Law Enforcement". In: *Proc. SPIE*. 1999.

[97] A. Belbachir and J.-A. Escareno. "Autonomous decisional high-level planning for UAVs-based forest-fire localization". In: vol. 1. 2016, pp. 153–159.

[98] B. R. Barmish and G. Leitmann. "On Ultimate Boundedness Control of Uncertain Systems in the Absence of Matching Assumptions". In: *IEEE Transactions on Automatic Control* 116.1 (1982), pp. 153–155.

[99] B.-j. Yang, T. Yucelen, and J.-y. Shin. "An LMI-based Analysis of an Adaptive Flight Control". In: *AIAA Infotech@Aerospace 2010* (2010).

[100] C. Cao and N. Hovakimyan. "Design and Analysis of a Novel L1 Adaptive Control". In: *IEEE Transactions on Automatic Control* 53.2 (2008), pp. 586–591.

[101] N. T. Nguyen and S. N. Balakrishnan. "Bi-objective optimal control modification adaptive control for systems with input uncertainty". In: *IEEE/CAA Journal of Automatica Sinica* 1.4 (2014), pp. 423–434.

[102] T. I. Fossen and S. I. Sagatun. "Adaptive control of nonlinear systems: A case study of underwater robotic systems". In: *Journal of Robotic Systems* 8.3 (1991), pp. 393–412.

[103] A. C. Huang and Y. C. Chen. "Adaptive sliding control for single-link flexible-joint robot with mismatched uncertainties". In: *IEEE Transactions on Control Systems Technology* 12.5 (2004), pp. 770–775.

[104] B. Meng, C. Gao, S. Tang, and Y. Liu. "Adaptive Variable Structure Control for Linear Systems with Time-varying Multi-delays and Mismatching Uncertainties". In: *Physics Procedia* 33.60974025 (2012), pp. 1753–1761.

[105] J. F. Quindlen, G. Chowdhary, and J. P. How. “Hybrid model reference adaptive control for unmatched uncertainties”. In: *2015 American Control Conference (ACC)* (2015), pp. 1125–1130.

[106] K. Astrom and B. Wittenmark. *Adaptive control (2nd ed.)* Reading, MA: Addsion-Wesley, 1995.

[107] G. Chowdhary, T. Yucelen, M. Muhlegg, and E. N. Johnson. “Concurrent Learning Adaptive Control of Linear Systems with Exponentially Convergent Bounds”. In: *International Journal of Adaptive Control and Signal Processing* 22.4 (2011), pp. 325–343.

[108] G. Chowdhary, M. Mühlegg, and E. Johnson. “Exponential parameter and tracking error convergence guarantees for adaptive controllers without persistency of excitation”. In: *International Journal of Control* 87.8 (2014), pp. 1583–1603.

[109] A. Parikh, R. Kamalapurkar, and W. E. Dixon. “Integral Concurrent Learning: Adaptive Control with Parameter Convergence without PE or State Derivatives”. In: *submitted to Automatica, see at arXiv:1512.03464* (2017).

[110] N. Cho and Y. Kim. “Basis Integral Concurrent-Learning Model Reference Adaptive Control”. In: *2016 European Control Conference* (2016).

[111] N. Cho, H.-S. Shin, Y. Kim, and A. Tsourdos. “Composite Model Reference Adaptive Control with Parameter Convergence under Finite Excitation”. In: *IEEE Transactions on Automatic Control* (2017), pp. 1–1.

[112] K. Oda, H. Takeuchi, M. Tsujii, and M. Ohba. “Practical Estimator for Self-Tuning Automotive Cruise Control”. In: *1991 American Control Conference* (1991), pp. 2066–2071.

[113] N. Yoshitani and A. Hasegawa. “Model-based control of strip temperature for the heating furnace in continuous annealing”. In: *IEEE Transactions on Control Systems Technology* 6.2 (1998), pp. 146–156.

[114] A. Vahidi, A. Stefanopoulou, and H. Peng. “Recursive least squares with forgetting for online estimation of vehicle mass and road grade: theory and experiments”. In: *Vehicle System Dynamics* 43.1 (2005), pp. 31–55.

[115] F. Fraccaroli, A. Peruffo, and M. Zorzi. “A new recursive least squares method with multiple forgetting schemes”. In: *Proceedings of the IEEE Conference on Decision and Control* 2016-Febru (2016), pp. 3367–3372. arXiv: 1503.07338.

[116] R. M. Johnstone, C. Richard Johnson, R. R. Bitmead, and B. D. Anderson. “Exponential convergence of recursive least squares with exponential forgetting factor”. In: *Systems and Control Letters* 2.2 (1982), pp. 77–82.

[117] Q. Zhang and A. Clavel. “Adaptive observer with exponential forgetting factor for linear time varying systems”. In: *IEEE Conference on Decision and Control (CDC)* 4.December (2001), pp. 3886–3891.

[118] S. Bittanti, P. Bolzern, and M. Campi. “Convergence and exponential convergence of identification algorithms with directional forgetting factor”. In: *Automatica* 26.5 (1990), pp. 929–932.

[119] L. Cao and H. Schwartz. “Directional forgetting algorithm based on the decomposition of the information matrix”. In: *Mediterranean Conference on Control and Automation (MED09)* (1999), pp. 1635–1644.

[120] L. Cao and H. Schwartz. “Directional forgetting algorithm based on the decomposition of the information matrix”. In: *Automatica* 36.11 (2000), pp. 1725–1731.

[121] G. Tao. *Adaptive control design and analysis*. New York NY: Wiley, 2003.

[122] R. A. Horn and C. R. Johnson. *Matrix Analysis*. Cambridge: Cambridge University Press, 1985.

[123] J. R. Magnus and H. Neudecker. “The Differential of a Determinant”. In: *Matrix Differential Calculus with Applications in Statistics and Econometrics*. Wiley, 1999.

[124] P. Ghorawat. “Adaptive, Neural and Robust Control of Wing-Rock and Aeroelastic System”. In: May (2015).

[125] S. Tatikonda and S. Mitter. “Control Under Communication Constraints”. In: *IEEE Trans. Automat. Contr.* 49.7 (2004), pp. 1056–1068.